ABSTRACT

Title of Document: DEVELOPMENT OF A NEW STRETCHABLE
                               AND SCREEN PRINTABLE CONDUCTIVE INK

                               Anwar A. Mohammed, Doctor of Philosophy, 2017

Directed By: Professor Michael Pecht,
                               Department of Mechanical Engineering

Stretchable conductive ink is a key enabler for stretchable electronics. This thesis research

focuses on the development of a new stretchable and screen printable conductive ink. After print

and cure, this ink would be capable of being stretched by at least 500 cycles at 20% strain

without increasing its resistance by more than 30 times the original resistance, while maintaining

electrical and mechanical integrity. For a stretchable and screen-printable conductive ink, the

correct morphology of the metal powder selected and the ability of the binder to be stretched

after the sintering process, are both indispensable. This research has shown that a bi-modal

mixture of fine and large-diameter silver flakes will improve stretchability. While the smaller

flakes increase the conductivity and lower the sintering temperature, the larger flake particles

promote ohmic connectivity during stretching. The bi-modal flake distribution increases

connection points while enhancing packing density and lowering the thermal activation barrier.

The polymer binder phase plays a crucial role in offering stretchability to the stretchable

conductive inks. The silver flakes by themselves are not stretchable but they are contained within

a stretchable binder system. The research demonstrates that commonly used printable ink binder

when combined with large-chain polymers through a process known as 'elastomeric chain

polymerization' will enable the conductive ink to become more stretchable. This research has

shown that the new stretchable and screen printable silver conductive ink developed based upon the two insights mentioned above; (1) bi modal flakes to improve ohmic connectivity during stretching and (2) elastomeric chain polymerized binder system which could stretch even after the ink is sintered to the substrate, can exhibit an ink stretchability of at least 500 cycles at 20% strain while increasing the resistance by less than 30 times the original resistance. Wavy print patterns can enhance the stretchability of stretchable conductors. The research also demonstrates that FEA modeling, simulating the total principal strain on the printed patterns, can be used to estimate the comparative resistance changes caused by stretching and these changes can be explained by some basic equations from Percolation Theory.

Development of a New Stretchable and Screen Printable Conductive Ink

by

Anwar A. Mohammed

Dissertation submitted to the Faculty of the Graduate School of the

University of Maryland, College Park in partial fulfillment

of the requirements for the degree of

Doctor of Philosophy

2017

Advisory Committee:

Professor Michael Pecht (Chair)
Professor Christopher Davis
Doctor Diganta Das
Doctor Michael H. Azarian
Professor Peter Sandborn
Professor Patrick McCluskey

DEDICATION

Dedicated to my parents, Abdul and Shirin Mohammed,

To my family, Ezmina, Ambar, Sanaa and Kausar Mohammed

&

To all the teachers who guided and counselled me for over the years.

ACKNOWLEDGMENTS

TABLE OF CONTENTS

LIST OF TABLES

LIST OF FIGURES

LIST OF SYMBOLS & ABBREVIATIONS

C	Celsius
K	Kelvin
W	Watts
W/mK	Watts per meter Kelvin
Ω	Ohms
ADL	Activities of Daily Living
CAGR	Compounded Annual Growth Rate
CNP	Carbon Nano Particles
CNT	Carbon Nano Tube
COP	Chronic Obstructive Pulmonary
CSAM	Confocal Scanning Acoustic Microscopy
CTE	Coefficient of Thermal Expansion
DOE	Design of Experiments
EC	Epileptic Crisis
ECG	Electro Cardio Gram
EDX	Energy Dispersive X-ray
EEG	Electro Encephalo Gram
EMG	Electro Myo Gram
f	Volume Fraction of Conductive Flakes
f*	Threshold Volume Fraction of Conductive Flakes
FD	Flexible Displays
FEA	Finite Element Analysis
HTCC	High Temperature Cofired Ceramic

IoT	Internet of Things
LED	Light Emitting Diode
LTCC	Low Temperature Cofired Ceramic
MEMS	Micro Electro Mechanical Systems
NFC	Near Field Emission
OLED	Organic Light Emitting Diode
PC	Poly Carbonate
PCB	Printed Circuit Board
PDMS	Poly Dimethyl Siloxane
PDT	Photo Dynamic Therapy
PET	Polyethylene Terephthalate
PI	Poly Imide
PUT	Poly Urethane
PV	Photo Voltaic
RH	Relative Humidity
SE	Stretchable Electronics
SEM	Scanning Electron Microscope
SIDS	Sudden Infant Death Syndrome
Sigma c	Composite Conductivity
Sigma f	Flake Conductivity
SOC	System on Chip
SWN	Single Wall Carbon Nano Tube
t	Conductivity Exponent
TC	Thermal Cycling
Tg	Glass Transition Temperature

TPU	Thermo Plastic Polyurethane
WE	Wearable Electronics
WT	Wearable Technology

Chapter 1: Introduction

The thesis work is broken down in seven chapters. The first chapter is an introduction to the flexible and stretchable products emerging in the Wearable Electronics (WE) industry, the second chapter covers the literature review and the third chapter discusses the methodology used for the thesis research. Chapters 4 and 5 address the two major research objectives of the thesis, Chapter 6 covers fine line screen printing, ending with the research summary and conclusion in Chapter 7.

In this introductory chapter the background of the WE industry is covered with a brief overview of the definition, market, products, applications and challenges of the WE industry. Stretchable Electronics (SE), also known as stretchtronics, is envisaged to play a pivotal role in expanding the capabilities of Wearable Electronics and also generating new applications. The last section of this chapter covers new applications that can be achieved by the introduction of stretchtronics.

1.1 Context

The key motivation and application space for developing stretchable and screen printable conductive inks is the Wearable industry. Wearable products have been around for decades, but it is only recently that they are becoming fashionable. The term 'wearable' was coined in the nineties and products like wearable hearing aids and pace makers have been around in the medical field for a long time. Wearable devices have generally been trendy within the academic community. The expanding wearable market, led by industry giants like Google, Samsung and Nike is now capturing the attention of a wider mass of professionals and technologists. One of the earliest companies to make a move in the wearable space was Adidas. In 2008 they acquired Tektronics and introduced a personal coaching system by collecting relevant data like heart rate obtained from embedded sensors in sports bras and vests.

The WE technology has evolved beyond the proof of concept stage to bona fide products worn by consumers. Some of these products include augmented reality eyeglasses, headbands for monitoring brain activity, concussion sensors nestled within a helmet, sensor-guided canes for the blind and smart T shirts for the soldiers in the battle field. Contemporary wearable products tend to be more integrated, seamless, transparent, comfortable, useful, reliable and practical compared to earlier versions. Wearable technology is on a fast track towards ubiquity. We may be witnessing the dawning of a new technology, and products like Fitbit (to monitor personal activities) and the Google lens (to monitor sugar level non-invasively) may just be the technology heralds of the future.

1.2 Definition

In 1991 Mark Weiser coined the word wearable computing and defined it as being pervasive, ubiquitous or invisible with emphasis that the device should not only behave in an unobtrusive manner but also be transparent to the user [1, 2]. A wearable device may be defined as an application enabled computing device which accepts and processes inputs. This device is generally a fashion accessory usually worn or attached to the body. The device could work independently or be tethered to a smartphone allowing some kind of meaningful interaction with the user. The wearable product could be on the body (like a smart patch), around the body (like a wrist watch or a head band) or in the body (like a sensor attached to the heart monitoring cardiac aberrations). Wearable is a broad term and covers many products like patches, bandages, diapers, glasses, rings, watches, socks, shoes, hats, under- garments, jewelry, tattoos, ties, scarves, apparels and many others. To find sustainable market success, smart wearables must offer compelling value proposition beyond just behaving as technology gadgets.

1.3 Market

A recent marketing report (Fig. 1) from Beecham offers a helpful approach in understanding the breadth of the WE market. It points out key sectors like Security and Safety, Medical, Wellness, Sports/Fitness, Lifestyle Computing, Communications and Glamor which are already benefitting from the WE boom. The report also emphasizes the importance of blending function with style.

FIGURE # 1:   BEECHAM 2013 Report on WE   SOURCE: BEECHAM

The WE market has witnessed significant deployments in the health and fitness arena. Established companies like Google, Apple, Samsung, Nike and Microsoft are making strategic moves within the WE sector. This bodes well for smarter and sophisticated WE products and for the development of a robust supply chain ecosystem. If current developments are any indication of the future, it appears that the WE segment is going to be a very crowded landscape with strong competition.

ABI Research estimates the global market for WE in health and fitness alone could reach 170 million devices by 2017. Juniper Research is predicting the smart glass shipments to cross 10 million units per year by 2018. The Credit Suisse report expects a WE market of approximately $40B by 2016.The research analyst firm Berg Insight is predicting a CAGR (compounded annual growth rate) of 50% by 2018. Juniper Research forecasts (Fig. 2) that the revenue for WE will reach $19 billion by 2018. The numbers vary but the upward market trend is obvious.
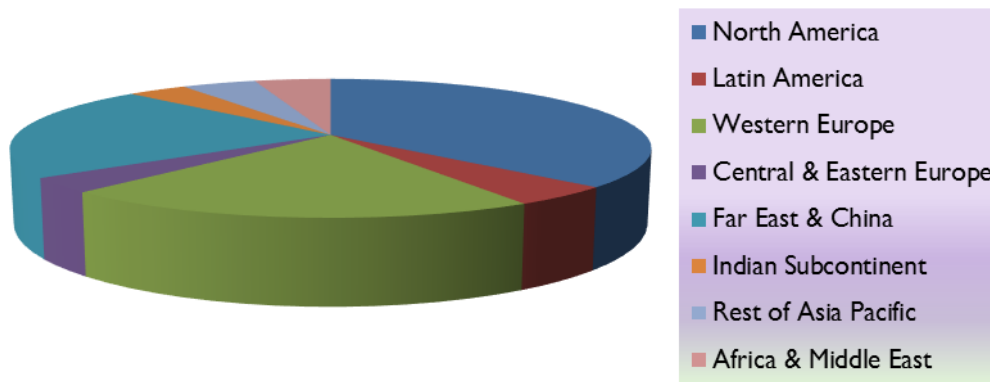
Global Smart Wearables Hardware Revenue
Total: $19 Billion by 2018

FIGURE # 2:   JUNIPER 2013 Research on WE   SOURCE: JUNIPER

1.4 Products

Current WE products in the market are creative but not close to leveraging the full power of this technology. Smart watches represent the biggest product segment in the current WE market. There are many product offerings but they are generally activity and position trackers with accuracy and algorithms that are not fully developed yet. Both Sony and Samsung have launched watches using OLED (organic light emitting diodes) displays, but they have not yet produced a bendable, wraparound display. Products like

the Google Glass try to stretch the technology envelope by demonstrating applications like doctors streaming live surgery to multiple different locations.

FIG # 3: Google Glass Source: GOOGLE   **FIG # 4: Samsung Galaxy Source: SAMSUNG**

Some products have been well received by the market like the Google Glass (Fig. 3) and the Samsung Galaxy Gear watch (Fig. 4). Experts point out that a WE product will succeed if attention is paid to comfort, value, portability, fashion and meaningful functionality.

As products get smaller and offer increased functionality the battery will become a critical differentiator. That is one of the reasons why printable battery suppliers like Imprint Energy are able to garner strong industry interest. New products are also in demand. Boston based MC10 (Figure 5) is developing conformal bandages and plasters which could be applied on the skin, providing a source for data collection. They are developing dissolvable patches that are strategically positioned near the heart or brain providing valuable diagnostics during surgery and dissolving innocuously after the operation.

1.5 Applications for Wearable Electronics

Lux Research highlights the significant opportunities in healthcare. The report accentuates opportunities for flexible and stretchable electronics to participate in the $300 billion healthcare market, pointing out that diabetic monitoring is expected to reach a $10 billion yearly turnover. Other opportunities include treatments like photodynamic therapy (PDT) where a stretchable light sensor can be targeted on light sensitive drugs applied on localized skin areas. PDT is also used to clean up acne- causing bacteria in the skin. Flexible and stretchable monitoring system has a strong potential for being used for remote health monitoring in senior health care [3, 4], where reliability is critical. Nuubo from Spain has developed smart vests for patients to monitor their health. These vests can offer medical quality cardiograms and heart activity monitoring. The bracelets from Nymi compare the wearer's unique electro cardiogram rhythms for identity validation.

Developers are also using near field communication (NFC) chips on rings and wristbands for seamless identification to pay for items or unlock doors.

1.6 Challenges

Many new products and technologies are converging at a rapid pace. Printable products like batteries [5, 6], antennas [7], LEDS, transistors and memory technologies are available, deposited on multiple substrate platforms such as flex, PET, TPU, paper and textile. New materials, such as flexible conductors [8] and anti- bacterial, self-cleaning, and water-resistant nano-materials [9], are now available using various deposition techniques like screen printing, stencil printing, and aerosol printing. The industry is seeing the introduction of many new products and technologies; however, there is a need for standardization on approaches for testing the reliability of these products.

Key product challenges include smaller device sizes, non-invasiveness and the ability to monitor multiple parameters while providing automated feedback for improving user behavior. This will require the integration of multiple sensors, different connectivity protocols and minimized power consumption. If garments and apparels are going to be electrically connected the robustness of the electronics will need to be improved and the garments will need to handle a minimal amount of washings.

Flexible OLED displays are still not ready for the market. In the interim, companies like Samsung are using curved displays which require rigidity and glass covers. Flexible batteries will enable more comfortable and mobile sensors for health care and a better understanding of piezoelectric will enable garments that could be charged easily.

Power will remain a challenge for a while. The Google Glass is being powered by a bulky battery behind the right ear, which is well hidden in the promotional pictures. There is progress being made in this field with promises of enhanced energy densities, longer battery lives and minimized charging times. Printable, flexible and chargeable batteries are being developed using leading edge technologies. Market competition is enabling the development of a diverse and strong supply chain eco-system.

Connectivity is another challenge worth considering. Currently the WE devices are generally hooked to the smartphone using Bluetooth connectivity. Which may be fine for now but eventually we might want to have our WE device independent of our smart phones.

As personal devices become ubiquitous, data storage and data privacy will become key areas of concern. The data collected could become part of a Human Cloud system, hosting and analyzing customer patterns to improve services offered by

companies and public organizations. We may have to develop cloud infrastructure to support the massive volume of generated data. It is evident that cloud computing is a strong enabler, however there are concerns of data privacy. Legal issues like taking a video of a movie or photographing people stealthily will need to be solved.

Medical insurance companies are already encouraging and rewarding their participants for using health improvement wearable devices. Generally, that is a good idea but it has room for potential mishandling and abuse of the data collected. There are many such legal challenges that need not be solved as WE gets popular with mainstream.

1.7Applications for Stretchable Electronics

Stretchable Electronics (SE) is a new paradigm. Nonetheless, there are many current applications that could benefit from this technology. Flexible displays, neuroprosthetics and cardio-stimulating implants, soft robotics, and other curvilinear systems require materials with high conductivity over a tensile strain of 100 percent [10, 11, 12]. Stretchable electronics which could be bent or twisted without compromising reliability would present significant value to biomedical applications for electroencephalograms (EEGs), electrocardiograms (ECG), photo detectors, and implantable devices [13, 14]. Other applications include highly flexible solar cells, wearable healthcare devices, implantable medical devices, sensors for artificial skin, and actuators for artificial muscles [15, 16, 17]. SE technology is well poised to play an important enabling role for emerging technologies like Internet of Things (IoT), Wearable Electronics (WE) and Flexible Displays (FD).

SE technology significantly extends the application horizons of current electronics technology. It is playing an increasingly important role in health management and biomedical applications. Close and accurate monitoring of "stretching" body organs like the heart and lungs require a SE solution. Smart stretchable patches on pregnant mothers for prenatal monitoring of high risk babies would be enabled by SE technology. Athletes wearing Lycra-based expandable garments, for example, would need SE on their attire to monitor their performance more accurately.

The human body is stretchable, soft, and curvaceous. For electronic devices to perform effectively in the human body, on the human body, and around the human body, they need to be compatible with the human body. Conventional integrated circuits tend to be rigid, planar and inflexible, whereas stretchable electronics are not. When conventional circuits are employed as implantable devices for the heart, brain, or the muscles, the human body identifies and eventually rejects them as foreign materials. This process is known as tissue scarring and is well documented regarding how it inhibits the performance of implantable devices. A soft and stretchable material analogous to our own tissues is necessary for long-lasting implants [18]. It would also be helpful for

diagnostic and surgical implants that work in close proximity to the human body while offering advanced therapeutics. Figure 5 depicts an example of a conformal skin patch that conforms to a baby's body for close and accurate monitoring.

Figure # 5: Conformal patch on a baby's body   Source: MC10

Stretchable electronic sheets could be wrapped around the contours of engine parts for efficient energy scavenging using thermoelectric principles. Stretchable LEDs, photovoltaics, sensory robotic skins, and biologically inspired designs for advanced cameras mimicking the human eye are potential application areas for this technology [19]. Figure 6 below depicts some of the products that can be enabled with stretchable electronics.
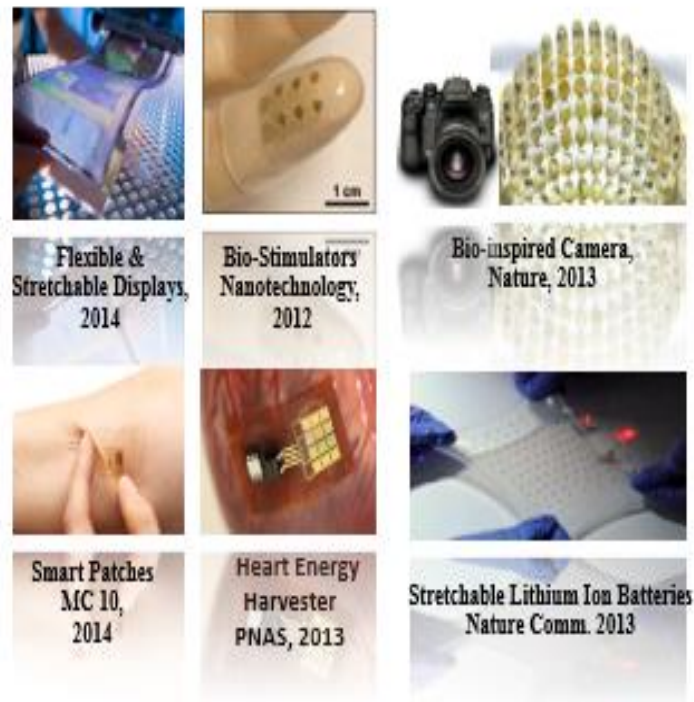
Applications:

- Flexible and stretchable displays
- Stretchable photo-detectors
- Wearable health care devices
- Long Distance Health Monitoring
- Implantable medical devices
- Sensors for artificial skins
- Actuators for artificial muscles
- Neuroprosthetics
- Soft robotics
- Stretchable batteries, antennas
- Stretchable sensors on garments
- Sports and Fitness Attire
- Connected Garments

Figure # 6: Some Applications for Stretchable Conductors.

1.8 Medical Industry

1.8.1   Long Distance Health Monitoring

Longevity has increased in industrialized countries and people are living longer but with multiple complicated health challenges. [8, 9, 20]. Because of advances in medical treatment survival from acute trauma has improved but this has resulted into the management of people with critical disabilities [21, 22]. WE has the potential of addressing many of the above problems because of the ability to diagnose and monitor health conditions in a long distance mode. Additionally, new cohorts of WE applications also offer motion monitoring like movement and walking, physiological monitoring like wound healing and biochemical monitoring like blood sugar and sweat readings [23, 24]. This could help patients with pulmonary, cardiovascular and neurological challenges like asthma, dysrhythmia, hypertension and seizures [22].

Remote health monitoring systems enabled by SE can play a significant role in mitigating access challenges [25]. About a fifth of the US population resides in rural

areas but only a tenth of the US doctors practice in rural areas [25]. Studies have shown that rural residents generally have worse outcomes than their urban counterparts for common conditions like heart attack and diabetes [26, 27]. SE, with remote monitoring can help improve the results. Figure # 7 offers a conceptual approach to achieve this.
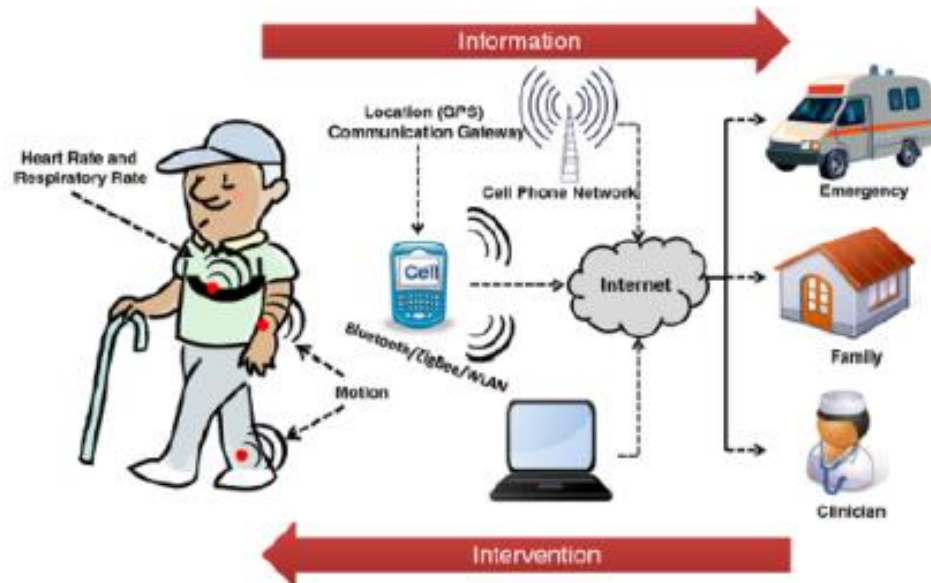
FIGURE # 7: A Conceptual Approach Towards Remote Health Monitoring [25]

Extensive research has been undertaken to validate the accuracy and efficacy of using SE for monitoring health conditions. Mathie et al [28] have established the feasibility of employing accelerometer sensors to monitor the activities of daily living (ADL). Giansanti et al have developed an accelerometer controlled wearable device for counting the steps of Parkinson patients [29]. Aziz et al have constructed a wearable device to monitor patient recovery after abdominal surgery [30]. Sazonov et al have installed a pressure sensor and an accelerometer in shoes to monitor ADL activities [31]. Studies have shown that wearable devices can play a very important role in monitoring the health status of patients. To encourage patients with weight challenges to undertake active and healthy lifestyle wearable products have been used successfully to monitor their activities and invoke clinical intervention when necessary [32- 35]. WE has also been proven effective in monitoring and managing patients with congestive heart failures [36, 37]. Currently, there are many wearable products available to carry out long term monitoring of important health indicators like steps taken, temperature, pressure, sweating, glucose monitoring, pulmonary oximetry, heart rate, blood pressure, ECG (electro cardiogram for heart monitoring), EMG (electro myography for muscle status) and EEG (electro encephalogram for brain monitoring). Table 1 offers a list of some currently available sensors [38].

Physiological Sensors	Parameters to be extracted	Related Use
Electrocardiograph (ECG or EKG)	QRS Complex Width RR Distance QT Interval	Presence of a heart block Heart Rate (directly) HR Variation
Electroencephalograph (EEG)	Alpha, beta, theta and gamma waves	Neural status
Pulse Oximeter	Heart Rate SpO2	A sudden change in HR Reduction in blood oxygenation (urgent medical intervention)
Accelerometer (3-axis)	Body Motion (activity)	Orientation and movement of body segment
Electromyography (EMG)	Surface EMG	Identification of motor tasks (muscle activity, numbness etc.)
Blood Pressure	Pressure Pulse	Hypertension Healthiness
Galvanic Skin Response (GSR)	Sweat Gland Activity	Sudden fear, stress etc.
Body Temperature	Skin Temperature	Fatigue and healthiness etc.
Respiration	Respiration Rate	Breathing activity and healthiness etc.

TABLE # 1: List of Currently Available Sensors for SE [38]

Several organizations have been running major research projects to evaluate the possibilities of leveraging SE devices for health status monitoring. Some notable ones include LiveNet, which is a system developed at the MIT Media Laboratory to measure ECG, EMG, galvanic skin response and 3D acceleration for monitoring Parkinsonian symptoms and detecting epileptic seizures [39]. LifeGuard is another system designed to monitor health statistics under extreme conditions including space travel [40]. AMON a European project uses a wrist worn device to study the medical condition of high risk patients with cardio-respiratory challenges by monitoring temperature, pressure, blood oxygen saturation and ECG [41]. Other European projects like MagIC [42, 43] and MyHeart [44] are designed for health monitoring of people in community settings using garment based wearable sensors.

1.8.2 Early Detection of Medical Issues

Flexible and stretchable devices have been studied to help the early detection of medical issues requiring clinical intervention. Patients showing chronic obstructive pulmonary (COP) disease can benefit by the early detection of the onset of an exacerbation episode. Excessive dyspnea (sudden and severe shortness of breath), cough and increase in the amount of the sputum can lead to functional impairment and disability. Early detection can trigger clinical intervention (visit to the doctor) to prevent grave consequences. Studies have shown [45, 46, 47] that a lowering of the daily activity level could be a useful indicator of a worsening condition leading to an exacerbation episode. A sensor worn in the ear, developed by Atallah et al [48] was used to monitor exertion levels and daily activities of COP patients. Using sophisticated algorithms, they

were able to predict the onset of an exacerbation event. In a similar study Belza et al [49] and Steele et al [50] were also able to predict an exacerbation event by monitoring the movements of the monitored patients.

Dementia is another disease which can be mitigated by early detection using stretchable technology. Also known as neuro-cognitive disorder, dementia results in a serious loss of cognitive capabilities in a previously unimpaired person. This loss would be above and beyond what would be expected as a result of normal aging. Over 30 million people globally suffer from dementia accounting for over $300B for medical care costs [22]. Early detection can be achieved by monitoring adult daily living (ADL) activities, medical compliance and changes in social behavior. Haiying et al [51] developed a wearable device for analyzing sleep patterns of suspected dementia patients. By evaluating the quantity, quality and rhythm of sleep the researchers aimed to identify the level of cognitive disorder of the subjects. Preliminary results suggest that subjects suffering from mild dementia have poorer sleep patterns. It is important that the monitoring devices need to be completely unobtrusive, transparent and should not involve patient intervention. Hayes et al were able to develop a home monitoring system using infra- red motion sensors which was completely unobtrusive [52].

Stretchable devices could also be used for the early detection of epileptic seizures. It is known that a sudden loss of consciousness can be caused by the onset of primary or secondary epileptic crisis (EC). These events are also accompanied by predictable patterns in the electroencephalogram (EEG) chart. During serious episodes the patient is unable to interact with the environment. Various types of wearable devices designed to monitor the onset of EC have been developed and tested successfully. EEG sensors, 3D accelerometers worn on the wrist, EMG sensors combined with accelerometers and electro dermal activity (EDA) sensors are currently available to distinguish EC patterns from normal patterns [53-56]. Dalton et al have developed wearable devices using the Nokia N810 platform to monitor EC [57].

Early detection of diabetes could be achieved by using products like the new Google lens (Fig. 8). This product is designed to monitor the blood sugar level of diabetics and potential diabetics by constantly analyzing the composition of the subject's tears using a wireless chip and a glucose sensor. Using miniaturized sensors and chips the lens can monitor glucose reading once per second. If a reading is out of the safe range an alert is issued using LED lights. This product was introduced in January 2014 and will still need some time to receive FDA approvals but it is a very good example of how miniaturized chip and sensor technology can be leveraged to help in early detection using very creative, unobtrusive and non- invasive approaches.
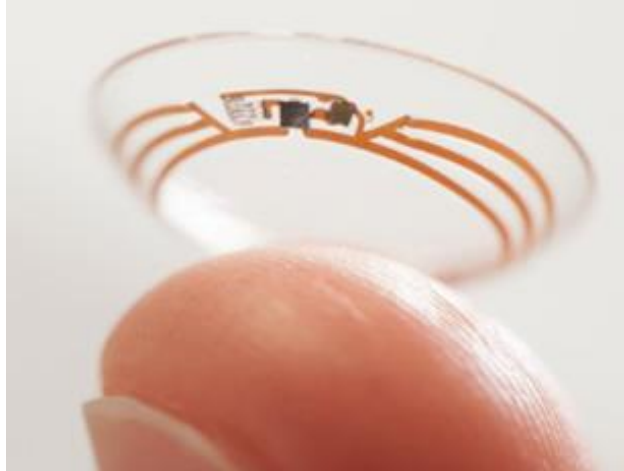
FIGURE # 8: Google Lens.   Source: GOOGLE

1.9 Safety and Security Industry

1.9.1   Fall Detection

Many seniors are prone to falls and this leads to serious medical consequences and increased medical billing. Wearable devices, using stretchable electronics are well situated to assist because of its unobtrusive nature and many systems have been developed to respond to the situation. Lanz et al [58] have developed smart canes (SmartFall) which utilize embedded accelerometers in walking canes to detect falls and relay the information wirelessly. Bourke et al [59] leveraged tri-axial accelerometers in a customized vest to detect and report falls. Bianchi et al [60] employed pressure sensors to detect falls while distinguishing it from regular daily activities. The current smart phones with their GPS sensors have also been used successfully for monitoring and reporting falls [61, 62]. The accelerometers combined with the GPS system was used by Yavuz et al [63] to develop a fall monitoring system. Since wrist bands are much less unobtrusive, fall detection systems have also been developed for wrist bands [64] however it is much more challenging to accurately detect fall events. The next level up is developing systems to prevent injuries caused by falls using airbag technology [65]. Accelerometers and gyroscopes are used to activate the inflation of airbag to mitigate fall related injuries.

1.9.2   Smart Security Garments

A new generation of smart garments is being developed for the security of people like soldiers in the battlefield and fire fighters. These apparels can monitor external environmental variables like temperature, pressure, humidity, heat flux and GPS location and are capable of transmitting stored information wirelessly. Supported by military funding, Georgia Tech introduced the digitized Smart Shirt (Fig. 9). Assembled with embedded sensors and optical fibers, this lightweight T-shirt can monitor vital signs of a

soldier and detect bullet wounds. It can monitor critical information like the location of the injury, the amount of bleeding and the GPS location of the soldier and wirelessly transmit the information to the nearest medical center. This shirt can also be modified for remote monitoring of infants at risk of sudden infant death syndrome (SIDS), for campers, trekkers, space- travel and law enforcement officers.
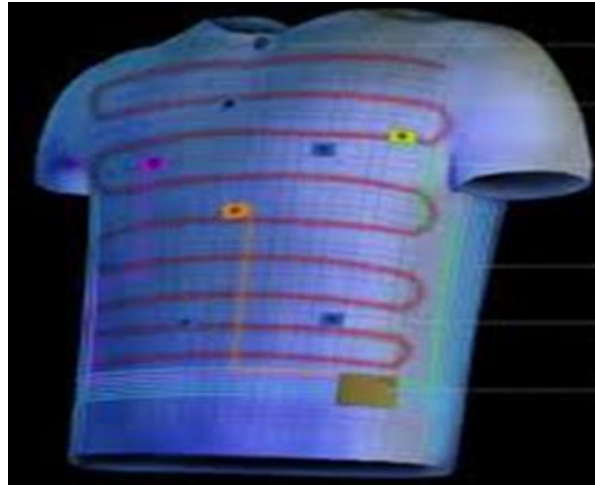
FIGURE # 9: Smart Shirt   Source: GEORGIA TECH

1.10 Technology Advancements

1.10.1 Microelectronics

Recent advances in miniaturization of microelectronics and sensors have played a strong enabling role in the development of stretchable technology. Current microelectronics can be miniaturized in the silicon level, the PCB level, the package level and the component level. Various technologies are being developed to make the microelectronics smaller, lighter, thinner and capable of handling higher power. Significant advances in the manufacturing of micro electro mechanical systems (MEMS) have assisted the assembly of inertial sensors that have been used in the monitoring of motor activities and other health monitoring systems. [22]. Batch fabrication of MEMS has also reduced the cost of these sensors. Component integration and miniaturization of micro- processors and communication circuits have resulted in System on Chip (SOC) implementations [66]. Recent developments in manufacturing and packaging allow the manufacturing of wearable products with attractive options in a cost sensitive manner. With the advent of printed, flexible electronics, conductive fibers, Bluetooth and miniaturized, low cost and low power sensors it is possible to integrate more and more high tech into regular clothing.

1.10.2 Smart Textiles

The development of smart textiles can now allow the integration of sensing capabilities within garments (Fig.10). Electrically connected clothing from IMEC can now have embedded sensors (Fig. 11) to collect information like electro cardio gram (ECG) and electro myographic (EM) data. These are sometimes referred to as body sensor networks. [67]. Safety, washability and low cost are some of the requirements for such networks. There are various means to establish electrical connectivity in these textiles. The electrical interconnect could be printed, deposited, embedded, patched in, wired in physically or by using conductive thread in the yarn [68]. The Fraunhofer Research Institute has developed a textile glove that can change color in the presence of toxic materials and Climaware has developed clothing that can change temperature according to the wearer's body temperature.
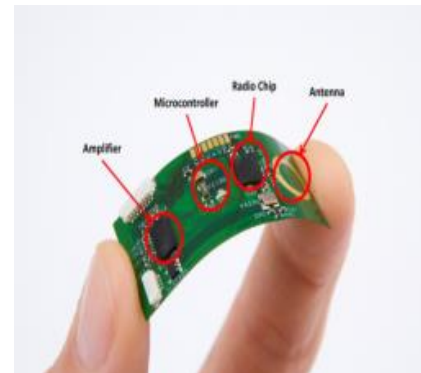
FIGURE # 10: Smart Textile from IMEC   **FIGURE # 11: ECG Sensor from IMEC**

1.10.3 Academia & Consortia

The academia plays an important role in envisioning and developing new technologies in the flexible and stretchable space. The concept of wearable computers, which led to the wearable movement started at the MIT Media Lab and the novel idea of stretchable conductors was given birth at the University of Chicago by Professor John Rogers, the cofounder of MC 10. Printable, flexible and chargeable batteries which hold such an important promise for future WE products was initially a PhD thesis for Christine Ho, a Cal Berkeley student and cofounder of Imprint Energy. There are many such examples. Consortiums also play a critical role in organizing the various players of the eco-system towards mutually shared technology visions and roadmaps. There are Research Institutes like IMEC in Belgium and Fraunhofer in Germany that undertake pioneering work in developing stretchable and flexible technology. In 2015 the US Government awarded a grant of $75M to establish NextFlex in California for the development of flexible and stretchable hybrid electronics.

Chapter 2: Literature Review

In this chapter we study the research accomplished so far in developing stretchable conductors. Different approached for developing them are covered and their feasibility for using them for stretchable electronics (SE) discussed. The review also focuses on the cyclical fatigue reliability of the various approaches and seeks to determine important gaps in the existing literature to develop research objectives for the current thesis. The literature surveyed could be broken down into the following four major process categories and each of the categories are carefully analyzed.

(1) Sputtering or etching conductive thin films on stretchable substrates
(2) Embedding conductive materials like CNT within stretchable substrates
(3) Thinning or developing meandering patterns on stretchable substrates
(4) Screen Printing conductive inks on stretchable substrates

Process #	Process	Advantages	Disadvantages	Comments
P1	Sputtering or etching conductive thin films on stretchable substrates	High stretchability with high cyclical fatigue reliability	Not cost efficient. Not suited for low volume/high mix products	Not suitable for low cost Stretchable Electronics (SE)
P2	Embedding conductive materials like CNT within stretchable substrates	High stretchability with high cyclical fatigue reliability	Not cost efficient. Not suited for low volume/high mix products	Not suitable for low cost Stretchable Electronics (SE)
P3	Thinning or developing meandering patterns on stretchable substrates	High stretchability with average cyclical fatigue reliability	Not cost efficient. Not suited for low volume/high mix products	Not suitable for low cost Stretchable Electronics (SE)
P4	Screen Printing conductive inks on stretchable substrates	Cost effective process (70% cheaper than P1,2 or 3). Established eco system. Well suited for low volume/high mix manufacturing	Screen printable conductive ink exhibit 'limited stretchability' with very poor cyclical fatigue reliability	Could be used for low cost SE. Need to develop screen printable conductive ink with improved stretchability and cyclical fatigue reliability.

TABLE # 2: Four ways in the Literature for developing Stretchable Conductors

2.1 Stretchable Conductors Overview

Stretchable electronics may be defined as electrical circuits which may be mechanically deformed by more than a few percent while retaining functional integrity [69]. Mechanical deformation could be caused by bending, compressing, stretching, twisting or deforming into arbitrary shapes [69]. Because of this behavior, they usually tend to be thin and laminar and generally fabricated from organic or inorganic materials in a nano-structured or a micro-structured form while integrated within some type of elastomeric substrates.

There is a need in the industry for a stretchable conductive ink that could also have fine printing capabilities. Since miniaturization is important, the fine line printing becomes very beneficial. There is research activity for developing stretchable conductors but nothing in the literature about conductive inks that are stretchable and printable. Of course, nothing also for stretchable and printable inks that are also capable to be printed in fine lines, usually around 50 microns. Organic conductive films are generally flexible but not stretchable. Flexibility is enabling for roll to roll printing (Fig. 12) processes and these films are generally printed on flexible substrates like polyimide (PI) or polyethylene terephthalate (PET) [70]. Presently, a gap remains for intrinsically stretchable conductive materials [71].
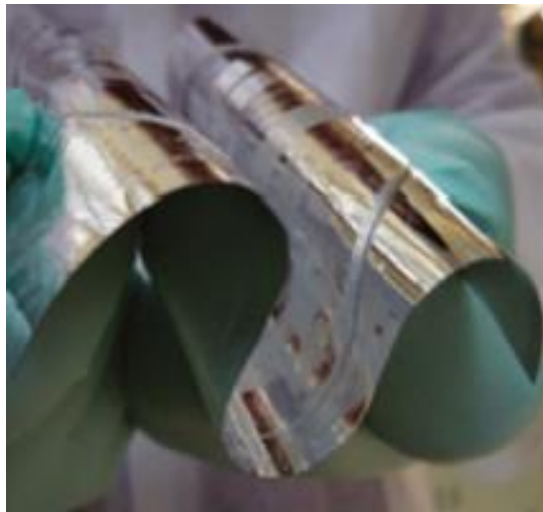
FIGURE # 12: A roll of bendable circuits   Source: Flex

Stretchable conductors which could be bent or twisted without compromising reliability would bring significant value to biomedical type applications for

16

electroencephalogram (EEG), electro cardiogram (ECG), photo detectors and implantable devices [77, 78]. Other applications include highly flexible solar cells, wearable health care devices, implantable medical devices, sensors for artificial skin and actuators for artificial muscles [79, 80, 81].

Several patterns for stretchable metal conductors have been proposed in recent years, such as out-of-plane, wavy or wrinkling conductors [82, 83]. Hsu et al [84] have done some work on horse shoe shaped wavy conductors (Fig. 13) on PDMS substrates and encapsulated by polymer. Two different line widths were compared; 900 microns and 1500 microns. It was experimentally determined that the 900 micron lines were stretchable up to 123% and the 1500 micron lines were stretchable up to 135% before exhibiting electrical rupture. These patterns were formed using photolithography and wet etching process on a copper foil which was encapsulated by PDMS substrates on both sides. They established that the coarse lines failed because of metal rupture whereas the finer lines failed because of delamination between the substrate and the copper metal.
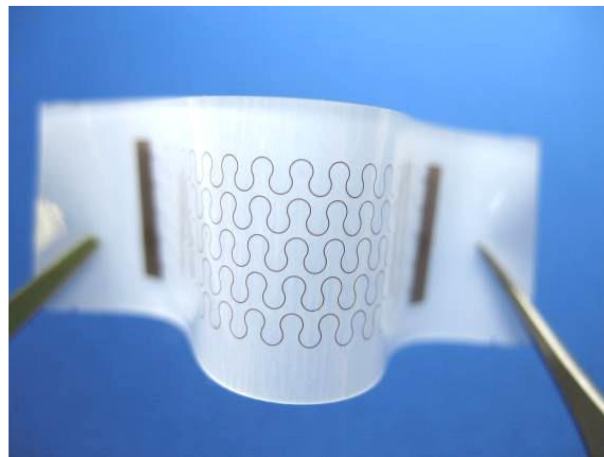
FIGURE # 13: Horse Shoe shaped pattern for stretchable conductors [84]

Another study on horse shoe shaped parallel conductors was carried out by Jahanshahi et al [85] where a PCB/foil based and a thin film based stretchable conductor was developed and the fatigue reliability of both the types was characterized. It was demonstrated that the continued exertion of plastic strain induced by the elastomer on the metal and the delamination of the metal from the substrate were the two main causes of failure. The paper stated that the factors affecting the reliability were Young's Modulus of the substrate, thickness of the substrate, the width of the substrate in comparison to the width of the copper metal and the composition of the copper.

2.2 Sputtering or etching conductive films on stretchable substrates (P1)

Stretchable conductors can be formed by sputtering thin Au films or etching thin Cu foils on to stretchable substrates like PDMS (poly dimethyl siloxane) or Polyurethane. Stretchable conductors are only meaningful on stretchable substrates. PDMS, PI (Polyimide), Polyurethane and Ecoflex are some substrates used for their stretchability. Ecoflex is also biodegradable [74].

Wenzhe Cao [75] deposited some Au thin films on PDMS substrates and was able to achieve electrical connection at 140% strain, meaning the system was stretched to 2.4 times the original length in the X direction. He was also able to achieve electrical connection at 16% radial strain, meaning strain in the Y direction. His research showed that the narrowest line exhibiting stretchability was 10 microns wide. He also postulated various models and approaches to predict the resistivity of a stretched system based upon the SEM pictures where the black nonconductive part was compared to the white conductive part to determine the amount of conductivity attained.

Thin copper foils were attached to PDMS substrates from both sides, after undergoing photolithography and wet-etching process to obtain the desired horse shoe pattern to form a stretchable conductor which could be stretched by 123% for 1.8 mm pitch horse shoe patterns and 135% for 3.0 mm pitch, without electrical failure. It was determined, both empirically and through finite element analysis, that the crest of the horse shoe was the weakest link. Delamination and metal rupture were deemed as failure mechanisms [84].

Sputtered gold patterns, using a horse shoe pattern on Polyimide (PI) films, were sandwiched into a PDMS substrates. 60,000 stretch cycles were observed at 20% strain without any failures [85].

Vardoy et al [86] developed stretchable electronics using metal coated polymer spheres which were packed into biocompatible silicone tubing. This particular material was designed to be used on textiles and it showed no drift in resistance up to 1000 cycles at 25% strain.

Thin sputtered gold film (~20 nanometers thick) were deposited on stretchable PDMS and silicone substrates to develop polymer actuators to manage fecal incontinence, which is the involuntary passage of bowel movement affecting around 45 % of retirement home residents and more than 12 % of the world adult population. Mechanical artificial sphincter implants for treating incontinence are available but they usually fail after five years. This new approach seeks to develop artificial muscle sphincters based on bio-mimetic electro-active polymer (EAP) actuators [87].

The advantage of this approach is that the products display high stretchability with high fatigue reliability, but because the set up cost for the sputtering or etching process per manufactured lot is quite high and because the stretchable electronics products tend to be in low volumes with a high skew mix, this is a cost prohibitive approach for SE.

2.3 Embedding conductive materials in stretchable substrate (P2)

Researchers have embedded carbon nano tubes (CNT) and conductive nano particles (CNP) on stretchable poly dimethyl siloxane (PDMS) to make stretchable conductive materials [72]. A CNT tube on polyurethane can handle up to 400% strain [72] and Ag nano wires on Ecoflex can handle up to 460% strain [76]. Researchers have successfully embedded Au nano- mesh in PDMS substrates [15] and metal coated polymer spheres have been fabricated within a biocompatible silicone tubing [17]. Stretchable electrodes using nanowires and graphene [18, 19] have also been embedded in various stretchable substrates.

Recently developed materials can also be used to make stretchable electronics. The most successful approaches are the ones that use elastic conductors as electrical interconnects between active devices that are rigid or slightly bendable [88]. Single-walled carbon nanotubes (SWNT) are grinded in an ionic liquid and then mixed with a fluorinated copolymer, making a black conductive substance commonly referred to as bucky gel [88]. Individual SWNTs form tangled mats in these gels (Fig. 14) that are able to reconfigure in response to applied strain. Another material that has attracted attention is graphene due to the fact that it can be used as an electrode because of its high conductivity and stretchability and can also be transferred to a substrate [89].
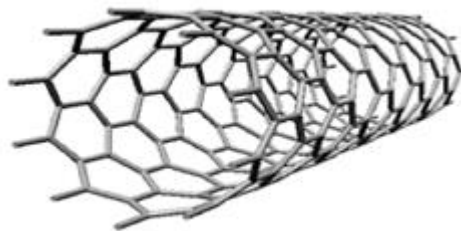
FIGURE # 14: Single Wall Carbon Nanotubing [88]

Highly stretchable strain sensors were developed by sandwiching Au nanowires on PDMS and other stretchable substrates like Ecoflex and Nitrile. The thin Au nanowire films exhibited strong mechanical stretchability up to 300% strain without any metal rupture or delamination [90].

Synthesized carbon nanomaterials like graphene and carbon nanotubes and metal nanomaterials like metal nanowires are also being embedded increasingly in various types of stretchable substrates to manufacture stretchable devices like electroactive polymer actuators, supercapacitors and capacitive sensors [91]. Graphene offers many attractive electrical, mechanical and optical properties that can be integrated into stretchable electronic devices for sensors and energy-harvesting devices [92, 93].

The advantage of this approach also is that the products display high stretchability with high fatigue reliability, but because the process for embedding the conductive material is non scalable and requires very skilled expertise, it is a cost prohibitive approach for the stretchable electronics products which tend to be cost sensitive and are manufactured in low volumes with a high skew mix.

2.4 Thinning or developing meandering patterns (P3)

In this approach we see processes where a material is rendered stretchable by thinning it or developing wavy, meandering patterns either mechanically or by deposition.

2.4.1   Pre-strained Substrate approach

This strategy leverages the basic mechanical idea that any material in a sufficiently thin form is flexible. Since silicon wafers are reasonably rigid, if enough strain is applied they crack or break. However, if the silicon is made into extremely small slices of nano-ribbons, it can be then stretched with ease. For example, the fabrication of thin silicon ribbons on a silicon wafer by conventional lithographic process with thicknesses of 100 nm experience peak strains of only 0.0005% upon bending to a radii of curvature of 1 cm [88]. These silicon nano-ribbons can be coupled to an elastomer such as polydimethylsiloxane (PDMS) through covalent –O-Si-O- linkages that form due to condensation reactions between surface –OH groups [94]. If these nano-ribbons are mounted on bi-axially pre-strained sheets with thicknesses of 20 mm, the strains (~0.1%) at similar bend radii, remain below the fracture limits (~1%) [88]. This can be improved further by moving the silicon away from the surface of the plastic, where the bending strains are largest, to the point in its depth where these strains are zero. After the bonding has been completed, peeling back the PDMS bonded with the ribbons from the silicon wafer and then releasing the pre-strain immediately will give the herringbone structure [88]. Formatted into sinusoidal waves by a controlled buckling process, a two-dimensional analog of a similar effect first observed in ribbons will give the result of a Si/PDMS construct that can be stretched and compressed reversibly, with a linear elastic

response to applied force [88]. The amplitudes and wavelengths of the waves change in response to induced deformations that avoid substantial strains in the silicon itself.

This approach depends on simple, linear elasto- mechanical responses, and can be applied to different materials, in various molecular structures, such as inorganic nano-ribbons, nano-membranes, carbon monolayers and nanotubes. Figure 15 below depicts the above strategy where nano ribbons of silicon are attached to pre-strained poly dimethyl siloxane (PDMS) substrate [95]. After the process has been completed the silicon nano-ribbons resemble a herringbone shape.
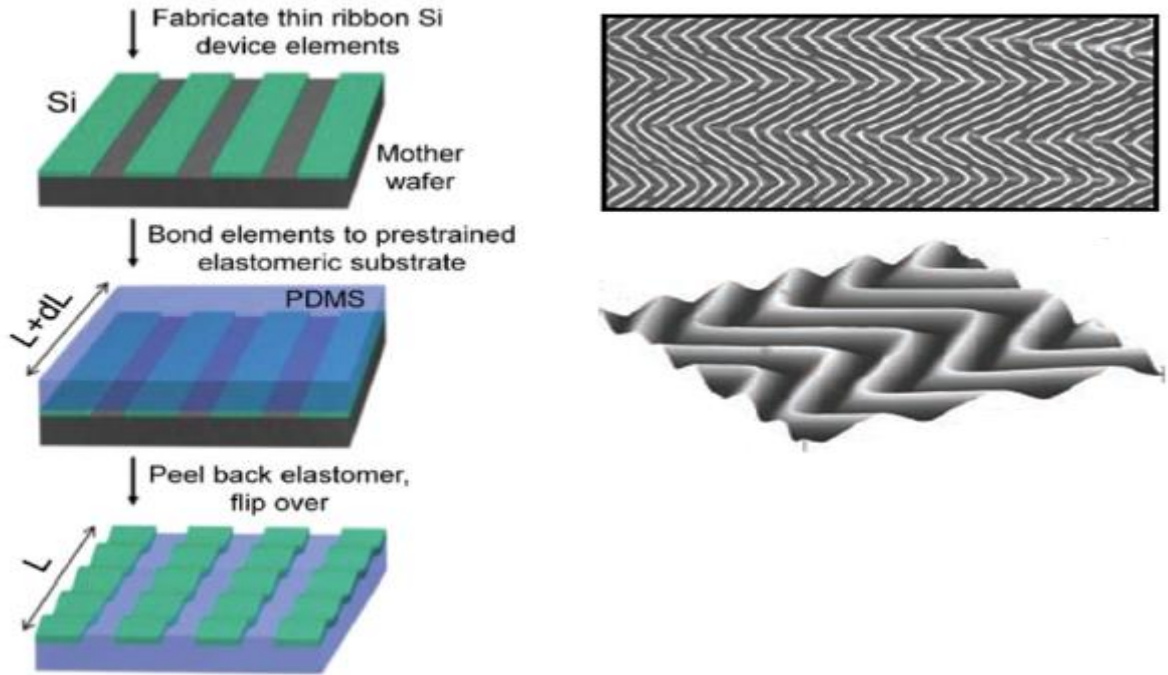
FIGURE # 15: Silicon nanoribbons on pre-strained PDMS substrates forming a herringbone configuration [95]

2.4.2 Localized node bonding approach

Localized node bonding is similar to the pre-strained bonding approach. This effect is achieved by structuring the sheet into a mesh and bonding the silicon nano-ribbons to the substrate only at the nodes (Fig. 16). The non-bonded, arc shaped regions can delaminate, and move freely out of the plane to accommodate applied strains, giving them a "pop-up" impression [96]. This provides a level of mechanical isolation for the nodes, or islands. The main advantage is that the buckled bridges allow optimization for stretchability. By using Young's Modulus, it is shown that this strategy is most effective when the bridge thickness is much smaller than the bridge length, and the sizes of the

islands are smaller than the distances between them [96]. For example, a bridge with thickness of 50 nm and length of 20 ums would have the strain in the bridge reduced by 6x, 21x, and 90x for pre strain 1%, 10% and 100% respectively, and the strain on the bridge can be further reduced for thin and long bridges [96]. The strain in the island is the same as the bridges for islands and bridges having the same elastic modulus and thickness. The strain on the island can be reduced even more as the island elastic modulus and thickness increase. The strains can be calculated by the following equations [96]:

$$\varepsilon_{bridge} = 2\pi \frac{H_{island}}{L_{bridge}} \sqrt{\frac{\varepsilon_{pre}}{1+\varepsilon_{pre}}}, \quad \varepsilon_{island} = \frac{E_{bridge}}{E_{island}} \left(\frac{H_{bridge}}{H_{island}}\right)^2 \varepsilon_{bridge} \qquad \ldots\ldots\ldots \text{EQUATION \# 1}$$

As with the pre-strained strategy, this localized node bonding strategy can also be implemented with ribbons, membranes or wires of various materials [96]

Cu

PDMS
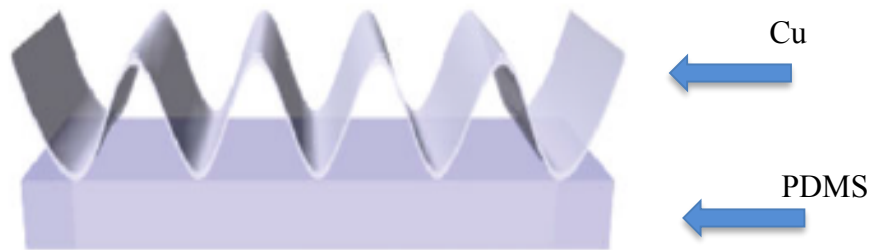
FIGURE # 16: Localized Node Bonding [96]

2.4.3   Helix structure approach

The helix structure (Fig. 17) strategy resembles the helical strands of DNA and is constructed in a serpentine fashion that allows substantial elongation. Although electronic circuits could be fabricated onto a helical structure, it would require microfabrication in 3 dimensions which is a process that still requires development. Therefore, planar microfabrication is used to create the same results. This can be done by having a thin film of a stiff material suitably bonded to a compliant substrate, then small strains are induced to the film and the film accommodates these strains by twisting out of the elongation [97]. A similar pattern can serve as a substrate on which entire electronic circuits can be fabricated using this planar micro-fabrication technology. When strain is applied, the circuits will be able to function without appreciable fatigue, the out of plane twisting of the p n. patterned substrate only affects the top layer leaving the bottom layer available for optional support or backing [97]. The elongation has several advantages, one, if the film is a metal such as copper, its electrical resistance increases with elongation in a way

predicted based on the assumption that it retains a rectangular shape. Secondly, the resistance of the film is unchanged leading to the prediction

$$R/R_0 = (L/L_0)^2 \qquad \boxed{\text{.........EQUATION \# 2}}$$

Where R and L are the electrical resistance and the length of the stretched film,]. respectively, and R_o and L_o are the resistance and length of the unstrained film, respectively [97].
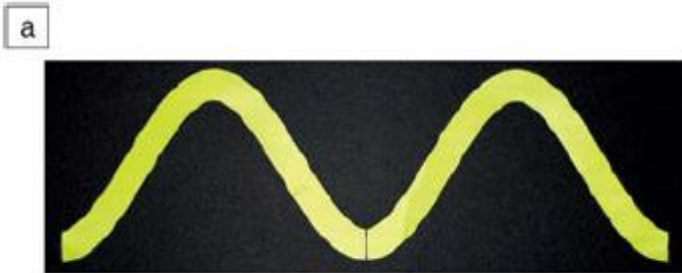
A serpentine strip cut out of a piece of paper and is initially flat.
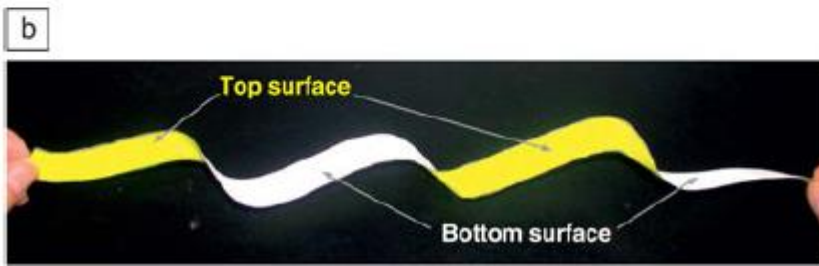
When the strip is pulled, it twists out of the plane acting like a

helical spring, elongates but keeps the strain small.
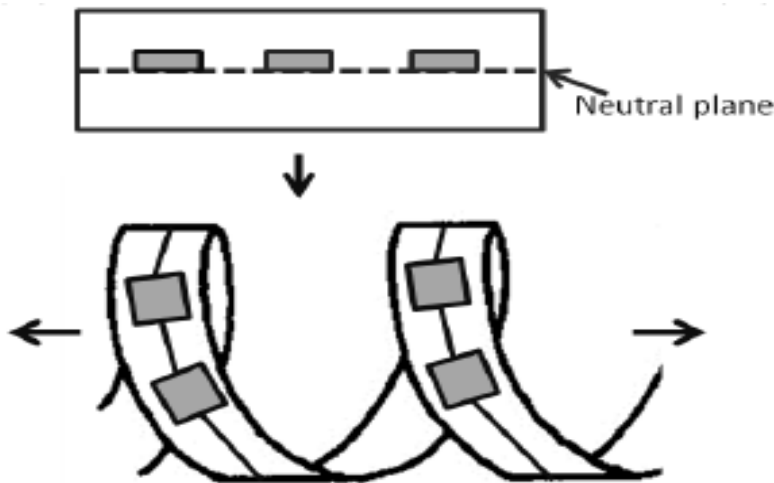
Process of micro fabricating silicon onto a stretchable structure of a helical pattern.

FIGURE # 17: Helix Structure [97]

23

It is interesting to note that the strain exerted on the helix structure can be estimated by using 3D finite modeling [98]. Figure 18 below enumerates the strain distribution for a 720° twist.
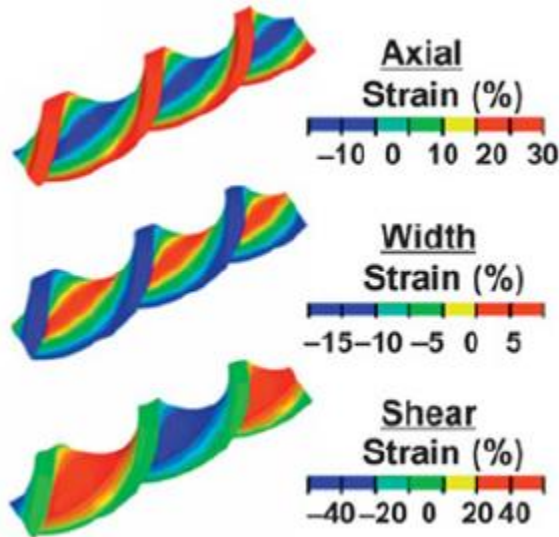
Strain distributions in the twisted substrates, calculated by 3D finite element modeling for the case of the 720° twist.

FIGURE # 18: Stress Distribution on a Helix Structure [98]

The advantage of this approach is that the products display high stretchability with average cyclical fatigue reliability, but because the fabrication is non scalable and requires very skilled expertise, it is a cost prohibitive approach for the stretchable electronics products which tend to be cost sensitive and are manufactured in low volumes with a high skew mix.

2.5 Screen Printing conductive inks on stretchable substrates (P4)

The literature does not have any mention of truly stretchable and screen printable conductive inks, because they are a new phenomenon. However, there are references of ink behavior with very limited stretchability. It is interesting to note that there is no evidence in the literature of a screen printed conductive ink which displays a cyclical fatigue reliability of more than 30 stretch cycles under stress, with the accompanying change in resistance.

2.5.1 Ag Conductors on Polyurethane

Araki et al have added silver flakes in elastomers on polyurethane substrates and achieved promising results [99]. Silver flakes embedded in a polyurethane binder and printed on stretchable polyurethane substrates were shown to tolerate up to 600% strain (Fig. 19) for a single cycle stretch. However, the increase in resistance after 1 cycle at 20 % strain was over 70 X and after 1 cycle at 80% was over 700 X the original resistance [99]. This was unacceptably high even though the electrical connection was intact.

The conductive ink showed excellent adhesion to the substrate and was cured at only 70C making it useful for cellulosic and textile based substrates. The authors stated that percolation theory was an important consideration in understanding the ink behavior [99].

No cyclical fatigue reliability data (important for stretchable electronics) was available for multiple stretching cycles. The increase in resistance after 1 cycle is also very high.
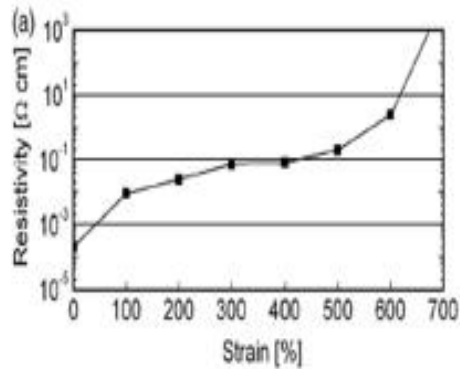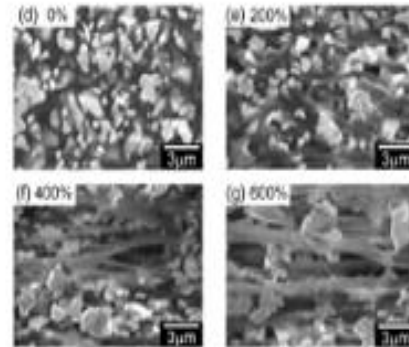
FIGURE # 19: Ag on Polyurethane, Resistance versus Strain [99]

2.5.2 Ag Conductors on PVC

The electrical performance and morphological study of a silver ink printed on a stretchable PVC substrate was investigated in strained and unstrained conditions. The goal of this study was to develop a strain sensor [100]. The silver ink studied contained a polyester binder resin, which was not an elastomer and the silver flakes used had a uni-modal distribution with an average of 9 microns. The conductive pattern used for the testing was 8 mm wide and 97 mm long. This pattern is suitable for developing antenna applications but is too wide for conductive interconnects [100]. It was argued that high filler content would lead to higher conductivity but may result into more brittle and less stretchable ink, because the cross linking of resins between fillers would become more difficult. [100]. The resistance versus strain graph was developed for a single cycle stretch of up to 50% strain (Fig. 20). Cyclical fatigue reliability data available for only 3 cycles.

Characterization of Silver Conductive Ink: Ag on PVC

Resistance and dimensions of conductors on PVC before and after the stretching.   **Max. data for cyclical strain is 3 cycles [100]**

Sample	Stretching	Resistance (Ω) before stretching	Resistance (Ω) right after stretching	Change in width right after stretching	Change in length right after stretching	Change in resistance (Ω)
1	1	1.0	1.6	0.1 mm - 1.3%	6 mm - 6.2%	0.6
1	2	1.5	2.4	0.2 mm - 2.5%	7 mm - 7.2%	0.9
1	3	1.0	2.6	0.2 mm - 2.5%	7 mm - 7.2%	1.6
2	1	0.6	1.5	0.3 mm - 3.7%	7.3 mm - 7.5%	0.9
2	2	1.1	2.1	0.5 mm - 6.2%	9.3 mm - 9.6%	1.0
2	3	1.0	3.2	0.4 mm - 4.9%	7.8 mm - 8%	2.2
3	1	0.5	1.3	0.3 mm - 3.7%	7 mm - 7.2%	0.8
3	2	1.0	2.5	0.2 mm - 2.5%	7 mm - 7.2%	1.5
3	3	1.0	2.1	0.3 mm - 3.7%	6 mm - 6.2%	1.1
4	1	0.5	1.3	0.2 mm - 2.5%	5 mm - 5.1%	0.8

FIGURE # 20: Characterization of Silver Ink on PVC [100]

2.5.3   Ag Conductors on other substrates

Screen printed electrically conductive silver ink patterns were characterized on paper, fabric and PET substrates. The conductivity breakdown was postulated due to several phenomena like the delamination from the substrate and loss of contact between filler particles, because of the decrease in the volume fraction of the filler materials during stretching. [101]

All three silver inks exhibited excellent bendability up to 10,000 bend cycles using a cyclical bending test (Fig. 21). The sheet resistance of the ink varied from 40 to 130 milliohms per square. Different curing temperatures from 20 to 180 C were tested revealing that the sheet resistivity decreased with higher cure temperature. The authors stated that the type and ratio of the polymer matrix, the size, amount, shape, distribution and orientation of the metal flakes had an effect on the electrical and mechanical properties of the silver conductive ink. [101]

No cyclical fatigue reliability data was available for multiple stretching cycles. Bendability testing is not an indicator of stretchability because bendability and stretchability have different failure mechanism and amount of stress.

Effect of cure temperature on ink sheet resistivity on paper substrates [101]
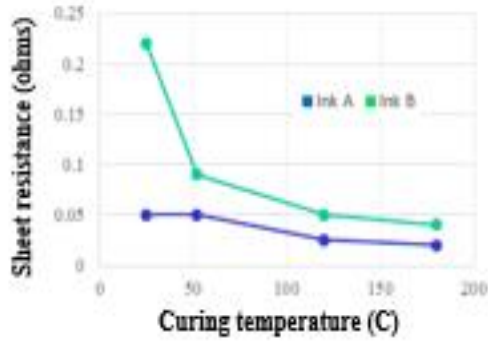
Bend cycling results of silver ink on PET [101]
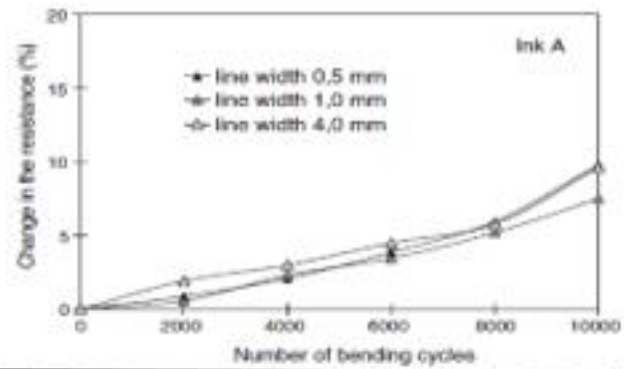
Cross Section of Ink A on fabric [101]
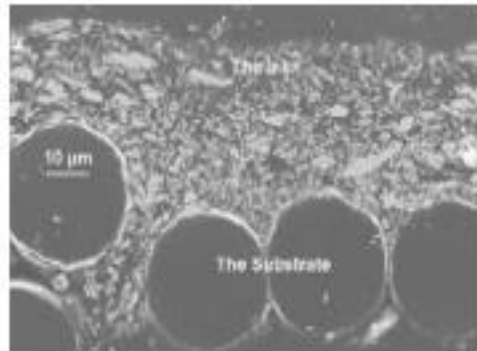
Cross Section of Ink A on PET [101
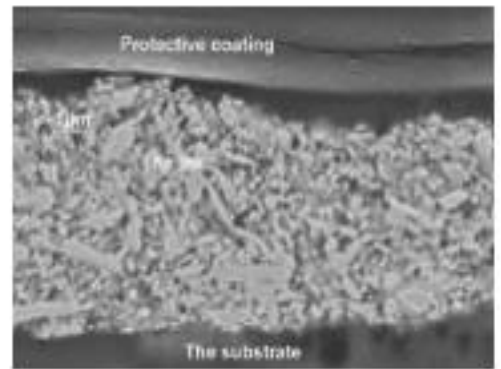
FIGURE # 21: Silver Ink on Different Substrates [101]

2.6 Literature Review Summary (P1-P4)

The literature review revealed that there are four distinct ways of developing stretchable conductors. (P1-P4) and they could be categorized as follows:

P1: Sputtered or etched thin films that have been fabricated within elastomer substrates [74,75,84-86]. The approach is to sputter or etch thin layers of metal film to an elastomer to make it stretchable.

P2: Stretchable conductors like CNT, CNP or Ag nano wires were embedded within elastomers making them stretchable [15, 17-19, 76, 89].

P3: Enabling stretchability by thinning and or meandering [88, 95, 96, 97, 98].

All of the above 3 manufacturing approaches (P1-P3) are not attractive for low volume, high mix products needed for SE because the set up costs are high and can only be cost justified for very high volume runs.

P4: Enabling 'limited stretchability' by screen printing conductive ink on stretchable substrates [99, 100, 101]. Attractive for low volume high mix products because the stretchable electronics products tend to be in low volumes with a high skew mix however, no meaningful cyclical fatigue study available because of unavailability of truly stretchable conductive inks.

2.7 Research Gaps and Objectives

In conclusion it is observed that many different approaches have been undertaken in the last few decades to develop stretchable conductive circuits, however none of them include screen printable conductive inks. There remains a clear gap for developing a cost -sensitive methodology, like screen printing, for manufacturing stretchable circuits. The current thesis focuses upon the development of a screen printable and stretchable conductive ink. The research objectives include the following:

(1) Develop a new stretchable and screen printable conductive ink which could be stretched more than 500 cycles, by at least 20% strain, without increasing the original resistance by more than 30 times.
(2) Run experiments to determine if the comparative changes in resistance caused by stretching, between a screen printed straight line pattern and a sine wave pattern can be estimated by calculating the total principal strain through Finite Element Analysis (FEA) modeling and explained by equations from Percolation Theory.
(3) Demonstrate the printing of 50 micron lines this newly developed ink.
(4) Study the feasibility of developing stretchable dielectrics

The first two objectives were addressed as contributions towards improving the current state of the art. The third objective was also completed but not as a contribution towards furthering the current knowledge in that space. Even though this was the first time a stretchable conductive ink would be used for the screen printing of 50 micron lines but this capability has been previously shown on non-stretchable screen printed conductive inks.

The fourth objective included a brief feasibility study of developing stretchable dielectrics, which along with the newly developed conductive ink would enable the development of stretchable capacitors and stretchable multi- layer circuitry.

Chapter 3: Methodology

This chapter covers the methodology and approach for achieving the research objectives. It includes the problem statement and the research scope, impact, approach and deliverables.

3.1 Problem Statement

Microelectronic screen printing technology is an established low cost manufacturing technology for developing low volume/high mix electronic circuits. The available screen printed conductive inks when this research started exhibited very limited stretchability and could not be used in applications requiring flexibility and stretchability. This research focused around the study of the failure mechanism of the available conductive inks with limited stretchability with the objective to generate recommendations for the development of a new screen printable and stretchable conductive ink, that could withstand over 500 cycles of stretching at 20% strain without increasing the resistance by more than 30 X the original resistance.

The research also focused around studying the comparative change in resistance caused by stretching, between a screen printed straight line pattern and a sine wave pattern. The objective was to determine if the resistance changes could be estimated by calculating total principal strain, using FEA modeling and explained by employing Percolation Theory.

The research also developed processing parameters required to print 50 micron lines to support miniaturization of the Wearable Electronics products and lastly it explored the possibilities of developing stretchable dielectrics by employing the same approaches used for the development of stretchable conductive ink.

3.2 Research Scope

This research centered around the development of a screen printable conductive inks, which could be stretched by at least 20% of the original length without exhibiting any mechanical or electrical failures. Based on the failure analyses of available inks, recommendations were made to improve the stretchability of the conductive ink. Few generations of the formulated ink were tried and evaluated until a suitable stretchable and screen printable conductive ink was developed.

The research also demonstrated that a printed sine wave pattern was more stretchable than a printed straight line pattern. It was postulated that the sine wave pattern

would behave like a spring coil that would open up when stretched and minimize the induced stress. The reduced stress would result into a smaller increase in resistivity when stretched. More importantly, the research was successful in estimate the change in resistance by calculating the total principal strain, using FEA modeling. Equations from Percolation theory were also used successfully to explain the resistance changes.

The research also demonstrated that the developed stretchable conductive ink could also be printed in fine lines as narrow as 50 microns wide. This would offer the capability to achieve miniaturization of the electronic circuit if required. Screen printing processing parameters were developed to enable the fine line printing.

The reliability studies were focused on the in situ monitoring of the electrical conductivity of the conductive ink as it was stressed and relaxed, for multiple cycles till it reached failure. This was carried out in a repeatable manner, using automated equipment for stretching and electrical reading. The electrical resistance of the printed stretchable conductive line was monitored in both the relaxed and stretched state. Failure analysis tools like Scanning Electron Microscope (SEM), Energy Dispersive X Ray (EDX), 3D Camera inspection and Confocal Scanning Acoustic Microscopy (CSAM) were utilized to understand the failure mechanisms. According to the literature [84, 85] metal rupture, metal delamination and substrate tearing were anticipated as potential failure causes. To check for delamination and rupture, standard tests like CSAM testing, temperature cycling and temperature humidity testing were also undertaken.

Regular microelectronics screen printing technology was used for depositing the stretchable conductive inks. Expensive processes like aerosol printing or photolithography were avoided to ensure the development of a cost effective approach which could be implemented for manufacturing, using currently available industry processes and equipment.

3.3 *Research Impact*
The goal was to enable the development of a screen printable stretchable conductive ink which would enable the commercialization of stretchable electronics. It is envisaged that stretchable electronics would play a key role in the growth of the emerging wearable technology and IoT products.

3.4 *Research Approach*
In this section we will review the conceptual research approach used for meeting the 3 key objectives of the current thesis; (i) Development and preliminary reliability studies of stretchable conductive inks (ii) Comparing the stretchability of a sine wave pattern versus a straight line using the stretchable conductive ink and (iii) Demonstrate

and develop recommended processes for printing 50 micron lines using the stretchable conductive ink.

3.4.1 Approach for Developing Stretchable Conductive Ink

For developing stretchable conductive inks, the approach depicted in the table # 3 below was undertaken.
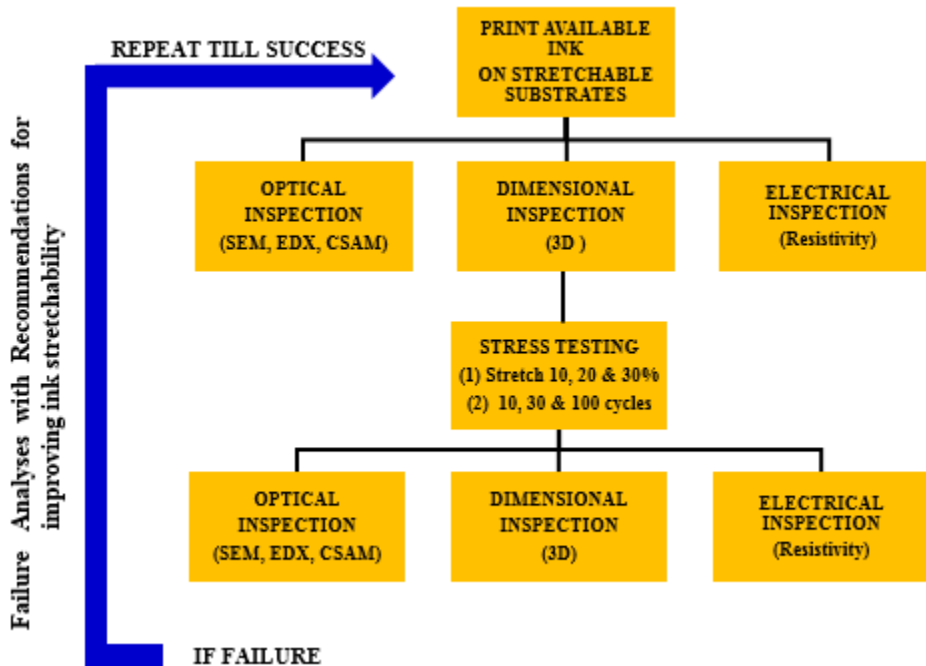
TABLE # 3: Stretchable Conductive Ink Development Flowchart

Compatible stretchable substrates were initially selected upon which the conductive inks were screen printed. The substarte selection was important because of potential compatibility, stretchability and delamination issues. Some initial stretchable substrate candidates included thermoplastic polyurethane substrate (TPU) substrates from American Polyfilms and Bemis and stretchable substrates like Cetes and Tyvek from DuPont. An initial filtering experiment was used to help downselect the appropriate substrate candidates. Similarly, potential candidates for stretchable conductive inks were selected from companies like Du Pont, Alpha, PPG and Nagase and an initial screening experiment was used to select the proper candidates. Before determining the final stretch conditions and the number of tested cycles for acceptability, initial pre-testing was

undertaken to help decide the final approach and save time. After testing a sample of conductive ink, reliability analyses was performed as necessary to determine failure analysis and generate recommendations for stretchability improvements. FEA modeling was be undertaken for the sine wave study, to compare with empirical results. A special test equipment, the universal flexibility tester, was designed and developed to automatically stretch and relax conductive lines with an accurate and repeatable predetermined stress for a given number of cycles. The equipment was able to monitor and record in situ resistance of the stretchable conductive lines in the stretched and relaxed state.

3.4.2   Comparing Stretchability of a Sinusoidal pattern

For studying the stetchability of sinusoidal wave patterns, special screens were designed and fabricated. Sample parts were printed depicting a sine wave pattern and a straight line pattern on the same substrate, at the same time using similar conductive inks processed and cured under similar conditions.The sample parts were stretched and tested to compare the levels of stretchability between the two different patterns. Stretchability was compared by calculating the percentage change of resistance of the conductive ink under similar stress conditions. Previous research [84,85] had shown that a horseshoe shaped wavy pattern is more stretchable than a stright line. However this research was done on much thicker lines (900 microns to 1500 microns thick) and they were not performed on screen printed lines but lines that were patterned using photolithography and wet etching of copper foils.

3.4.3   Approach for Developing 50 micron lines

Lastly for developing fine line printing capabiities, the stretchable conductive ink was printed on stretchable substrates using screen printing techniques developed specially for depositing fine lines. The current research demonstrated the capability to print 50 microns wide fine lines with stretchable conductive inks. This required the development of printing techniques specially suited for stetchable conductive inks on stretchable substrates. A recommended set of parameters for printing 50 microns wide fine lines was developed. Previous research [102] had shown the capabiities of printing screen printed lines that were 50 microns wide, but this work was not done on stretchable conductive ink but on conductive inks that were specially designed for fine line screen printing. Stretchable inks, because of their polymeric binder base are not designed for fine line printing. The fineness of the deposited ink also depends upon printing techniques like squeege blade material and angle, squeege presure, squeege speed, wire mesh and emulsion thickness. The ink rheology and morphology also play a significant role. The screen printer used would be a DEK or an equivalent printer which is capable of printing 50 micron lines.

3.5 Research Deliverables

The research deliverables include the following:

(1) Completed thesis dissertation.
(2) Samples and test data demonstrating the development of a new screen printable and stretchable conductive ink, that can withstand over 500 cycles of stretching at 20% strain without increasing the resistance by more than 30 X.
(3) Experimental data demonstrating that the comparative change in resistance caused by stretching, between a screen printed straight line pattern and a sine wave pattern can be estimated by calculating total principal strain by FEA modeling and graphically explained by employing equations from Percolation theory and comparing them to experimental data.
(4) Samples and test data demonstrating samples of 50 micron wide lines using the newly developed screen printable and stretchable conductive ink.
(5) Samples and preliminary test data for a screen printable and stretchable dielectric ink

Chapter 4: Development of Stretchable Conductive Inks

4.1 Introduction

In this section is covered the research activities related with the development and preliminary reliability testing of screen printable silver conductive inks which could be stretched uni-axially by at least 20% of the original length without exhibiting any mechanical or electrical failures and while keeping the increase in resistance to lower than 30X of the original resistance.

A screen printable conductive ink composition generally includes a functional phase which includes metal powders like Pt, Pd, Ag, Au or Cu and it may include some nano- materials technology to improve the sintering and low temperature curing of the ink. The binder phase of the conductive ink is designed to attach the ink to the substrate, during, before and after the curing process. The role of the vehicle phase is to become the carrier for the metal powders during the screening process and up until the curing process and it includes volatile solvents and non-volatile organic polymers.

For a stretchable conductive ink, the morphology of the metal powder selected and the ability of the binder and the vehicle to carry this powder during the printing and curing process is important. The binder plays an important role in enabling the ink to adhere to the substrate and by offering stretchability in the post cure state. The most important ink requirement is the ability to stretch after the curing has taken place in such a way that it still maintains connectivity between the metal powder flakes.

For an ink to be screen printable the rheology of the ink plays a very important role. Generally, an ink rheology depicting non-Newtonian. thixotropic behavior is desired where the ink viscosity falls down quickly under stress by the print squeegee (during the printing process) and does not move once the squeegee pressure is removed.

Areas covered in this section include literature review of conductive inks, methodology, sample preparation, stress testing, SEM/EDX/CSAM/3D analyses, preliminary reliability studies, development of a universal flex tester and conclusion.

4.2 Literature Review for Screen printed Conductive Inks

When the electrical resistance of a material is dependent upon external straining, the material is said to exhibit piezo resistivity. Generally, when elastomers are screen printed with silver conductive ink, the composite structure tends to exhibit piezo resistive behavior [103]. The conductivity of this structure depends upon the external stress and also upon the volume fraction of the conductive flakes (f). As f keeps on increasing an inflection point is achieved when the resistance increases sharply, because of the loss of ohmic contact. This point is referred to as the threshold volume fraction (f*). This

behavior can be explained by the percolation theory originated by Broadbent and Hammersley in 1957 and validated by others like Gurland, Kirkpatrick and Cohen. The percolation theory has been updated by few researchers like Pike and Balberg. Taya et al have proposed in 1986 the following fiber percolation model which can predict the conductivity of a piezo resistive composite structure [103]:

$$\sigma_c = \sigma_f(f-f^*)^t \text{ for } f>f^* \quad \boxed{..........\text{EQUATION \# 3}}$$

σ_c = composite conductivity σ_c
σ_f = flake conductivity
f = conductor volume fraction
f * = critical conductor volume fraction when a percolating network of conductors is just established when f is higher than f *
t= conductivity exponent (generally considered to be 2 for 3D structures)
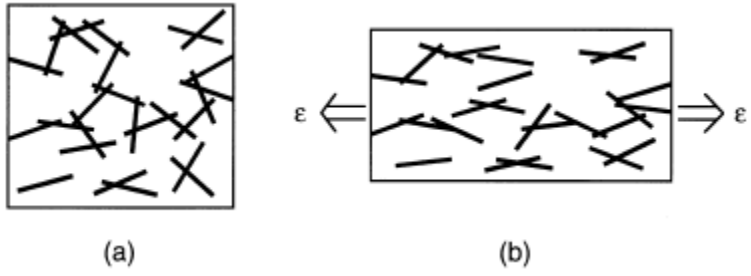
(a)   (b)

(a) Percolating, electrically conductive prior to straining
(b) Non percolating, electrically non- conductive after straining

The critical conductor volume fraction (f*) is generally between 10 to 20% volume ratio of the flakes, depending upon the particle size [104, 105, 106] and the f* increases in proportion to the strain exerted on the circuit [103]. The modeling exercise carried in the paper by Taya et al studies the behavior of a nickel coated graphite conductive on rubber substrate.

Roberson et al [107] have undertaken extensive SEM analyses to demonstrate that ink microstructures containing large flake sizes exhibit higher conductivity and lesser porosity. Other studies [108, 109] have also shown similar results. The microstructures are dependent on the thermal processing of the conductive ink and sometimes the microstructures could be improved by printing a double ink layer prior to curing [107]. Other factors effecting sintering is surface diffusion which is dependent upon the contact points available between adjacent particles [110]. The work carried out by Robertson et al used non stretchable substrates and inks.

Saraf et al [111] in their paper discuss the desired qualities of a conductive paste for fine line printing (around 200 microns) and high electrical conductivity (around 20 micro ohms per centimeter), to be used as a conductive interconnect for a multichip module (MCM) type process. The conductive ink designed consisted of a thermoplastic polymer, solvent and silver flakes at a diameter of 5 microns. They recommend that the rheological properties play an important role in obtaining fine resolution printing. It should be mentioned that the silver conductive ink used for this project was a non-stretchable ink.

Jahanshahi et al [85] point out that the factors affecting the reliability of a copper conductive trace patterned on a substrate and laminated between plastic foils are the Young's modulus of the substrate, the thickness of the substrate, the width of the substrate compared to the width of the copper trace and the composition of the copper trace.

Hsu et al [84] point out that there are at least two different methods for defining stretchability of a stretchable substrate. One would be based on the electrical resistance where a stretchable system could be stretched up to a point where an electrical failure is observed because of metal rupture. The second would be the limit where the circuit starts failing due to other reasons like metal delamination from the substrate. Others have suggested that a stretchable system may be deemed failing once the electrical resistance upon stressing has reached a preset limit, like thirty times the resistance of the original stress- free state.

4.3 Methodology

The research objective for this section is the development of screen printable conductive inks, which could be stretched by at least 20% of the original length without exhibiting any mechanical or electrical failures and while keeping the increase in resistance to lower than 30X of the original resistance. The approach used to obtain the research goal was to evaluate available inks and study the failure mechanisms during stretching and offer recommendations to improve the performance and reliability of the conductive ink. Equipped with this insight, new generations of inks were developed until a satisfactorily stretchable conductive ink was achieved. Multiple generations of the stretchable ink were formulated and the following methodology was successfully employed. (Table # 3).
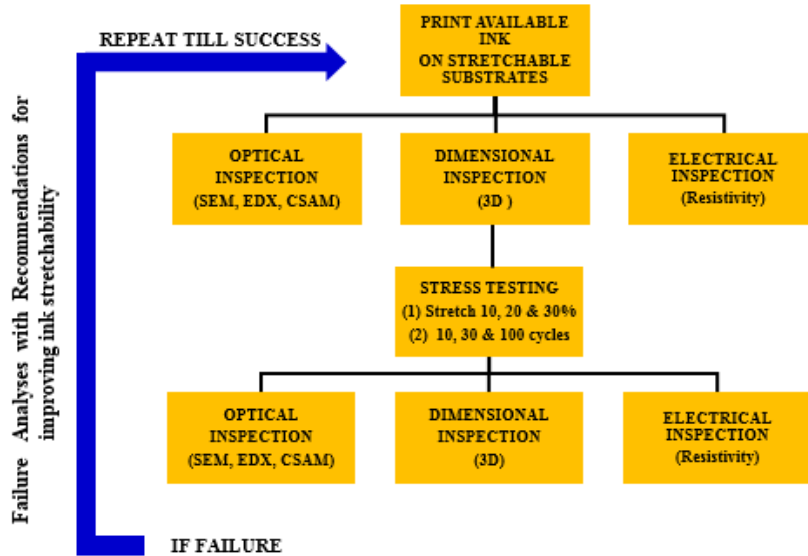
TABLE # 3: Stretchable Conductive Ink Development Flowchart

4.4 Sample Preparation

This section describes the process by which the experimental samples were obtained. The first phase undertaken was the down-selecting phase. Instead of testing many different types of materials for long hours, various substrates, conductive inks, ink curing approaches and screen printing processes were subjected to an evaluation process to filter down the most promising candidates. It was discovered during this process that the comparative stretchability performance of the system could be determined early enough by straining the system uni-axially by 20% and perform in situ resistivity measurement during the first 30 cycles.

After evaluating different types of substrates like polyethylene terephthalate (PET), polyimide (PI), poly dimethyl siloxane (PDMS), polycarbonate (PC), polyethers (PE) and thermoplastic polyurethane (TPU) substrates, it was decided to use TPU stretchable substrates from American Polyfilm because they were very stretchable (more than 100 % and in some case as much as 400%), they were suitable for screen printing and they were able to handle the thermal curing temperatures required for curing the available stretchable conductive inks (around 130 C for 20 minutes). Additionally, TPU substrates like the Bemis ET 315 show a stretch hysteresis effect of less than 1% when the substrate was relaxed after stretching 100 percent. It is also printable, can be cured as high as 165 C and is also washable up to 40 cycles. TPU substrates from both American Polyfilm (AP) and Bemis were selected as final candidates for substrates for the sample development of the multiple generations of conductive inks.

Various available stretchable and screen printable conductive inks were obtained and screen printed on different types of TPU substrates. After the parts were cured following the manufacturer's curing recommendation the parts underwent some stretch testing (up to 20% stress for 30 cycles). More than 90% of the conductive inks tested failed within 10 stretch cycles. The best performing ink, DP 178X, was chosen as the first generation (Gen 1) stretchable conductive ink material.

The Gen 1 ink was printed on TPU substrates from AP and Bemis. Based upon the learnings from the failure analyses studies of the Gen 1 ink, recommendations were constantly shared for the development of the next generation ink. After few attempts, this finally led to the development of Gen 2 ink (N 6301X). The Gen 2 ink was also printed on TPU substrates from AP and Bemis and underwent the detailed methodology depicted in Table # 3.

For all generations of ink, the following processes were performed sequentially:

(A) The substrate was plasma cleaned (Fig 22) with Argon to enhance the adhesion of the conductive ink to the substrate.
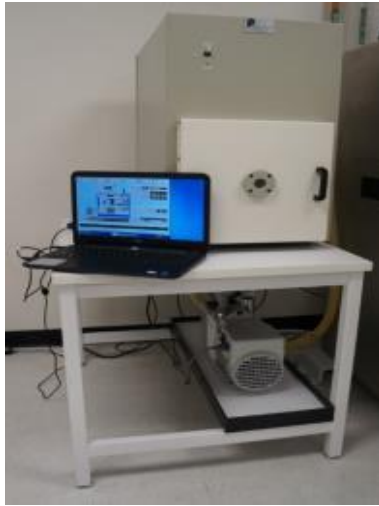
FIGURE # 22: Plasma Etching Machine-Model PE 100

(B) The parts were printed using a screen printing process using a screen that was made from stainless steel wires using a 400 mesh screen with the wires attached in a 45-degree angle. A special screen pattern was developed to evaluate printing of stretchable conductive inks. The following screen patterns (Fig 23) and printing test vehicles (Fig 24) were some of the patterns developed for the study and development of stretchable conductive inks.
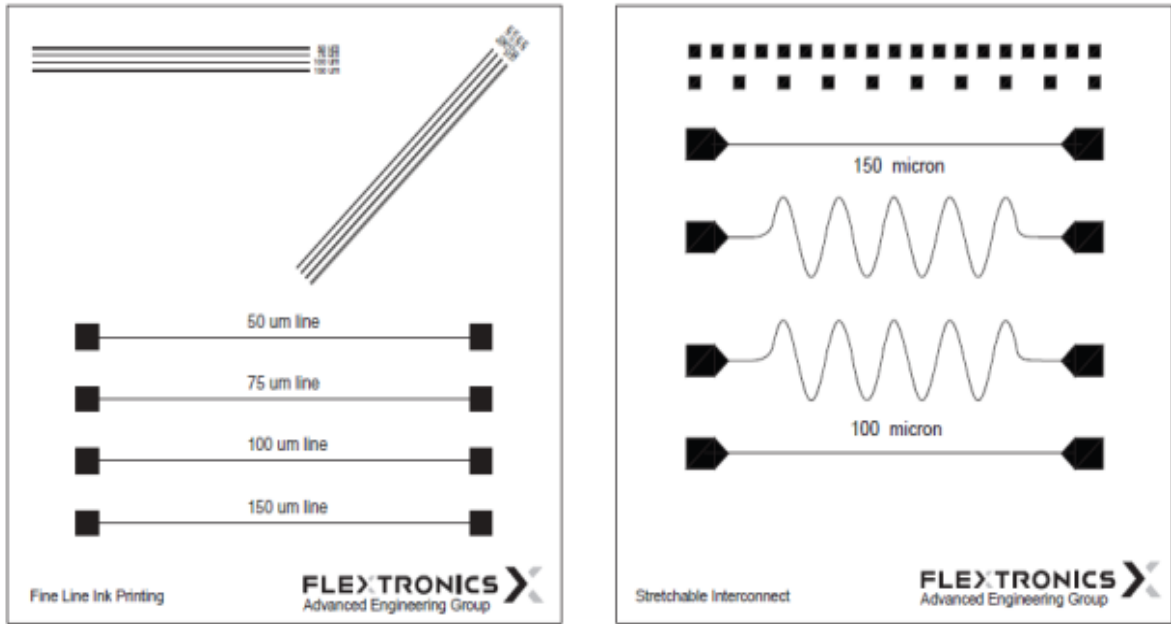
Figure # 23: Screen patterns developed for current research

Printed Conductive Ink Test Vehicle
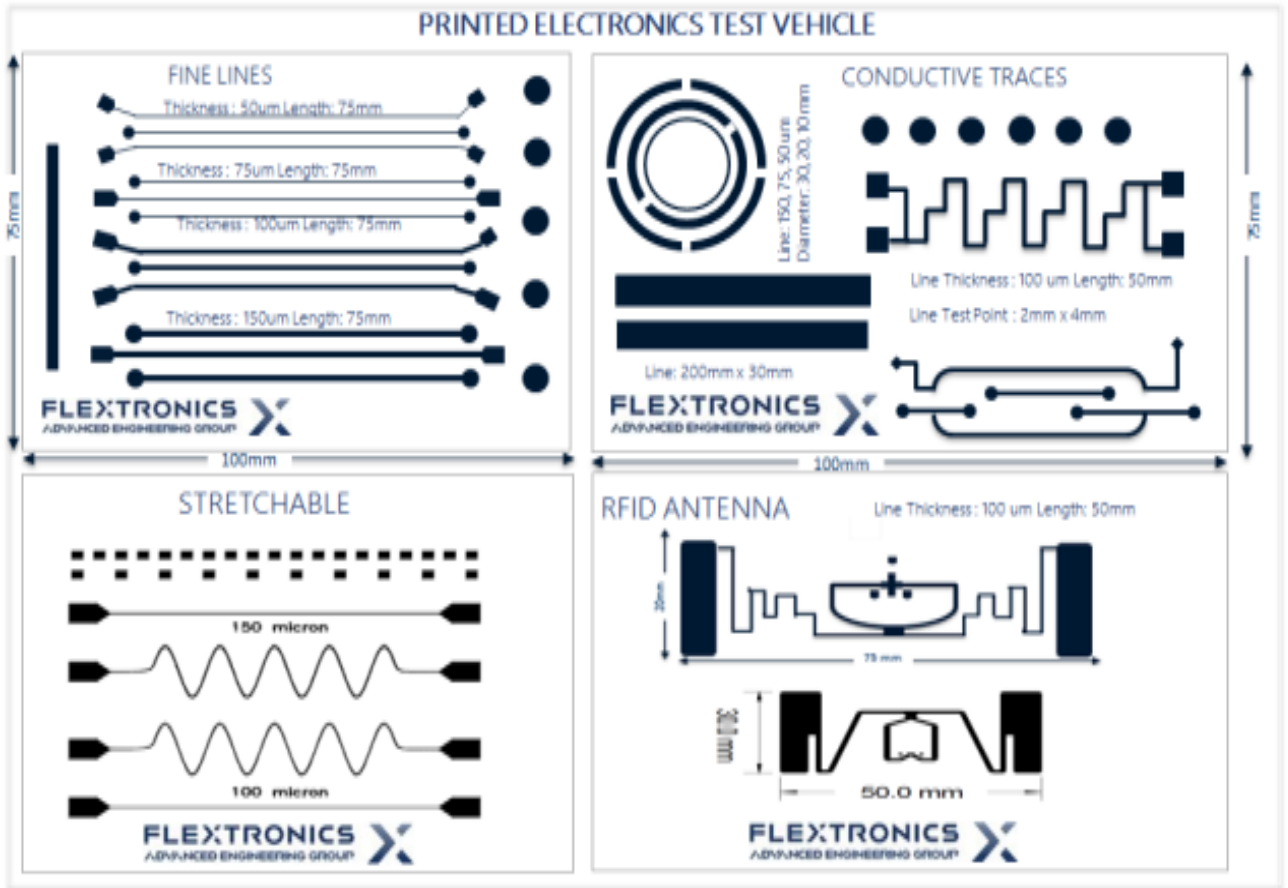
Figure # 24: Printing Test Vehicles developed for current research

The screen printing equipment used was ATMA 45PA (Fig 25) and the DEK model number LPiX (Fig 26). The ATMA was not used in the development of any fine line printing because the DEK machine has better capabilities for fine printing.

Figure # 25: ATMA Printer- Model # AT 45PA   Figure # 26: DEK Printer- Model # LPiX with attached screen

(C) The printed conductive ink was cured using an ambient air oven (Fig 27) heated at 120 C for 20 minutes. The oven was made by Despatch and the model # is Loc1.

Figure # 27: DESPATCH Batch Oven- Model # LOC1

(D) The parts were individually labeled and inspected using Scanning Electron Microscope (SEM), Energy Dispersive X Ray (EDX) (Fig 28) and Confocal Scanning Acoustic Microscopy (CSAM) (Fig 29) techniques. The parts also underwent a 3D (Fig 30) camera inspection to measure the ink width, ink- height and surface roughness. Lastly, the parts were electrically measured and the normalized resistivity recorded.

Figure # 28: JEOL SEM & EDX Machine
Model # JSM-6010 LV
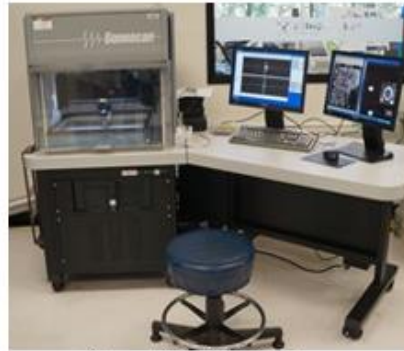
Figure # 29: CSAM Machine
Model # D9500
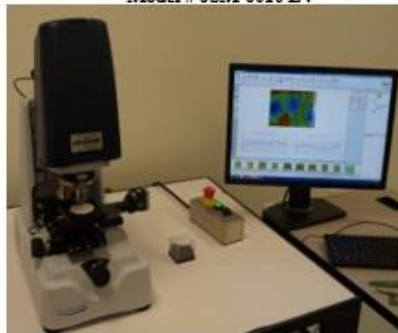
Figure # 30: 3D Camera
Model # Bruker 3D

Figure # 31: Dage Instron
Model 4000 plus

(E) The next few steps involved the cyclical stretching reliability studies. The parts were first stretched using a Dage Instron (Fig 31) machine at 10, 20 or 30% strain levels. The strain was applied at a constant speed of 0.1 mm/sec. The parts were relaxed after each strain cycle and the resistivity was measured in situ in the stretched state and the relaxed state. The stretch data was obtained for 10, 30 or 100 cycles, depending upon the failure point of the ink.

(F) The stretched parts were once again inspected using SEM, EDX and CSAM techniques. They also underwent a 3D (Fig 30) camera inspection to measure key parameters like ink width, ink- height and surface roughness.

(G) A failure analyses review was undertaken and reports were developed to offer suggestions to help improve the stretchability performance of the ink.

4.5 Stretch Testing Reliability Results

As mentioned earlier, the first Gen 1 ink was the best available ink when this study was started and after developing multiple generations of ink, Gen 2 ink was finally obtained with a satisfactory stretchability behavior. This section reviews the comparative stretchability performance between Gen 1 and Gen 2 ink, showing the superior stretchability performance of the Gen 2 ink.

(A) Gen 1and 2 Ink: Two generation of samples (Fig. 32)
(B) Gen 1 and 2 sample line width and height (Fig. 33)
(C) Resistivity Calculations of Gen 1 and Gen 2 Inks (Fig. 34)
(D) Stress Comparisons- Gen 1 & Gen 2 at 58% Strain (Fig. 35).
(E) Stress Comparisons up to 100% Strain: Gen 1 and Gen 2 Ink (Fig. 36)
(F) Gen 1&2 Ink at 60 % Strain compared to an ideal ink (Fig. 37)
(G) Gen 2 Ink stretched 1000 Cycles at 20% Strain (Fig. 38)
(H) Gen 1 and Gen 2 inks comparison at 1000 cycles at 20% (Fig. 39)
(I) Stretchability Testing to Failure under Increasing Load (Fig. 40)
(J) Stretchability and Compatibility of the Developed Dielectric Ink (Fig. 41)

Gen 1 samples use DP 178X ink printed on AP and Bemis polyurethane samples whereas Gen 2 samples use N 6301X ink printed on AP and Bemis substrates (Fig 32). Gen 2 ink was developed after inputs and insights obtained from failure analyses and reliability studies of multiple generations of the inks generated by this research. The recommendations developed for improving the stretchability of Gen 2 ink are covered in Section 4.8.

Generation 1 and 2 Samples

Generation1:
DP178X Ink, AP Substrate
Substrate Thickness: A ~0.27 mm; B ~0.18 mm

Generation1:
DP 178X Ink, Bemis Substrate
Substrate Thickness: ~ 0.06 mm

Generation2:
N 6301X Ink
AP Substrate
Substrate Thickness: A ~0.27 mm

Generation 2:
N 6301X Ink
Bemis Substrate
Substrate Thickness: ~.06 mm
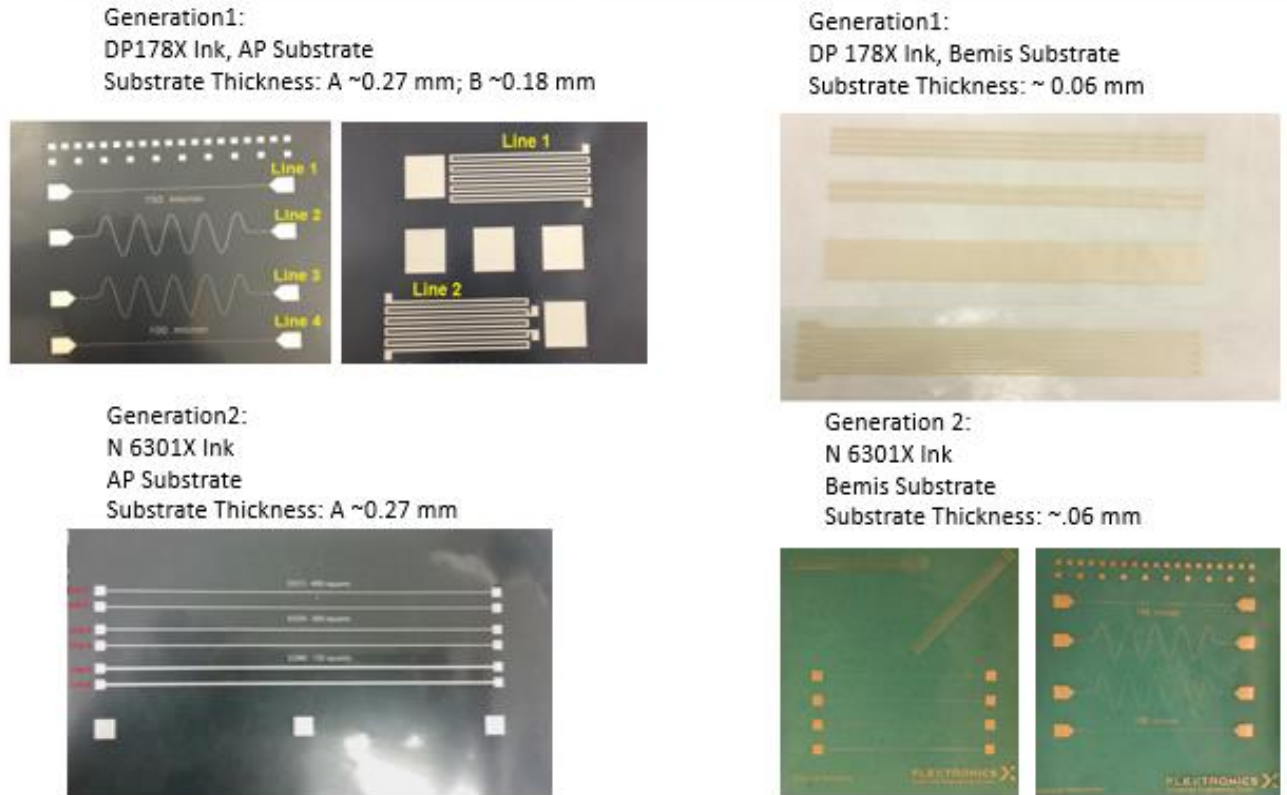
Figure # 32: Gen 1 and Gen 2 Ink: Two Generations of Samples

Different types of screen patterns were developed to study various ink characteristics like the stretchability of the conductive ink, the printability of fine line features and for comparing the stretchability between a sinusoidal pattern and a straight line. As discussed later even more screen patterns were used than the types shown above in Figure 32. To have a better understanding of the resistivity, it was necessary to measure the line width and height of the cured ink using 3D cameras. This enabled to obtain the normalized resistivity of the cured ink during the relaxed and stretched state (Fig 30). Gen 1 ink has a resistivity range 1.08E-06 to 1.82E-06 ohms/m and Gen 2 ink has a resistivity range of 2.25E-07 to 6.58E-07 ohms/m (Fig 31). In comparison pure silver has a resistivity of 1.59E-08 ohms/m. The Gen 2 ink exhibits better conductivity but a wider spread.

Line Width and Thickness – Gen 1 vs. Gen 2

Gen 1
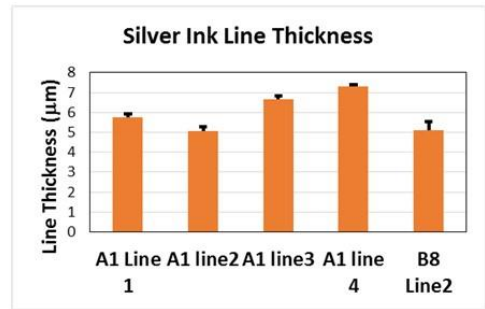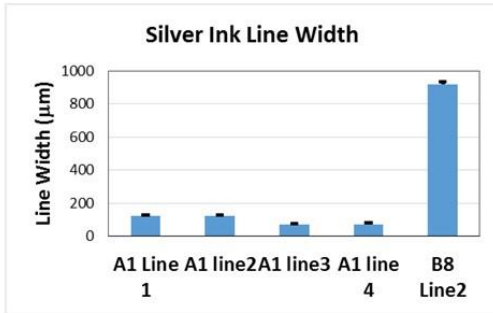
Gen 2
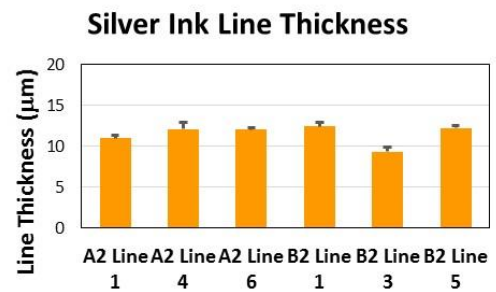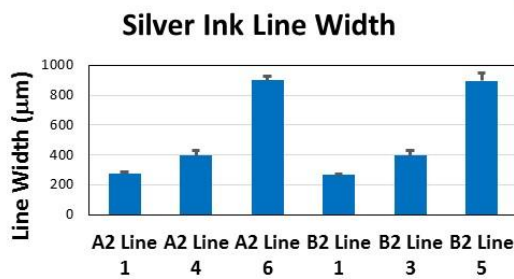
Figure # 33: Line Width & Thickness of Gen 1 and Gen 2 Inks

Resistivity Calculations - Generation 1&2

Gen1 Resistivity: 1.08E–06– 1.82E–06 Ohms.m
Resistivity of Silver is: 1.59E–08 Ohms.m

Resistivity: $\rho = R\frac{A}{\ell}$, R is the resistance, A is the cross section area, l is the length
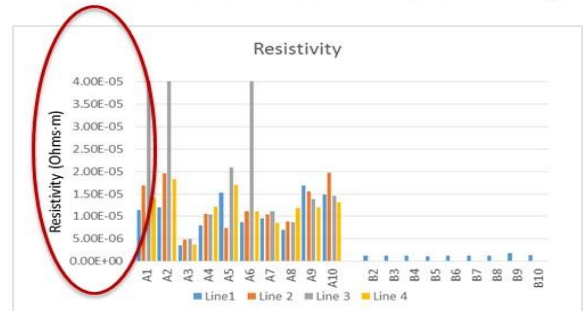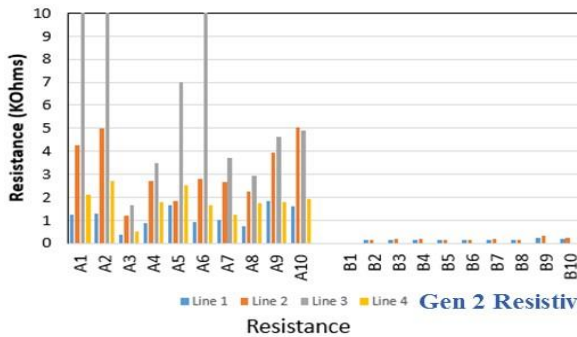
Gen 2 Resistivity: 2.25E–07–6.58E–07 Ohms.m
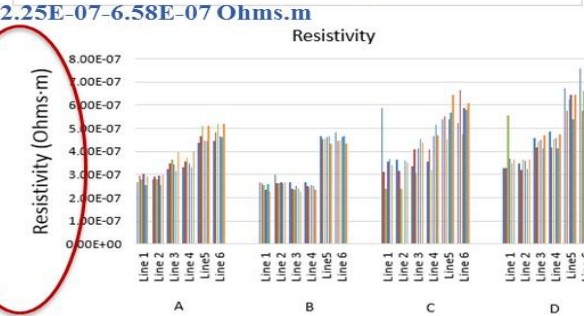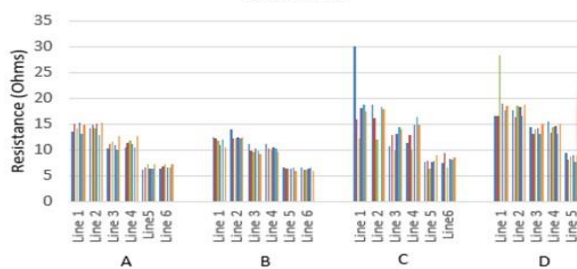
Figure # 34: Resistivity Calculations of Gen 1 and Gen 2 Inks

46

The ink samples were hooked on to the Dage Instron machine where the resistance of the cured ink was monitored in situ as the samples were being stretched and relaxed continuously at the rate of 0.1mm per second. In Figure 35 we see that the Gen 1 ink sample increased in resistance from 3.6 ohms to 1467 ohms, an increase of over 400 times, upon being stretched gradually at the rate of 0.1mm/sec to 58% strain with most of the jump occurring after 50% strain. The Gen 2 ink sample increases from 2.1 ohms to 59 ohms upon being stretched gradually at the rate of 0.1mm/sec to 58% strain, showing an increase of 28 times. The rate of increase in resistance is comparatively slower and gradual in the Generation 2 ink. In the graph on Figure 36 we see the Generation 2 ink being stretched gradually at the rate of 0.5mm/sec to 100% strain and compressed back at the same rate to 0% strain. The ink maintains electrical connectivity even after a strain of 100% but the resistance increases from 2.1 ohms to ~ 825 ohms at 100% strain and back to 2.4 ohms at 0% strain, which was very close to the original resistance of 2.1 ohms. In all of the three cases above AP VLM 3301 substrates were used and the substrate thickness was ~.28 microns.

Figure # 35: Stress Comparisons- Gen 1 & Gen 2 at 58% Strain

Gen 1 & Gen 2 Stretch Comparisons: Strain

Gen 1 Ink under 58 % Strain

Resistance versus Strain Curve

Gen 1 ink could only survive 58% strain

Gen 2 Ink under 100 % Strain

Resistance versus Strain Curve

Gen 2 was able to survive 100 % strain
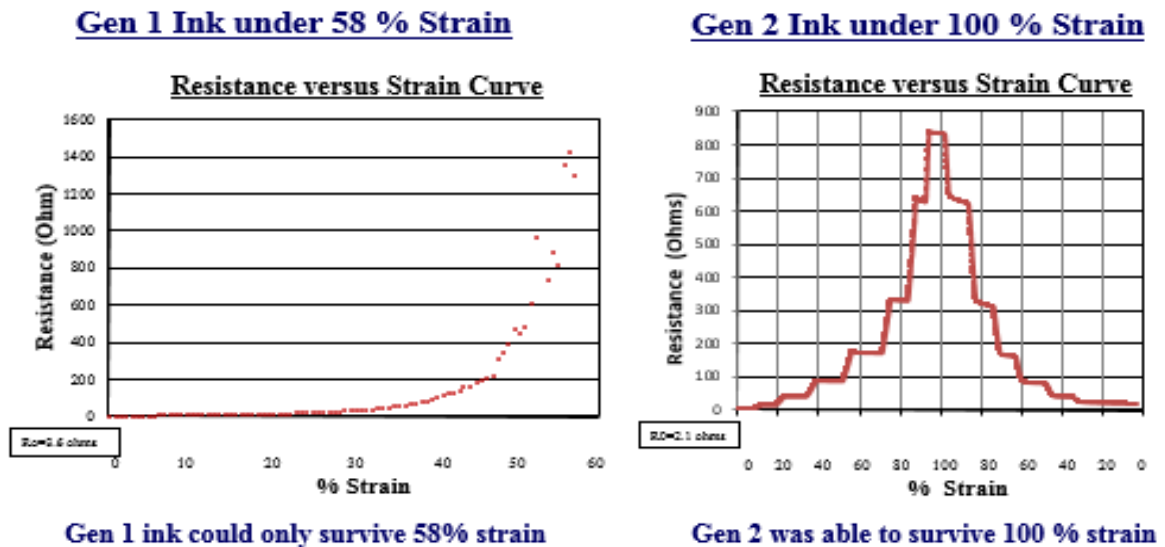
Figure # 36: Stress Comparisons up to 100% Strain: Gen 1 and Gen 2 Ink

Having determined that the Gen 2 ink performed much better than the Gen 1 ink, some experiments were carried out on the Gen 2 ink to understand the effect of the substrate thickness on hysteresis. The samples were exposed to a strain of 10% for 30 cycles accompanied with an in situ measurement of the change in resistivity. The 1.5 mil thick substrate increased in resistance about 7 times and the 7 mil thick substrate increased in resistance about 6 times after 30 cycles at 10% strain. The zero stretch reading for each of the 30 cycles was measured showed a gradual increase in each cycle. For the 1.5 mil thick substrate, it eventually returned to the original zero stress reading after a wait of 2000 seconds without stress It was interesting to note that for the 7.0 mil thick substrate, even after 4000 seconds without stress, the zero stress reading was not close to the starting point. This meant that some substrates display better hysteresis performance than others and it is possible that the substrate thickness was playing a role. After trying various experiments, it was determined that the Bemis TPU substrates displayed > 99 % recovery and were better than American Polyfilm TPU substrates for hysteresis performance, for substrates with the same thickness.

An ideal stretchable conductor would behave such that the stretched resistance value would be predictable according to the following equation # 4 [103]. Assuming that we have a continuous printed film where the volume of the film does not change before and during stretching. If Lo is the original length of the film and L is the final length of

the film and assuming there is no change in resistivity during stretching, in other words, assuming an ideal stretchable conductor then we would have:

$$R/R_0 = (L/L_0)^2 \longrightarrow R/R_0 = (1+\varepsilon)^2 \qquad \boxed{\text{..........EQUATION \# 4}}$$

Where Ro is the initial resistance and R is the final resistance. In Figure 37 we see the resistivity behavior of Gen1 and Gen 2 ink compared to an ideal stretchable conductor, for a single cycle strain up to 67%. We see that the Gen 1 ink has the resistivity jumping up around 40% strain and the Gen 2 ink depicts a much more tempered increase up to 50% strain. The black line in the chart of Figure 34 is the predicted behavior of an ideal stretchable conductive ink.

Gen 1 and Gen 2 Ink Stretch Test : Single Cycle ~ 60% Strain

Assuming no change in volume and resistivity of the conductive ink.
Assume increase in length (more resistance) and a decrease (more resistance) in width.
The black line is the behavior of an ideal stretchable ink which does not change its resistivity.

Change in Resistance (R/Ro) with Strain

The rate of increase in resistance is faster in Gen1 than Gen 2
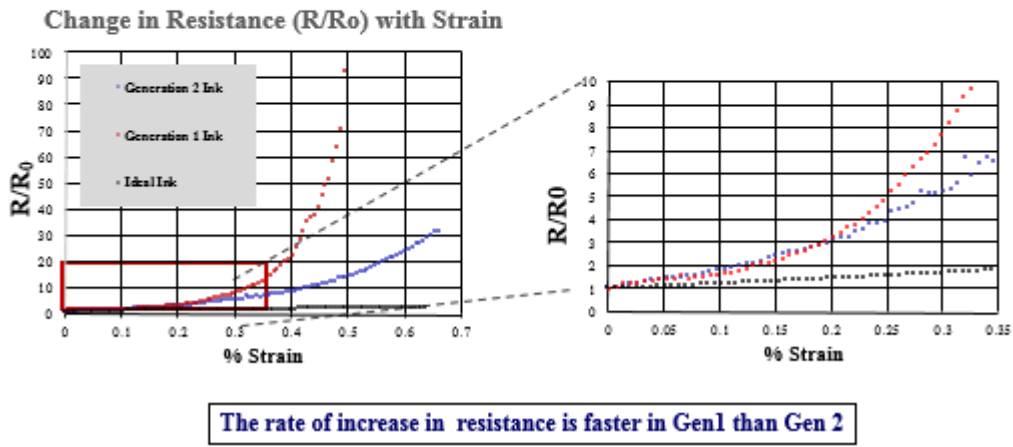
Figure # 37: Gen 1&2 Ink at 60 % Strain compared to an Ideal Ink

The next experiment was to determine what happens to the conductivity of the Gen 1 and Gen 2 ink after they have been stretched to hundreds of cycles at 20% strain. When the Gen 2 Ink was exposed to 1000 cycles of stretch at 20 % strain the results showed that it displayed good conductivity up to 750 cycles (Fig. 38). Beyond 750 cycles the resistivity started increasing unpredictably. Comparative results also show that the Gen 1 ink was no longer conductive after only 30 cycles (Fig. 39). The failure in both the

inks was due to the ink delaminating from the substrate. No evidence was seen for metal rupture. Even though the performance of Gen 2 ink is significantly better than the performance of the generation 1ink, it will still need to be developed further. This would be a good area of research for future investigation. Enhanced polymer chemistries used for the ink binders that can handle multiple stress cycles would need to be developed. Future wearable technology products would demand good electrical connections for at least 2000 stretch cycles at 20% strain.
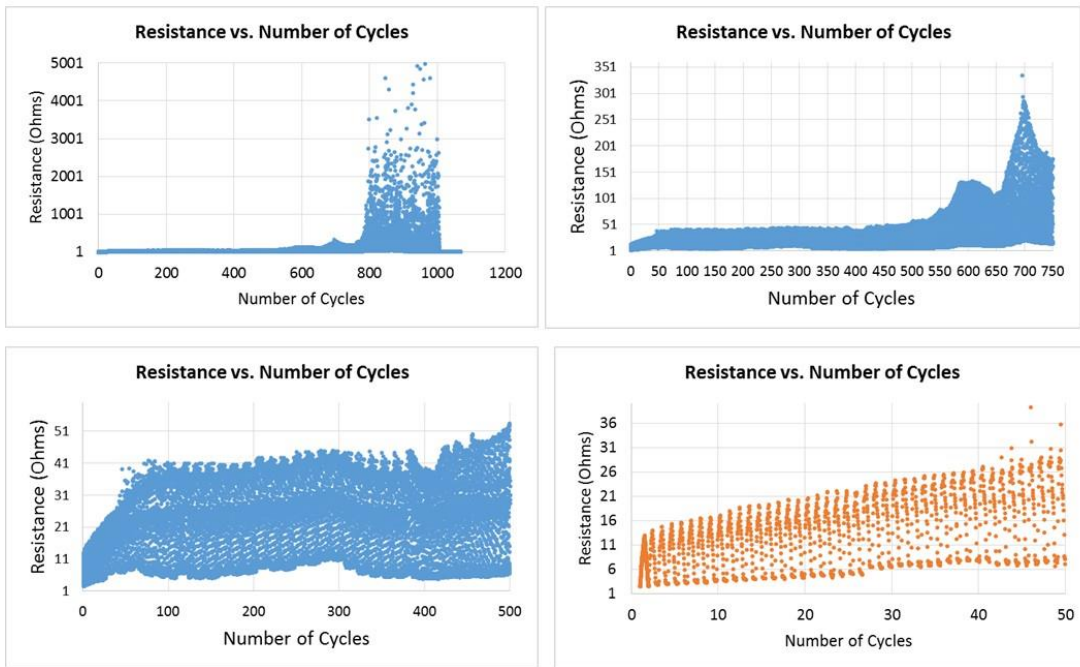
Figure # 38 A: Gen 2 Ink stretched 1000 Cycles at 20% Strain
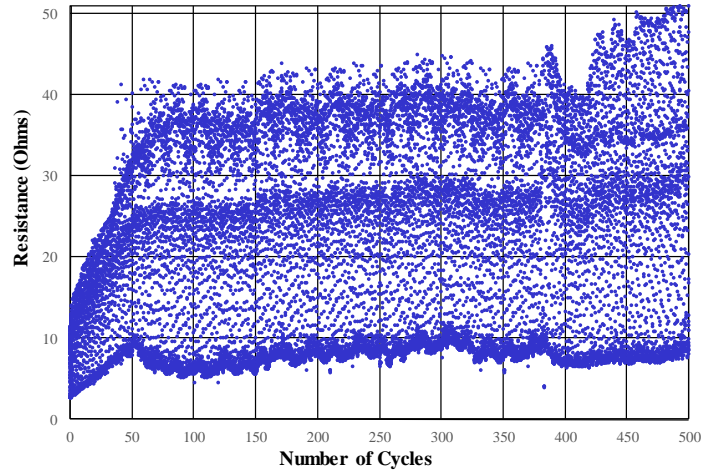
Figure # 38 B: Closer View: Gen 2 Ink after 500 cycles at 20% strain showing a starting resistance of 2.6 ohms and a final resistance of 50.9 ohms after 500 cycles
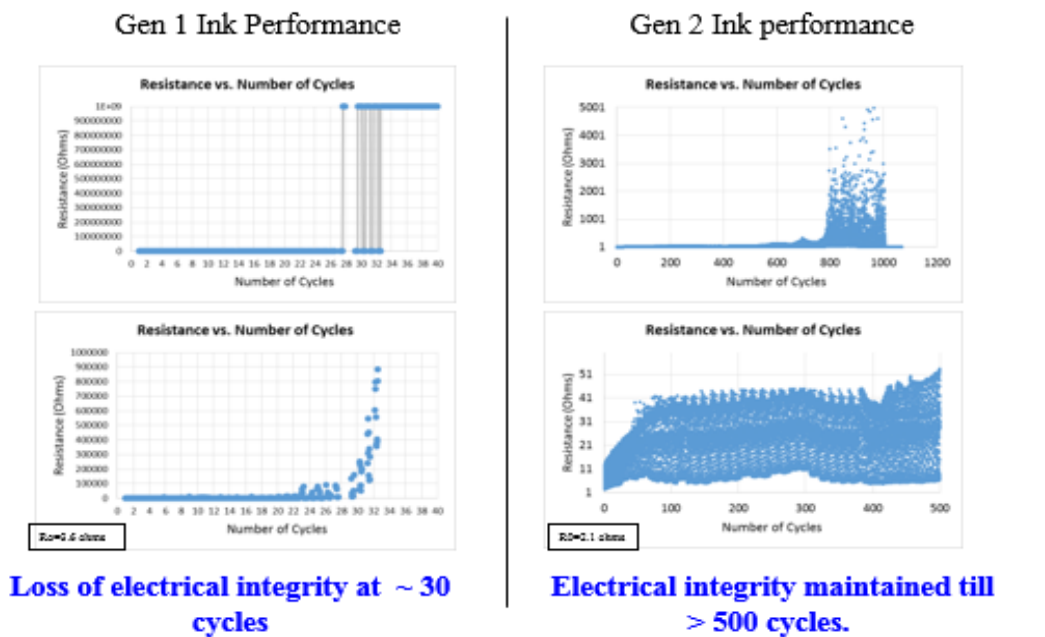
Figure # 39: Gen 1 and Gen 2 inks comparison at 1000 cycles at 20%

Another set of experiments were run to understand the failure point of the Gen 2 ink under increasing strain load. This was to understand the effect of fatigue as a possible cause of failure. The failure point for these experiments was deemed as the point when the original resistance at zero stress increases to more than 30 times the initial resistance, Figure 40 below shows that as the load increases the quicker does the ink succumbs to failure.

Cycles to Failure
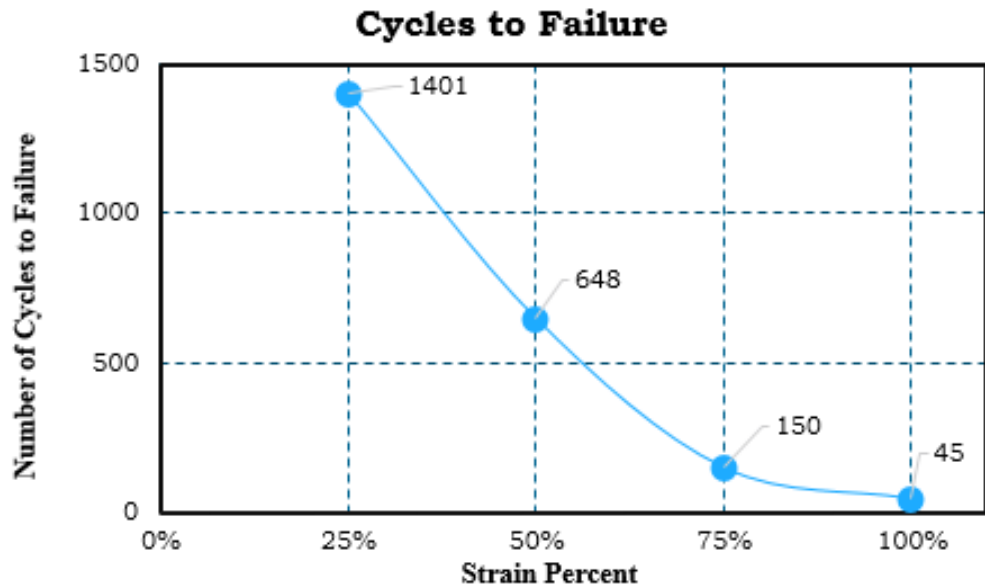
Failure was deemed when the resistance reached 30 X the original resistance at no stress

Figure # 40: Stretchability Testing to Failure under Increasing Load

For Gen 2 ink to be a valuable interconnect tool for circuit development it needs to have the capability for complex multilayer circuitry. Using the same basic binder chemistry and without using the silver flakes, a stretchable dielectric was developed to enable the development of stretchable capacitors and stretchable multi metal layer circuitry, as shown in the drawing below.
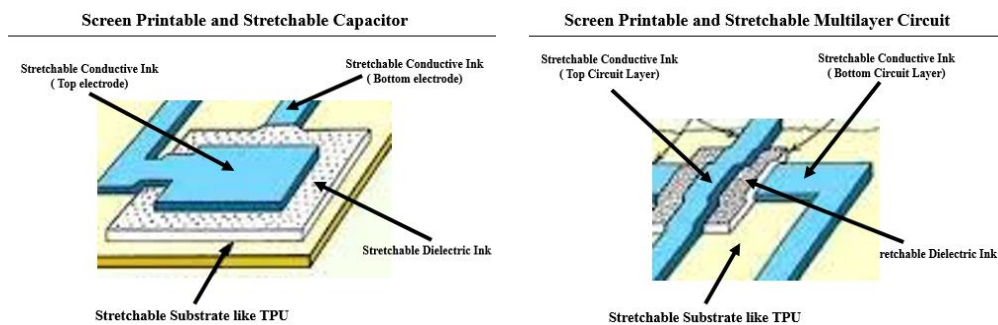
Figure # 41 shows that the stretchability of the developed dielectric layer is acceptable and compatible with the stretchable conductive ink. They are both stretchable because they contain elastomeric chain polymers for the binder system along with the normal screen printing binder. Both inks could be cured using similar curing temperatures because they contain similar organic solvents. Finally, both the inks are also screen printable, since they possess an essentially similar Non-Newtonian, thixotropic rheology (Fig 42), where the viscosity decreases when any shear is applied.

Gen 2 Stretch Test: With and Without Stretchable Dielectric Layer

Impact on Resistance as Substrate is Stretched (No Dielectric Layer)
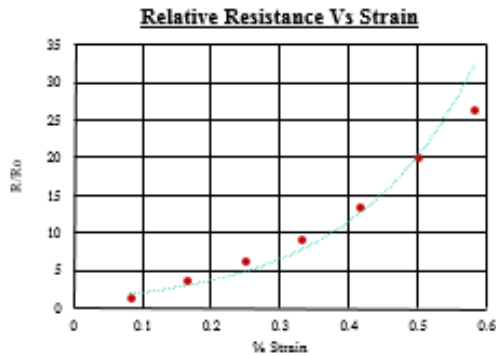
Impact on Resistance as Substrate is Stretched (With Dielectric Layer)
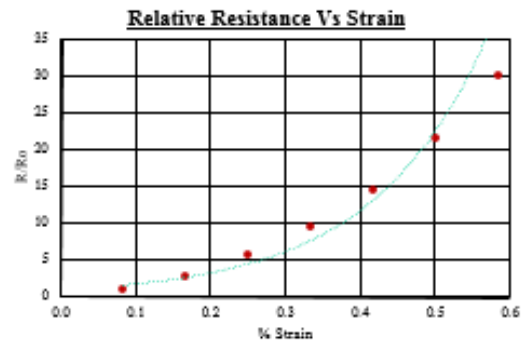
- Dielectric layer is stretchable and compatible with the conductive ink, does not impede stretchability
- Dielectric layer increase the resistance slightly and can serve as an encapsulant and enable multilayer circuitry and stretchable capacitors

Figure # 41: Stretchability and Compatibility of the Developed Dielectric Ink

STRESS VERSUS STRAIN RHEOLOGY CURVE FOR STRETCHABLE AND SCREEN PRINTABLE CONDUCTIVE AND DIELECTRIC

STRETCHABLE CONDUCTIVE CURVE,
~ 85% SILVER FLAKES,
NON-NEWTONIAN, THIXOTROPIC

STRETCHABLE DIELECTRIC CURVE,
NO SILVER FLAKES,
NON-NEWTONIAN, THIXOTROPIC
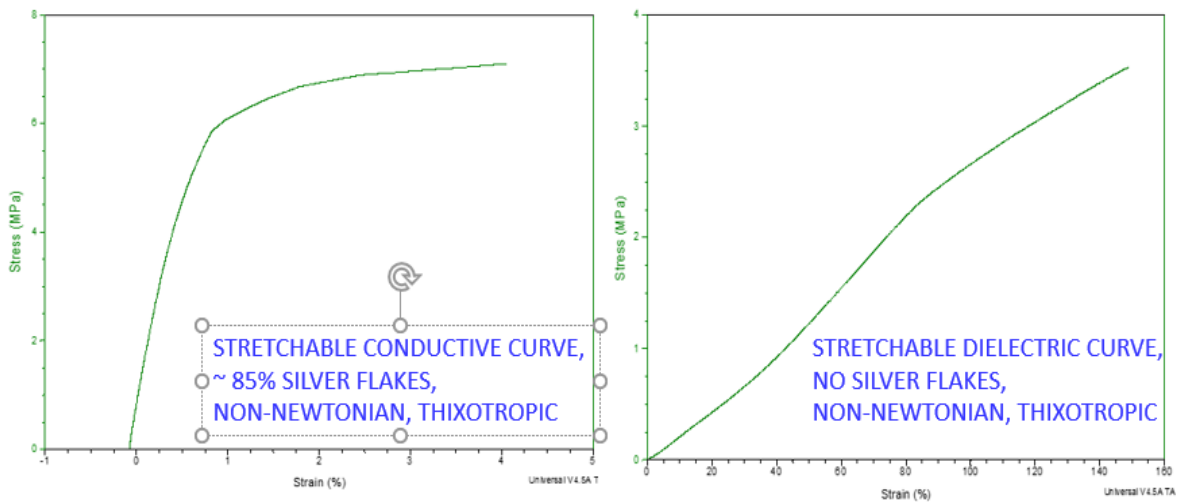
Figure # 42: Rheology Curves for the Stretchable Conductive and Dielectric Ink

4.6 Failure Analyses: SEM/EDX/CSAM/3D

Failure analysis studies played an important role in the current research focusing upon the development of stretchable conductive ink. The approach to develop better stretchable inks was centered on undertaking failure analyses studies to understand the failure mechanisms of the existing material and offering recommendations for the development of the next generation of stretchable inks. In this section is reviewed the various SEM, EDX, CSAM and 3D analyses undertaken and how it led to the development of recommendations for the next generation inks.

4.6.1   SEM Analyses

The top view SEM analyses of DP 178X ink (Gen 1 ink) and the N 6301X ink (Gen 2 ink) revealed that the silver flakes in Gen 1 ink are more densely packed than the Gen 2 ink. It also shows that Gen 1 ink has a tighter distribution of the particle size of the silver flakes ranging from 0.5-8 microns, whereas Gen 2 ink has a wider distribution from 0.5-20 microns (Fig 43).
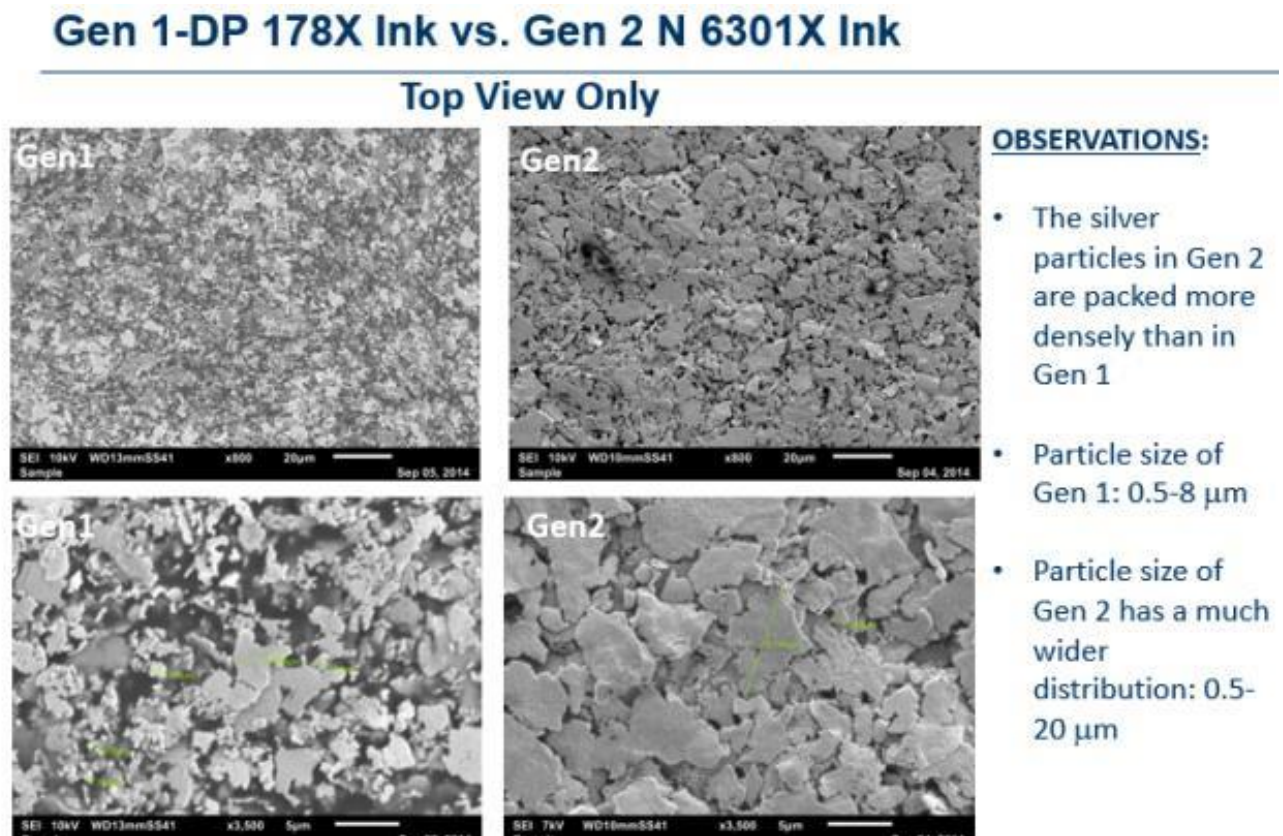
Figure # 43: Gen 1 & Gen 2 SEM Analyses   Top View Only

The particle size readings from the top view were verified with a cross sectional reading which confirmed that Gen 1 ink has a distribution of 0.5-8 microns (Fig 43). The thickness of the silver flakes was measured around 1 to 2 microns for both the Gen 1 and Gen 2 ink (Fig 43 and 44). The silver flakes are aligned parallel to the print direction.
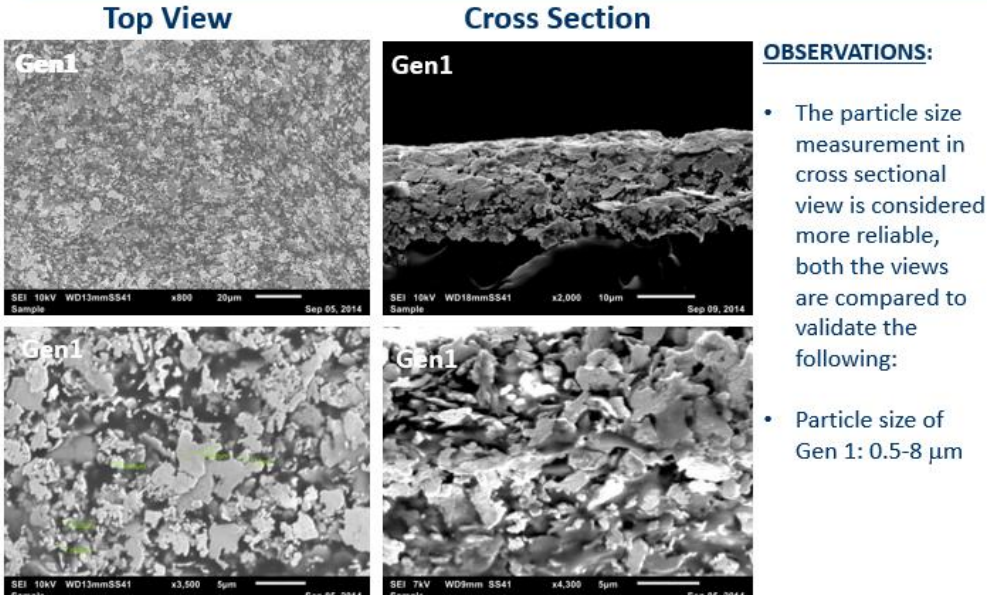
Figure # 44: Gen 1 SEM Analyses   Top & Cross Sectional View

Similar cross sectional SEM analyses with the Gen 2 ink revealed that the particle size readings have a distribution range of 0.5-15 microns (cross sectional view) and of 0.5-20 microns for top view (Fig 45). Because of the higher packing density and larger particle size of the flakes in the Gen 2 ink samples, it makes sense that we see a higher conductivity of Gen 2 samples.

Gen 2-N6301X Ink: Top view & Cross Sections Comparisons

Top View

Cross Section

OBSERVATIONS:

- The particle size measurement in cross sectional view is considered more reliable, both the views are compared to validate the following:

- Particle size of Gen 2 is determined to be in the range of 0.5 -15 µm
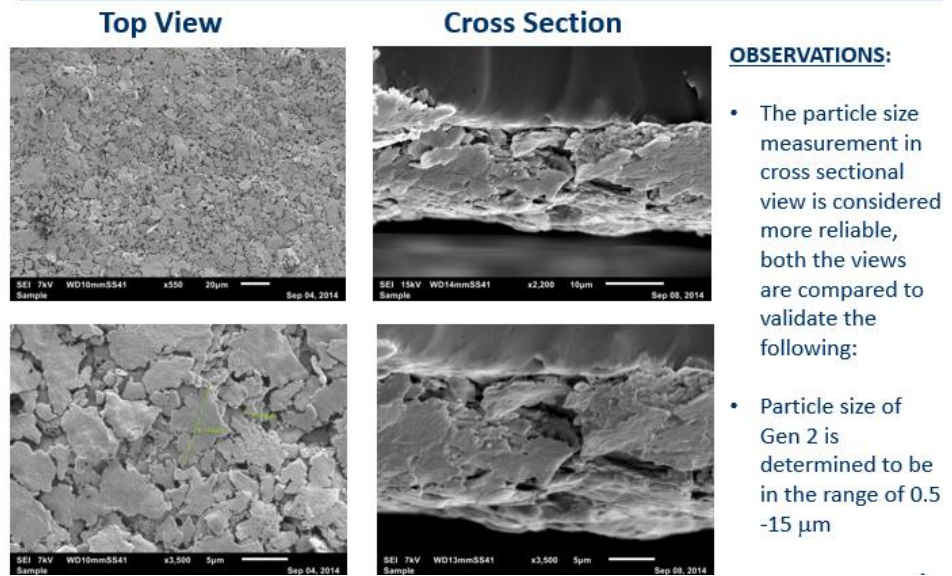
Figure # 45: Gen 2 SEM Analyses   Top & Cross Sectional View

Comparative SEM images are very helpful in determining failure analyses and understanding ink behavior. In Figure 46 we have comparative SEM images of the Gen 1 and Gen 2 ink after they have undergone 500 cycles of stretch under 20% strain. In Figure 46 we observe that the silver flakes in the generation 1 ink are more homogenous. The dark areas are the regions where we do not see any silver flake or the polymer binder and we are looking at the TPU substrate. We see more of the substrates in the generation 1 ink denoting there are more cracks. The generation 2 ink is more heterogeneous and depicts much lesser dark areas denoting comparatively lesser cracks and better conductivity.

SEM image Comparison after 500 cycles at 20% strain
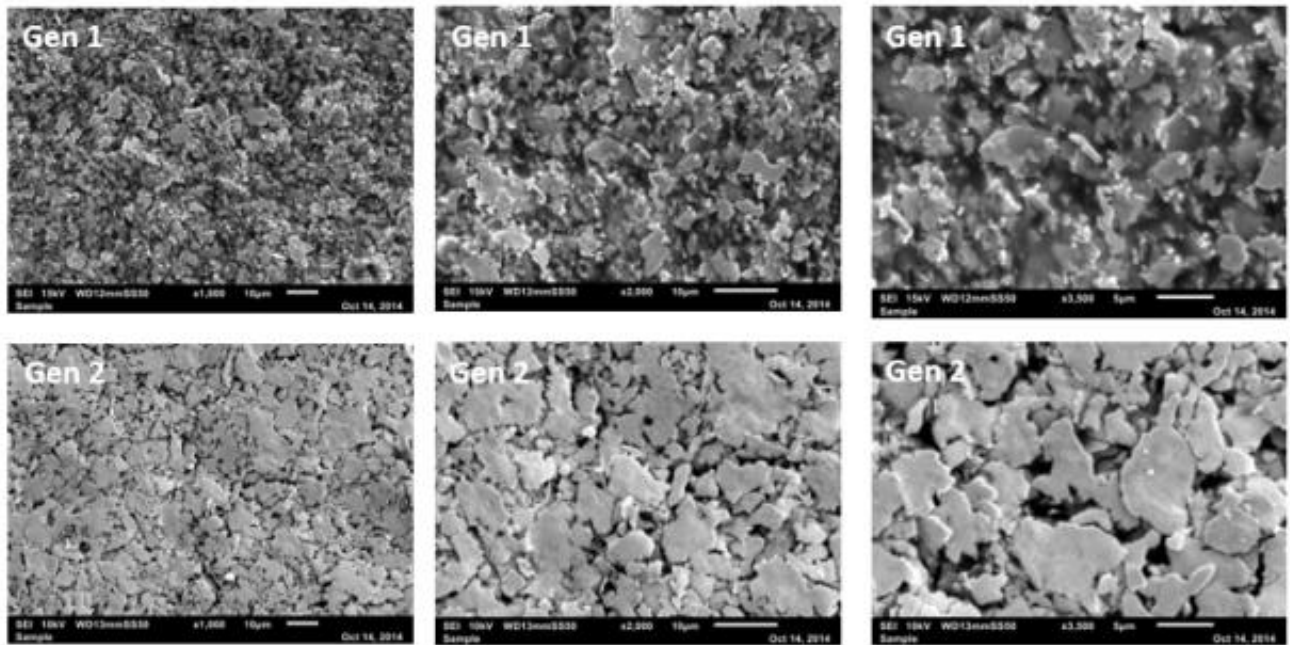
Observations:
Gen 1 Ink: More homogeneity in silver flakes, more dark spaces denoting more substrate area and cracks
Gen 2 Ink: Less homogenous silver flake distribution, less dark spaces denoting less substrate area and cracks

Figure # 46: Gen 1 & Gen 2 Ink Comparative SEM Analyses after 500 cycles at 20% strain

In Figure 47 we have comparative SEM images of the Gen 1 and Gen 2 ink at 50% and 100% strain. We observe that as the strain increases we see more cracks on the conductive inks as expected. We also note that the nucleation of the silver flakes in the generation 2 ink is much better clustered allowing better conductivity. This is believed to be because of the designed bimodal distribution of the silver flakes in the generation 2 ink allowing more contact points and better surface diffusion.

SEM Images : Gen 1 and Gen 2 Ink at 50% and 100% strain

S1=Stretching of Gen 1 ink at 50% and 100% strain
S2= Stretching of Gen 2 Ink at 50% and 100% strain

Top view
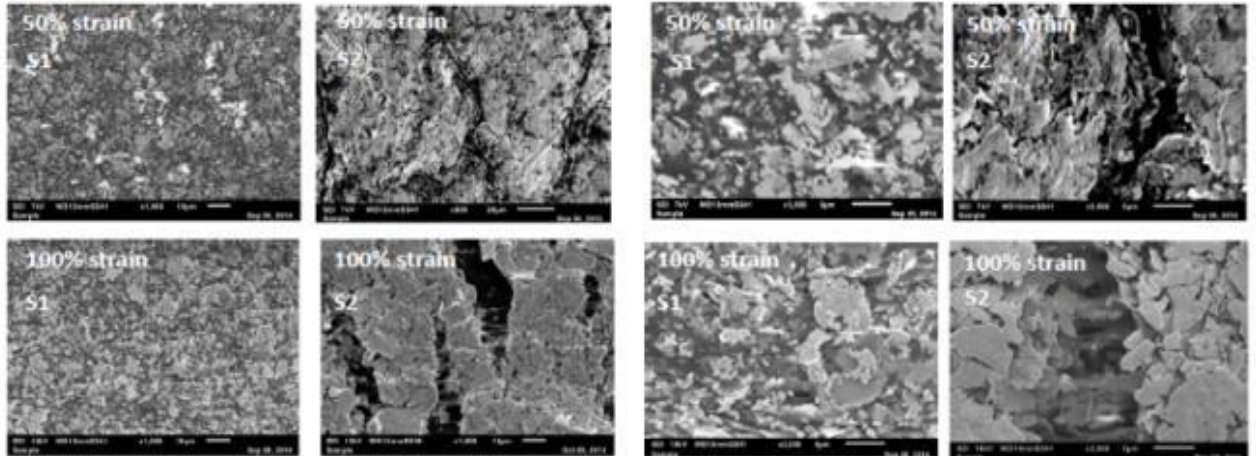
Observations:
As strain increases the cracks in the ink becomes wider for both Gen 1 and Gen 2 Inks
The nucleation of silver flakes in Gen 2 ink is much better clustered during strain allowing reduced electrical connectivity
The nucleation of Gen 1 ink is collapsed under strain leading to opens and no electrical conductivity

Figure # 47: Gen 1 & Gen 2 Ink
Comparative SEM Analyses 50% and 100% strain

4.6.2   EDX Analyses

EDX analyses help in validating our understanding of the SEM images by giving us an understanding of the percentage atomic content of the area we are looking at. Through EDX analyses of the generation 1 ink in Figure 45 we can validate that they grey area of the SEM pictures denotes silver flakes (73.37 atomic % silver), which is obvious, but it also shows us that the dark area is the TPU substrate because that area has no silver content. It also allows us to learn that the stretchy whitish grey area is the binder because it has a much small atomic percentage (4.5%) than silver.

EDX Analyses to Validate SEM Images of Conductive Inks
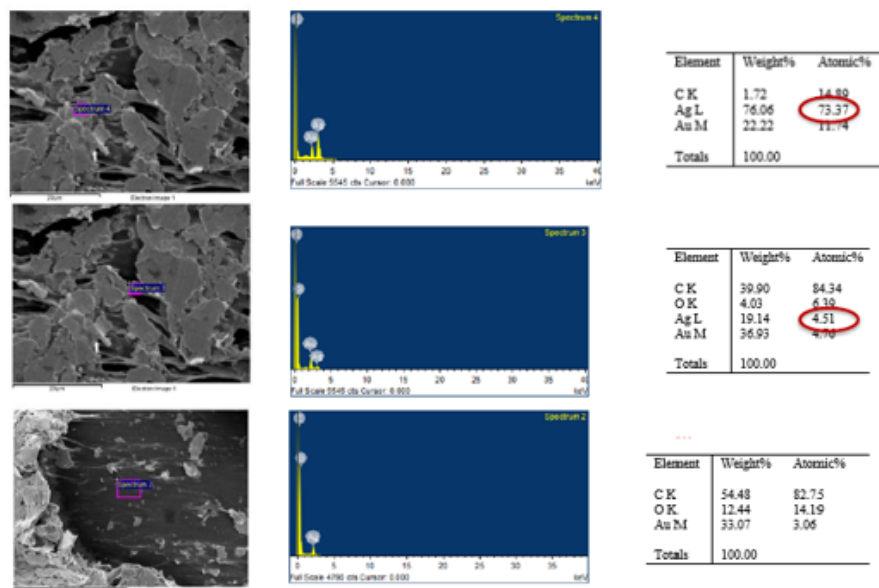
Observations:
The EDX reading for the spot (grey area) on the top SEM validates the positioning of silver flakes (73.37 % silver)
The EDX reading for the spot (stretchy area) on the middle SEM validates the positioning of the ink binder (4.51% silver)
The EDX reading of the spot (dark area) in the bottom SEM validates the positioning of the TPU substrate (no silver)

Figure # 48: Validating silver, binder and substrate regions for Gen 1 Ink

Figures 48 and 49 help in validating that the generation 1 ink has a lower weight percentage of silver (72.6%) versus the generation 2 ink with 84.8 % of silver. Generally speaking, the higher the silver content, the more brittle is the silver and that would lead to higher cracks and loss in conductivity during straining. However, in our case the generation 2 ink has been designed to have a bi modal, heterogeneous distribution of conductive flakes which allows better nucleation of the silver flakes which can manage strain better. It is believed that homogenous flakes have a higher critical conductor volume fraction (f*) compared to an ink with heterogeneous conductive flakes [103]. It is also an established fact that heterogeneous conductive flakes have a lower thermal activation energy compared to homogeneous conductive flakes [112], hence we see better nucleation and clustering of silver particles which allows the flakes to maintain connectivity when strained.

Figure # 49: Elemental Contents of Gen 1 and 2 Inks

4.6.3 CSAM Analyses

Confocal Scanning Acoustic Microscopy (CSAM) analyses help us in detecting failure modes like metal delamination or metal rupture. Along with torn substrates these were determined as the main causes for failure for stretchable conductive circuits [84, 85]. Generation 1 and 2 ink samples were cycled for 1000 cycles under 20% strain and the parts were analyzed under CSAM (Figure 50) for failure detection. The results showed delamination failures for both generation 1 and 2 inks however the amount of delamination was much higher in generation 1 ink. No failures were observed for metal rupture or torn substrates. Processing enhancements like plasma cleaning and corona cleaning can also improve the adhesion to minimize delamination. Material improvements on the binder side and the substrate side can also help overcome the occurrence of delamination.

CSAM of Gen 1 and Gen 2 Inks

Gen 1 Ink No Stretch

Gen 2 Ink No Stretch

G1 ink after 1000 cycles

G2 Ink after 1000 cycles
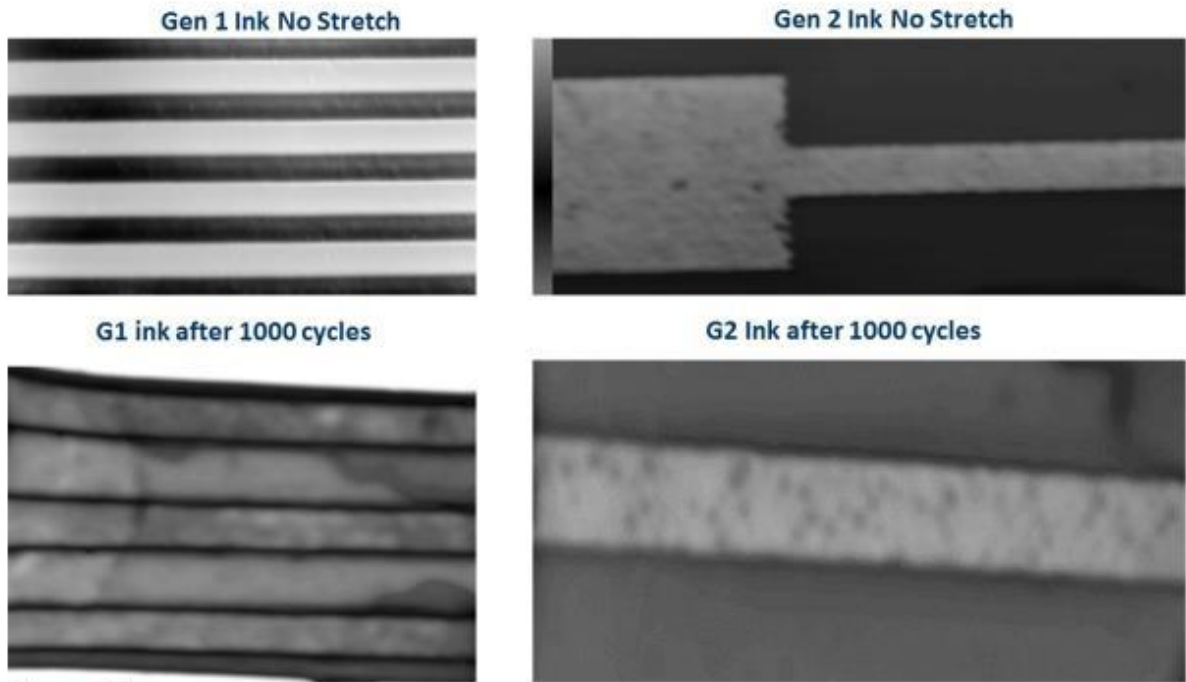
Observations:
Multiple delamination in Gen1 & 2 Ink after 1000 cycles. Delamination area in G1 is greater than G2

Figure # 50: CSAM Results showing Delamination Failures

4.6.4   3D Analyses

3D camera readings are very useful in determining the dimensional characterization of the screen printed conductive inks. Accurate dimensional analyses also allow the determination of the resistivity of the printed ink based upon the following formula:

$$\rho = R\frac{A}{\ell} \qquad \boxed{\text{..........EOUATION \# 5}}$$

Where normalized resistivity is equal to the resistivity (R) multiplied by the cross sectional area (A) of the printed ink divided by the thickness of the printed ink (l). Figures 51- 54 show the conductive line thicknes and width for both generation 1 and generation 2 conductive inks.These numbers were used to compare the normalized resistivity of the two inks.The height measurement of the cured ink is the thickness (l) measurement.

Generation 1, DP 178X Line Width
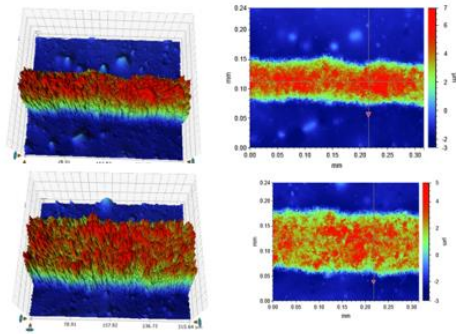
Average Line Width: 870 microns

Figure # 51: Gen 1 Ink Silver Line Width

Generation 2, N 6301X Line Width
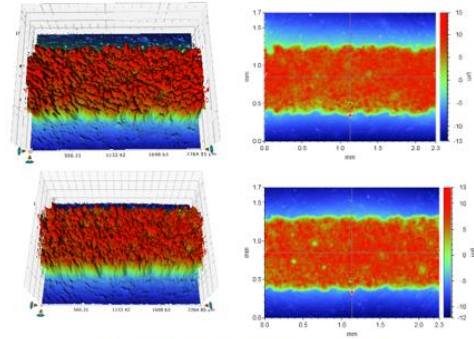
Average Line Width: 850 microns

Figure # 52: Gen 2 Ink Silver Line Width

Gen 1 Ink- DP 178X Height Measurement (7.33 μm Average)

Y Profile: ΔX=0.0344 mm; ΔZ=7.3283 μm
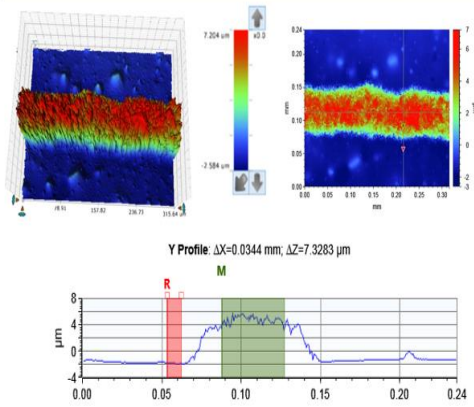
Figure # 53: Gen 1 Ink Silver Line Height

Gen 2 Ink- N 6301X Height Measurement (12.36 μm Average)

Y Profile: ΔX=0.1507 mm; ΔZ=12.2723 μm
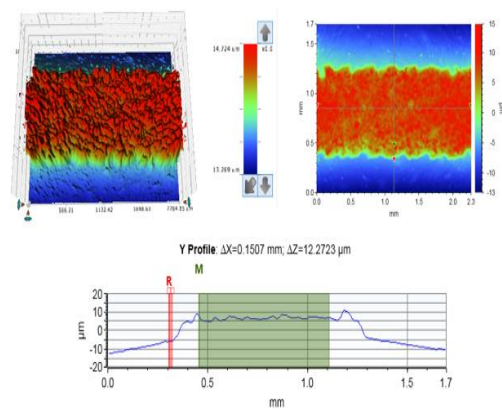
Figure # 54: Gen 2 Ink Silver Line Height

4.7 Reliability Studies

In addition to the stretchability reliability studies, two other types of general reliability studies were also carried out to understand the basic reliability capability of the process. The samples were subjected to Thermal Cycling and 85/85 Relative Humidity testing.

4.7.1 Thermal Cycling

The parts from generation 2 ink were subjected to 250 hours of thermal cycling from -55C to 125C at 15C/min. Multiple cracks were formed and there was a significant increase in the resistance of the part (Fig 55).
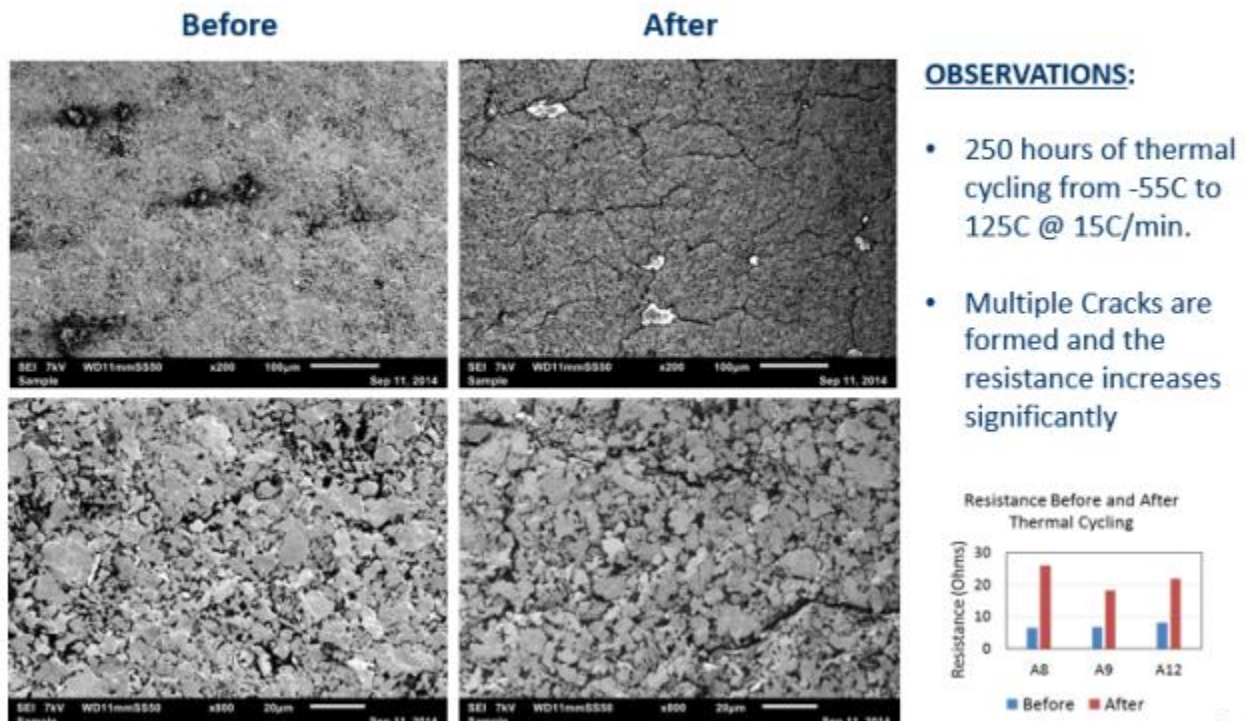
Figure # 55: Thermal Cycling from -55C to 125C, 250 hours

In another temp cycling test with a less stringent temperature change from -20C to 90C and with a protective dielectric layer, the Gen 2 ink samples showed much better results with an acceptable level of resistance increase. (Fig 56).

Environmental Testing – Thermal Cycling

Gen 2 N6301X Ink with stretchable Dielectric
Substrate : American Polyfilm
Substrate Thickness: 4 mil
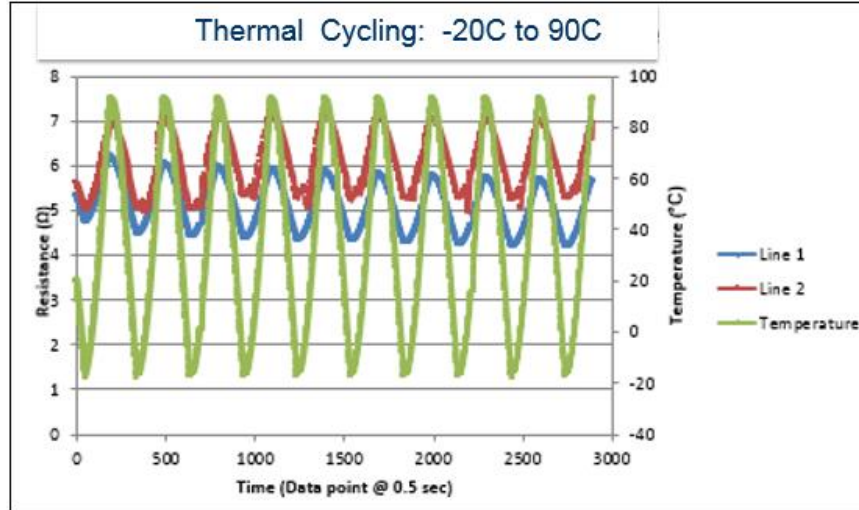
Figure # 56: Thermal Cycling from -20C to 90C, 10 cycles

4.7.2   85/85 Temperature Humidity

It was interesting that the Gen 2 ink after being exposed to 500 hours of 85C at 85 percent relative humidity showed an improvement in conductivity (Fig. 57). The SEM analyses also showed an improvement on the discontinuity region of the silver flakes.
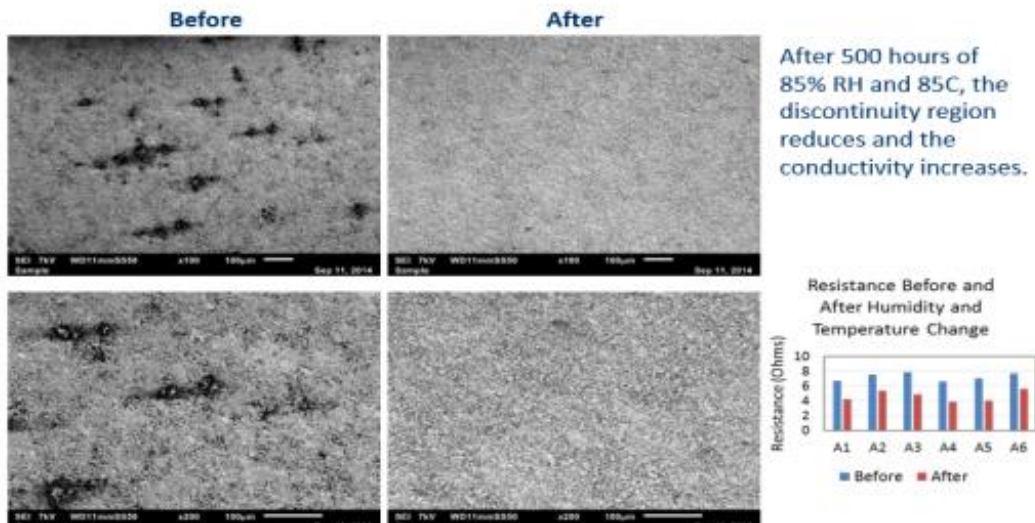
Figure # 57: 85%RH, 85C Humidity and Temperature exposure, 500 hours

The experiment was repeated again for validation with a slight variation. The Gen 2 ink (N6301X) was subjected to 85% RH and 85C and the resistance was measured at 0, 24 and 48hours (Fig 58). The conductivity once again improved and most of the change in the resistance took place in the first 24 hours. The length of the sample also underwent a shrinkage of about 8% but the increase in resistivity was noticeably more than 8%.

85%RH and 85C @ 0, 24 & 48 Hours

Gen 2 Ink: N6301K
Substrate: AP
Thickness: 4 mil
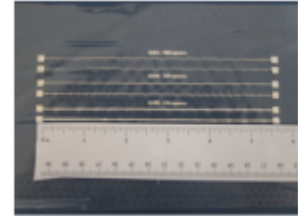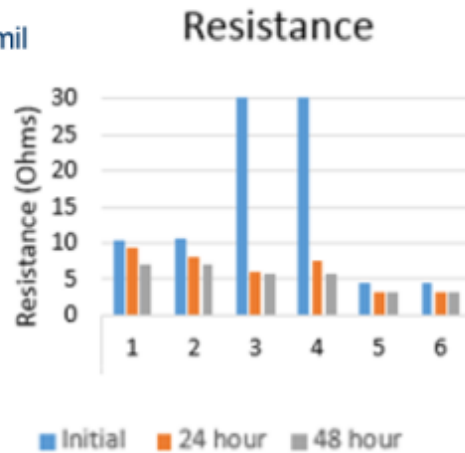
A shrinkage of ~8 % in the length of the sample was noted 48 hours after the 85/85 testing

Figure # 58: 85%RH, 85C Humidity and Temperature exposure, 0, 24 and 48 hours

4.8 Recommendations for the Development of Gen 2 Ink

Based upon the failure analyses and reliability studies carried out on the generation 1 ink, the following recommendations were developed to formulate the next generation of conductive inks which eventually led to the development of Gen 2 ink.

Ink Improvement Recommendations:

Improved stretchability will result from minimized metal rupture/cracks and delamination of the ink to the substrate

A. Improve stretchability of the ink by introducing bi- modal flake distribution of the silver conductive particles to minimize metal rupture/cracks

B. Improve stretchability of the ink, by making the ink binder more stretchable through elastomeric chain polymerization while maintaining adhesion to substrate. This will minimize delamination.

<u>Relationship of Recommendations with Desired Properties of Gen 2 ink:</u>

- Able to be stretched at least 500 cycles (A, B)

- With a minimum strain of 20% (A, B)

- Without losing electrical (A), mechanical (B) and functional (A, B) integrity

- With a resistivity increase of < 30 X (A)

- Minimize metal rupture (A) or delamination from the substrate (B)

Insights were generated from the Percolation Theory [95].

$$\sigma_c = \sigma_f (f - f^*)^t \text{ for } f > f^*,$$

Some improvement $\quad \sigma_c \quad$ = composite conductivity

$\sigma_f \quad$ = flake Conductivity

f $\quad$ = conductor volume fraction

f * $\quad$ = critical conductor volume fraction

A percolating network is just established through the composite when f is greater than f *
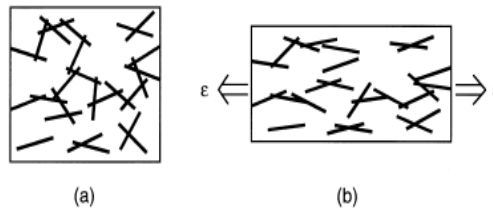
(a) $\qquad$ (b)

(a) Percolating, electrically conductive prior to straining

(b) Non percolating, electrically non-conductive during straining. Absence of ohmic contact.

It is important to note that Ohmic contact plays a critical role, hence we need to maintain ohmic contact during stretching.

Bimodal flake distribution performs better than uni- modal flake distribution in improving the stretchability of the screen printed conductive ink. This hypothesis was derived after reviewing the SEM pictures and reviewing the percolation model proposed by Taya et al [103]. The smaller size flakes fit in between the larger size flakes and paly in important role to maintain connectivity during the stretched stage. It should be noted here that the insights obtained from the literature studies [113] were very helpful in

66

analyzing the SEM pictures of the failed generation 1 parts. The generation 1 ink has essentially homogenous, uni-modal silver flakes ranging from 0.5 microns to 8 microns in particle size. In the case of a bi-modal, heterogeneous distribution the larger sized flakes maintain the electrical and physical connectivity during the stretched state with the assistance of smaller sized silver flakes (Fig. 59). Additionally, a bimodal distribution also offers increased contact points, better surface diffusion and lower thermal activation energy to help clustering of the flakes. The optimal ratio of the bimodal flake distribution is determined by a DOE (Design of Experiments) analysis carried out by the ink supplier and kept as proprietary information.
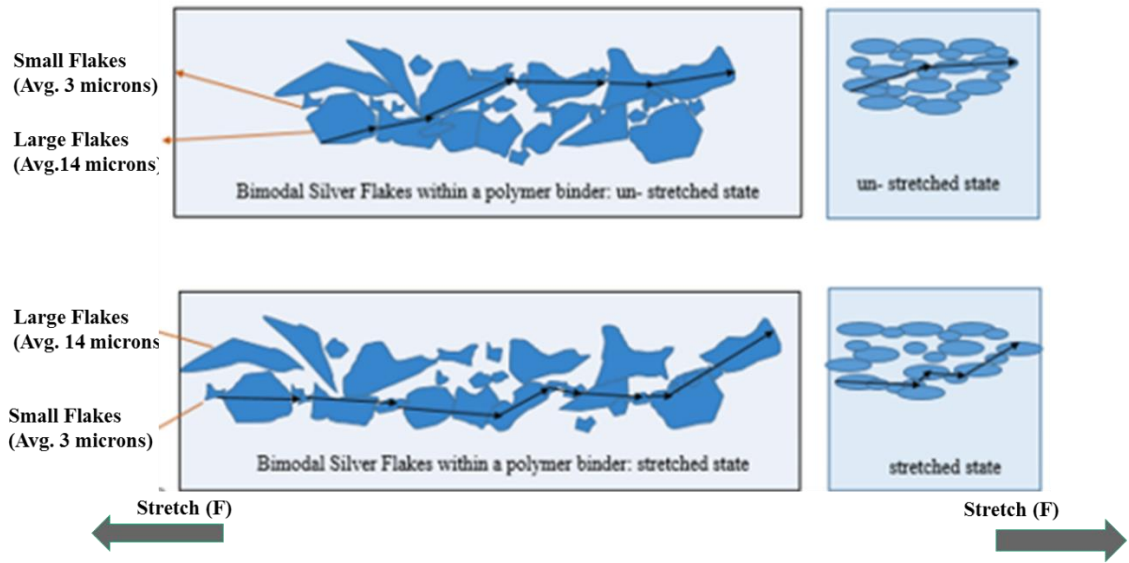
Figure # 59: Advantage of Bimodal flake distribution during stretching- a conceptual approach

Bi-modal flake distribution offers higher surface area, increased contact points, lower thermal energy of activation and better packing density [103, 110]. It is suggested that during stretching the larger and smaller sized flakes maintain electrical conductivity (ohmic contact) by staying physically connected using an altered connection route, with a higher resistance reading. The bi-modal flakes range from .5 microns to 20 microns in length and their individual thickness is around 2 microns and they lay flat along the direction of the screen print. The thickness of the cured ink is ~~ 11 microns.

To achieve enhanced stretchability it is better to use micron level metal flakes instead of nano- level metal flakes (Fig 60). This hypothesis was also derived after reviewing the SEM pictures of stretched and failed generation 1 samples and after studying the percolation model [103]. Nano- level silver flakes are very popular and they help lower the curing temperature and enhance the ink packing density and conductivity but because of their smaller volume they do not allow sufficient connectivity during the stretched

stage. The average silver fakes are around 15 microns whereas the nano- flakes are a thousand times smaller.

Un- stretched state: nano flakes offer higher packing density and increased conductivity

Stretched state: nano-flakes are too small to assist effectively in maintaining connectivity
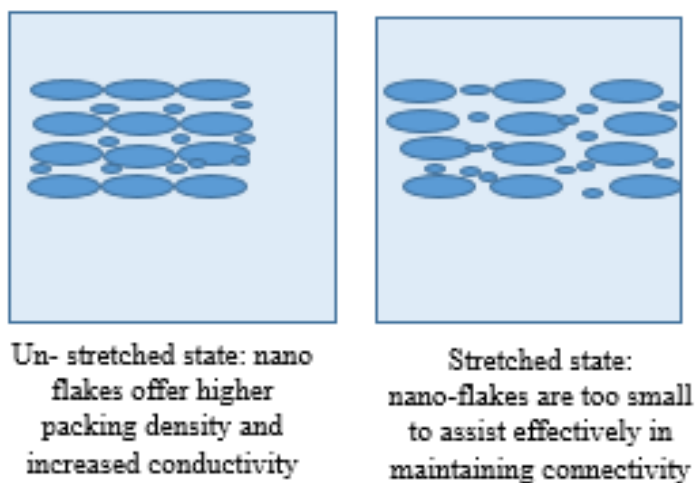
Figure # 60: Advantage and Disadvantages of nano- silver flakes- a conceptual approach

The polymer binders should have two amorphous resin blends to carry out various requirements of a binder in an efficient manner. The polymer binder system plays a pivotal role in offering stretchability to the stretchable conductive inks. The silver flakes by themselves are not stretchable but they are contained within a stretchable binder system. One way of increasing the stretchability is by employing large chain polymers which tend to be flexible and stretchable. But the issue is that the binders also play a very important functional role also. In addition to carrying the flakes before, during and after the curing process it is also the function of the binder to attach the ink to the substrate. All of these roles cannot be effectively carried out by large chain polymers. One solution (Fig 61) is to have a blend of two different types of amorphous binders. One binder offers the stretchability and the other carries out the functional responsibilities. Since they are amorphous they can stretch and compress as needed during stretching. High power (3500X) SEM pictures of conductive inks obtained under 100% stress level and EDX analyses were instrumental in offering insights to come to this conclusion. The optimal binder ratio is determined by a DOE analysis carried out by the ink manufacturer and is deemed proprietary. The idea of using 'elastomeric chain polymerized binder' is common in the tire industry. This process is known as 'toughening', the novelty in our approach was to use this as part of a two-part binder system for stretchable conductive inks.
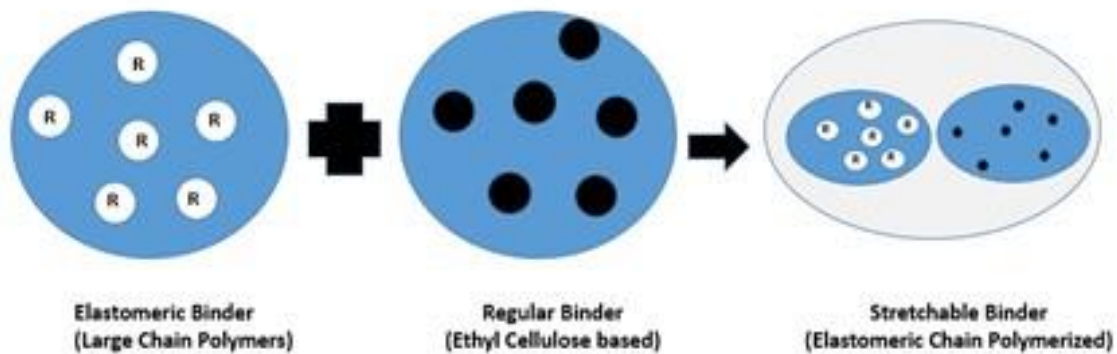
Figure # 61: Double Resin binder system for stretchable inks- a conceptual approach

The conductive silver flakes are not stretchable, so they are designed to be contained within a stretchable binder system. The regular/functional binder needs to carry the flakes before, during and after the curing process while enabling the ink to be attached to the substrate after curing. It was recommended that the stretchable binder system should be a mixture of at least two amorphous binder systems. One binder would be a large chain elastomer, offering stretchability and the other would be designed to carry the regular, functional role of the ink binder. The stretchability comes from the long chain, elastomeric polymeric binders to reconstitute themselves to respond to an applied stress. The elasticity comes from the covalent cross-linkages, enabling the elastomeric binder to return to its original shape upon stress removal. The recommendation was to use essentially the same ingredients besides the bi-modal silver flakes and the elastomeric chain polymerized binder system. It was also recommended that the same type of TPU substrates to be used with the same screen printing and processing methodology as used for generation 1 samples.

All of the above recommendations were implemented in the development of the final generation 2 ink which exhibited much better stretchability than the generation 1 ink, but it still needs to be improved further. Currently it can only be stretched predictably for ~750 cycles at 20% stress. It needs to be stretched by at least 2000 cycles to meet most wearable electronics requirements. The generation one ink was able to be stretched predictably for only 30 cycles at 20% stress.

The following figure (Fig. 62) shows a comparison between the differences in the performance and characteristics of the generation 1 ink and the generation 2 ink based upon the results of the current research.

Comparison of Gen 1 and Gen 2 Ink

Generation 1 Ink

Unimodal Silver Flake Distribution

.5 microns   8 microns

Single Polymeric Binder

Ethyl cellulose binder resin

Sheet Resistivity of ~ 70 milliohms per square,
Weight % of Silver: ~ 73%
Curing temperature of 140 C, 10 minutes
Prec-cure Ink Viscosity: 70 PaS ,
Rheology: Non-Newtonian, Thixotropic
**Can be stretched for ~ 30 cycles at 20% strain with
>1000X increase in resistance**

Generation 2 Ink

Bimodal Silver Flake Distribution

.5 microns   20 microns

Dual Binder System (Amorphous)

**Polybutadiene elastomer + ethyl cellulose resin
(with large backplane)**

Sheet Resistivity of ~ 30 milliohms per square,
Weight % of Silver: ~85%
Curing temperature of 120 C, 10 minutes
Pre-cure Ink Viscosity: 10 PaS,
Rheology: Non –Newtonian, Thixotropic
**Can be stretched for >500 cycles at 20% strain with
< 30X increase in resistance**

Figure # 62: Comparing Characteristics of Gen 1 Ink with Gen 2 Ink

4.9 Developing a universal tester for stretchability and related testing

The diversity of wearable electronics application includes activity trackers, smart athletic wear, conformable electronic textiles, and sensor skins, etc. [113-118]. Stretchable conductors play a key role in providing conductive pathways as interconnects. When the wearable electronics are subjected to a one-time or repeated deformation (e.g. stretch, bending, twist), the stretchable conductors are deformed quite differently between the film and substrate which tends to degrade the device performance [119-121]. Hence, it is important to evaluate the mechanical deformability and its effect on the electrical conductivity of the stretchable conductors under varying stress conditions.

The mechanical reliability testing of stretchable electronics poses some special demands. For example, the test equipment needs to tethered to an external resistance meter, so that the resistance can be monitored in situ during the stretching and relaxation.

For bending tests, a higher bending radius of 3-20 mm is needed to induce failure [122], which is generally beyond the range of a typical bend tester. To meet these requirements, traditional mechanical tests methods including tensile [100, 123], bending [120, 122, 124-126], and torsion tests [127, 128] have been adjusted or upgraded for various purposes.

A new universal flexibility tester was conceived and developed to simulate the various use conditions of stretchable conductors. Four key categories of mechanical testing were developed; stretchability test, bending test, multi modal torsion test, and compression crush test. Additionally, six different types of bending tests were included in the bending test category which included variable radius testing, sliding plate flexibility testing, variable angle bend testing, variable diameter rolling testing, free arc bend testing and multi-mode bend testing.

The universal mechanical flexibility tester (Fig 63) is composed of six subsystems; the specimen, a load fixture to hold the specimen, an actuation system to apply a prescribed load or displacement, a load cell to measure the force carried by the specimen, a module to measure the displacement, and a computerized data collection. The test fixtures can handle stretchable conductors as long as 150 mm. It has a vertical travel range from 0 to 650mm while horizontally it can move as far as 150mm. It can exert a vertical force as high as 120 Kg and the maximum torque motor force of 25 kg with a step angle of 1.8. Relevant data such as displacement, load and rotation angle can be communicated and stored within the computer.
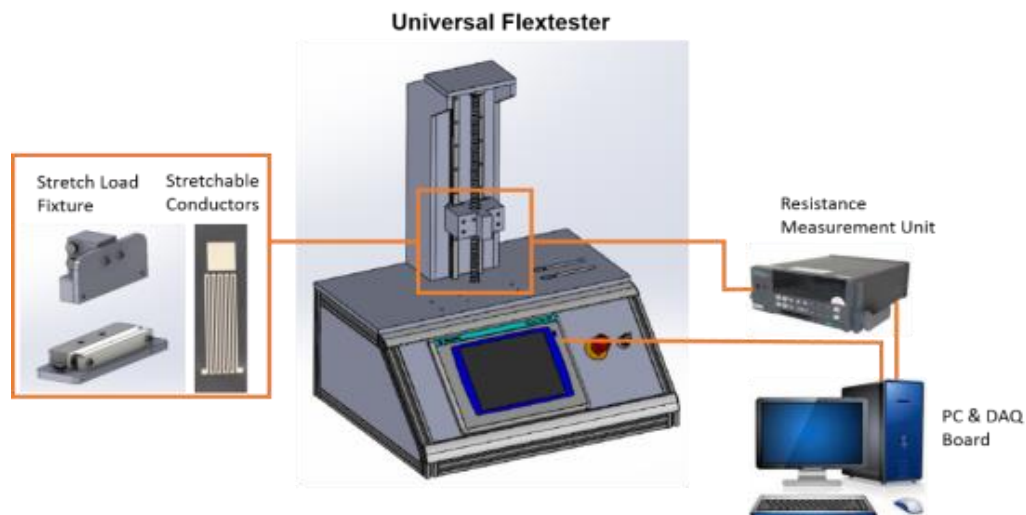
Figure 63. Universal flexibility tester for stretchable conductors

Some common failure mechanisms for stretchable conductors are substrate modulus, volume fraction of the filler material of conductor, particle size and shape in the filler material, etc. [123, 124]. Hence tensile stretchability test becomes an important mechanical test. Uniaxial tensile testing is performed with either one single cycle or multiple cyclic stretch testing. During the single cycle stretch test, the strain is increased at a constant speed until the conductor fails showing no electrical reading or the resistance stretches beyond a pre-set range, for example 30 times the original resistance reading. Cyclical reliability stretch testing involves a large number of stretch cycles with a few percent of stretch, e.g. 10% or 20% to determine the estimated lifetime of the stretchable conductors under a particular strain. Three sets of resistance are generally measured, before, during and after stretching (Fig 64) and a graph comparing the resistance with strain is used to represent the stretchability. Because stretchable substrates are generally viscoelastic polymers with time-dependent properties, a hold time between each test cycle is recommended to allow the sample to relax. The hold time depends on the mechanical properties of the substrate, however a strain rate of less than 1.0×10^{-3} s^{-1} is recommended.
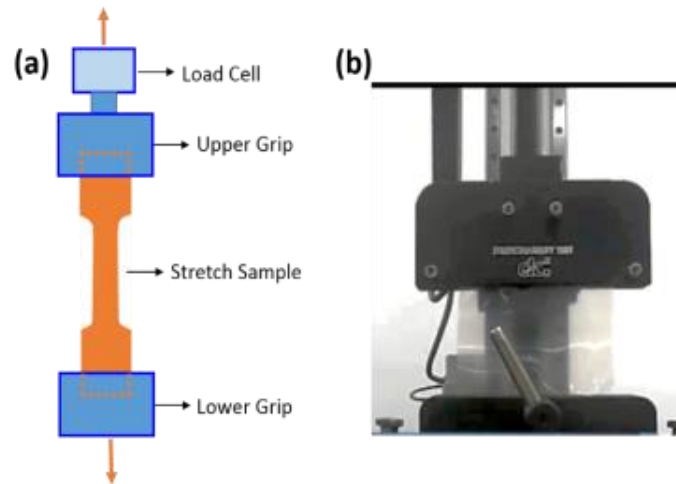
Figure 64. (a) Schematic setup of stretch load fixture; (b) Stretch load fixture

During bending the outer surface of the conductor film experiences tensile stress whereas the inner surface experiences compressive stress. Metal rupture, substrate delamination, film cracking, channeling, film adhesion and film cohesion may occur [120, 122, 124-125]. Hence bending test is also very important to understand the reliability of stretchable conductors.

The simplest method is bending the sample to a given radius r while the resistance is measured simultaneously at different bending radius (Fig 65 a). For the variable radius bend test the sample is positioned between two parallel plates, and is bent between the plates by decreasing the separation distance (Fig 65 b). For the variable angle bend

testing, the sample is held in a flat position between a fixed plate and a co-planar plate and then bent by varying the angle (Fig 65 c and d).
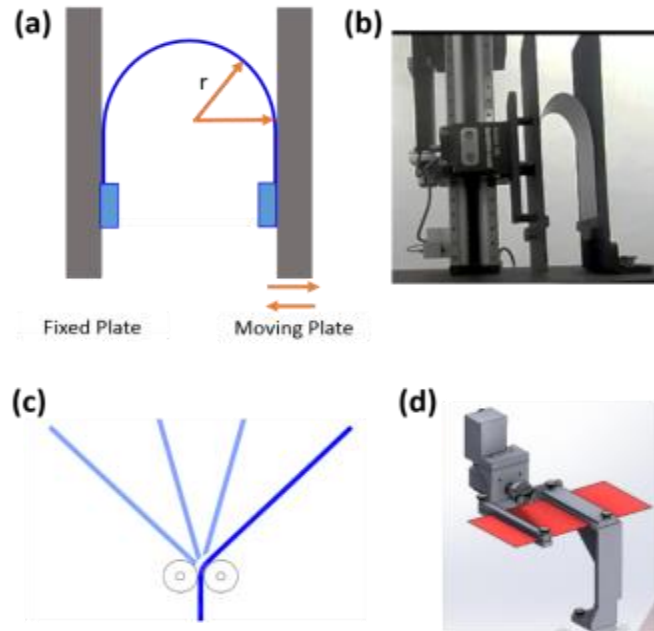
Figure 65. (a) Schematic setup of Variable Radius Test fixture (b) Variable Radius Test fixture (c) Variable Angle Bend Test fixture and (d) Variable Angle Bend Test fixture

Besides the two bending tests discussed earlier, four other bending tests can also be performed. They are sliding plate flexibility test (Fig 66 a, b), variable diameter rolling test (Fig 66 c, d), free arc bend test (Fig 66 e, f) and multi-mode bend test (Fig 66 g, h).
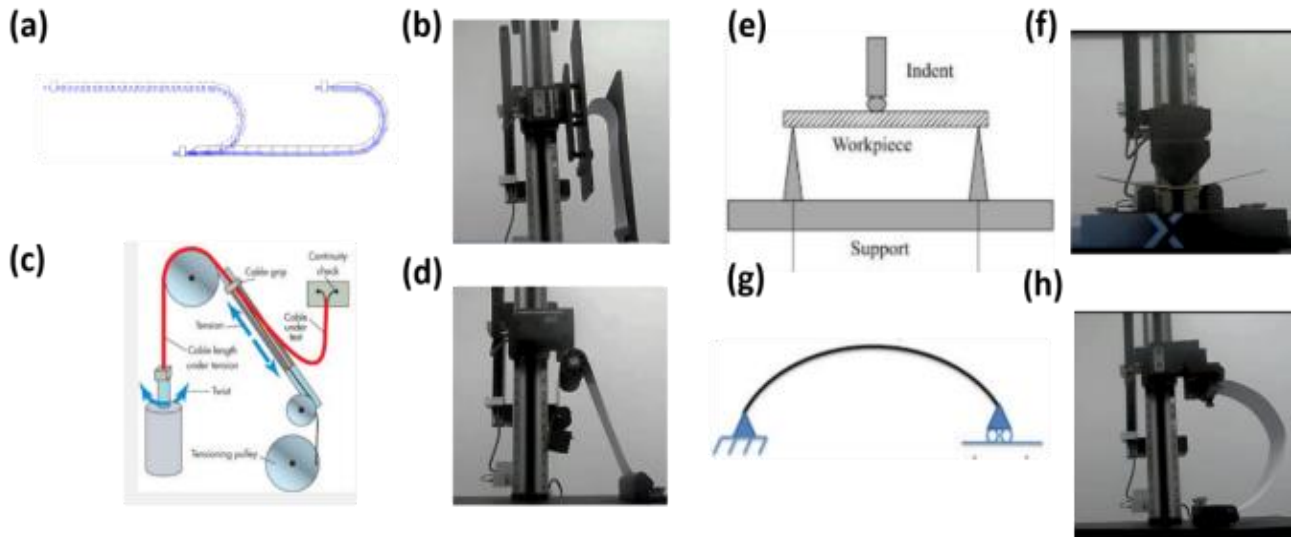
Figure 66. (a) (b) Sliding Plate Flexibility Test (c) (d) Variable Diameter Rolling Test (e) (f) Multi-Mode Bend Test (g) (h) Free Arc Bend Test.

Torque testing have the potential to help improve the design of wearable products [127, 128]. Figure 67 a and b shows the setup of Multi Modal Torsion Testing. The sample are twisted by exerting a controlled strain between 0 to 135°, while moving at a speed of 0 to 1000 rps. The resistance is also measured when varying the rotation angles allowing the capability to graph the relationship between resistance and torqueing.
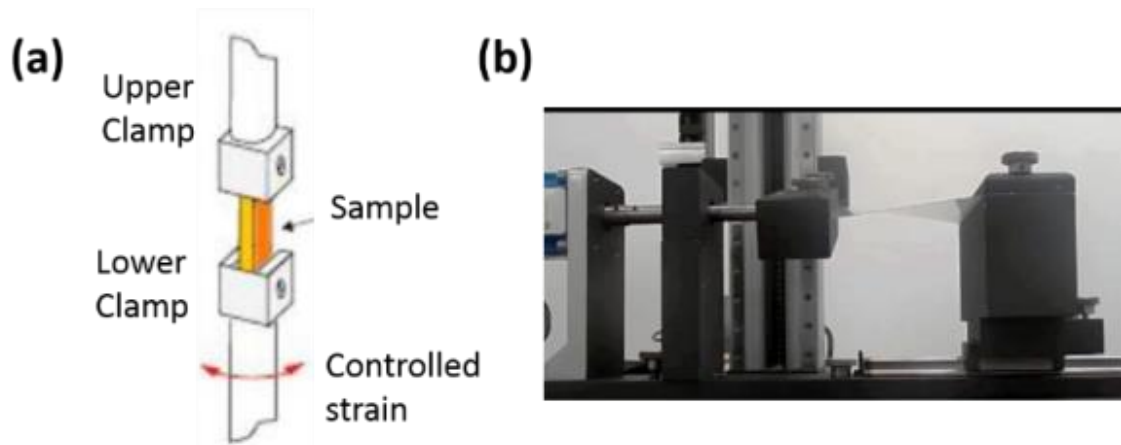
Figure 67. (a) Multi Modal Torsion Test fixture (b) Multi Modal Torsion Test fixture

Compression Crush Testing (Fig 68 a and b) can help evaluate the reliability of a circular or flat sheet of stretchable conductors. Uniaxial compression testing is performed using a constant speed on the test materials. Delamination and buckling of conductor films under compressive strain are common failure modes. The resistance variation graph with increasing compressive strain can help understand better the mechanical stability.
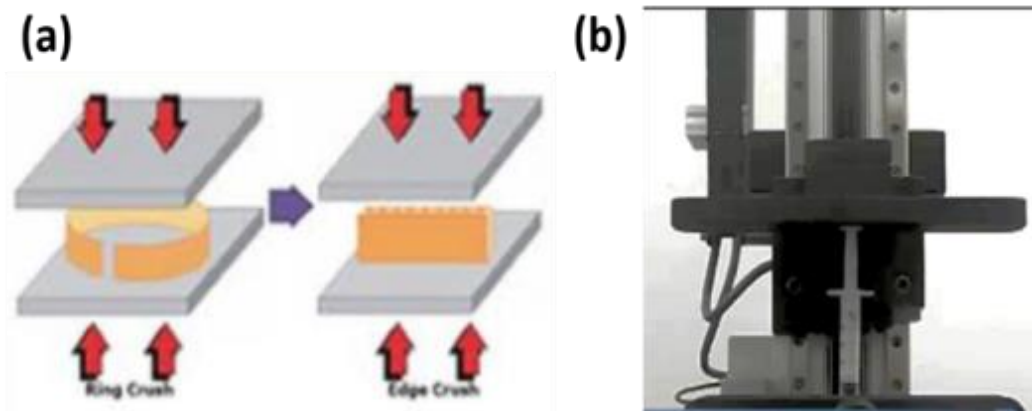
Figure 68. (a) Schematic setup of Compression Crush Test fixture (b) Compression Crush Test fixture

The development of the universal flexibility tester enables the evaluation of the reliability of stretchable electronics. Flexible integrated circuit boards, flexible transistors, smart textiles and other multi-layered electronics devices can also be tested. The tester creates a standard platform for consistent, systematic and repeatable mechanical testing. Stretchable electronics is a nascent technology and the industrial standards defining the mechanical testing methodology are not available and there is an absence of consensus and established references for testing. To enable the growth of stretchable electronic devices, shared and systematic test procedures need to be agreed upon which should also cover the understanding of the physics of failure and offer suggestions for test conditions and setting parameters.

4.10 Conclusion

The current research demonstrates successfully the development of a new screen printable and stretchable conductive ink, that can withstand over 500 cycles of stretching at 20% strain without increasing the resistance by more than 30 X.

The SEM/EDX/CSAM and 3D analyses undertaken during this research helped significantly in undertaking failure analyses studies that led to the development of the new stretchable and screen printable conductive ink. The two key critical insights that led to this development were the use of bimodal flake distribution to maintain ohmic contact during stretching and the use of elastomeric chain polymerization to develop a binder system that would enable stretching after the ink was cured and attached to the substrate.

The research also demonstrates the successful development of a compatible, stretchable dielectric to work along with the stretchable silver conductive ink enabling the development of multi-layer circuitry and stretchable encapsulants and capacitors.

A universal flexibility tester has also been designed and developed from scratch to enhance a deeper understanding of the mechanical behavior and reliability of stretchable substrates.

Preliminary reliability studies were also performed using thermal cycling and temperature humidity testing. It was interesting to note that the conductive ink jumped up in resistance after undergoing thermal cycling. Our research shows that protecting the conductive ink with a stretchable dielectric can mitigate the effect significantly. The current work also demonstrated that exposure to 85% RH and 85C will reduce the resistance of the conductive inks.

It was also shown that these stretchable conductive inks could be stretched at least by 100 percent and still maintain electrical and mechanical integrity even though the resistance jumps up to ~200 times the original value.

Chapter 5: Stretchability of Wavy Patterns

5.1 Introduction

The second research objective of the current thesis work was to demonstrate that the comparative change in resistance caused by stretching, between a screen printed straight line pattern and a sine wave pattern can be estimated by calculating the total principal strain using FEA modeling and explained by using equations from Percolation theory.

Employing wavy patterns is an intuitive mechanical technique to enhance the stretchability of a stretchable electronics. A sine wave, screen printed pattern using a stretchable conductive ink on a stretchable substrate, is more stretchable than a similarly fabricated straight line pattern. Stretchability in the printed conductor context, is defined as the percentage change in resistance of the printed conductor when exposed to an induced uni-axial stress. The lower the change in resistance the better is the stretchability. The hypothesis is that the wavy or meandering patterns will behave like a spring coil which will open up when stretched and should exhibit higher stretchability. Meaning, it could be stretched the same amount as a straight line but would depict a smaller increase in resistivity.

The literature covers the enhanced stretching behavior of a horseshoe copper lines [84] which were created using a photolithographic process and were covered on both sides within a PDMS substrate. Another paper [85] which also discusses horse-shoe patterns, demonstrates that meandering patterns with circular shapes exhibit a lower mount of plastic strain. The samples prepared use a PCB (printed circuit board) approach and a thin film based, polyimide supported approach. In both the papers [84, 85] it was demonstrated that the horseshoe pattern will exhibit lower stress than a straight line and that the highest stress concentration was found in the crest of the horseshoe.

After achieving the stated objectives above, an attempt was also made to determine if one could design the best printed conductor pattern with the most optimal stretchability, using total principal strain obtained from FEA modeling.

5.2 FEA overview

Finite element analysis of ink stresses on a sine wave and a straight line screen printed pattern were analyzed. The substrate and ink were modeled as a multilayered structure with a bonding interface model connecting the substrate and ink to simulate the screen printed process. The objective of the analysis was to assess the influence of the two different printed shapes on the resultant stresses on the printed pattern. The shapes

were printed on the same substrate using similar printing and curing process. This analysis was designed to estimate which shape would exhibit lower stress and by what percentage. The equipment utilized for performing this FEA analysis was ABAQUS, version 6.6. The material properties (Figure 69) were obtained from the substrate and ink supplier. The plan was to compare the numerical results with our experimental results.

Material Name/Type	Substrate	Ink
Flexural Modulus (MPa)	11.55	1034.21
Poisson's Ratio	0.45	0.25
Density (ton/mm^3)	1.2e-09	2.2e-09

Figure # 69: Material Properties used for FEA

Based upon the results obtained from our 3D camera studies, the FEA model was developed with the understanding that the ink thickness was .005 mm and the substrate thickness was .1 mm (Figure 70). Because of symmetry along the X direction a half model was deployed. 20% elongation stress is deployed uni-axially along the X axis (Figure 71).

t_A= 0.1mm
t_B= 0.005 mm
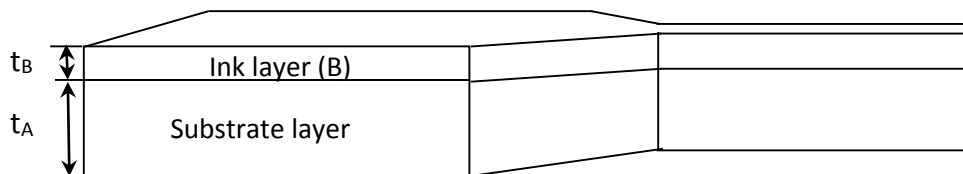
Figure # 70: Ink and Substrate thickness for FEA
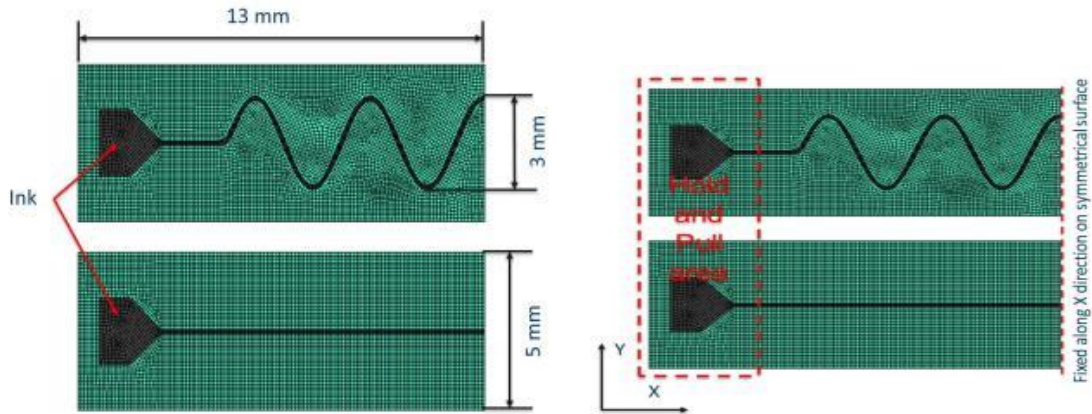
Figure # 71: FEA Symmetrical Half Model

The FEA analysis shows that it was reasonable to expect about 1.5 times higher strain on the straight line versus a sinusoidal line, assuming everything else was constant (Figure 72). The maximum principal strain on the straight line was 1.5 times higher than the sine wave pattern. The Principal stress and Von Misses stress for both the patterns were also compared (Figure 73). The predicted number 1.5 times is compared later (Figure 76A) in this chapter with our actual experimental results.

Component	Pattern	Max. Principal Strain	Von Mises Stress (Mpa)	Stress Relation (Straight line/sine wave)
Ink	Straight line	0.205	214	1.5 (MPS) 1.7 (VMS)
	Sine wave	0.135	127	
Substrate	Straight line	0.331	3.22	0.95
	Sine wave	0.339	3.38	

OBSERVATIONS:
- Straight line pattern would see more stress than a sine wave pattern
- Using maximum principal strain the straight line would see 1.5 times more strain

Figure # 72: FEA Results Summary
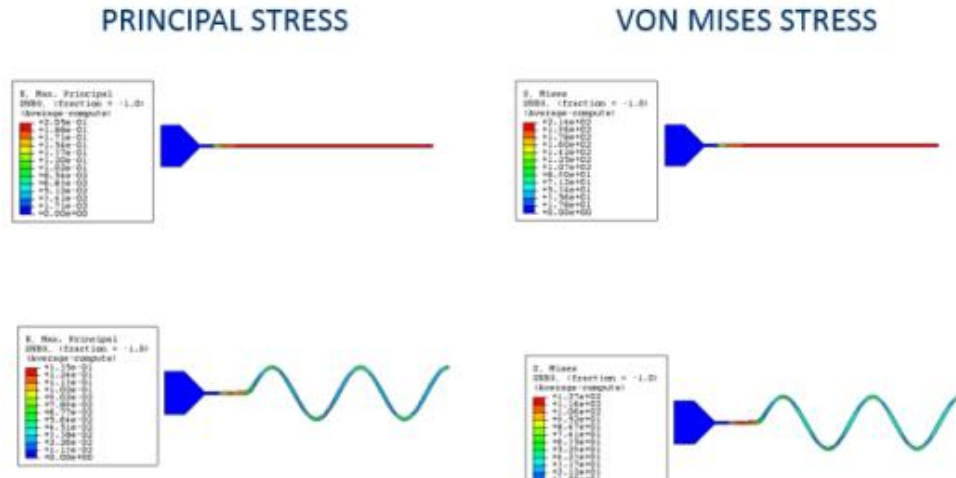
Figure # 73: Comparison between Principal and Von Misses Stress

5.3 Methodology

The approach was to run experimental studies and simultaneously run FEA modeling to compare the modeling results with the experimental observations. Appropriate stretchable conductive ink and substrate were selected and a screen pattern was designed to help us obtain our research objectives. The following methodology was developed.

(A) Fabricate test samples having a straight line and a sine wave pattern on the same substrate, side by side, using the same stretchable conductive ink using similar processing conditions.
(B) The line width of both the straight line and sine wave patterns would be similar and two different widths were tried; 100 micron lines and 150 micron lines.
(C) The samples would be subjected to optical, dimensional and electrical inspection and the results documented.
(D) The samples would be stretched at 20% strain for 100 cycles. In situ resistivity reading were recorded for each of the 100 cycles.
(E) The samples would be subjected again to a final optical, dimensional and electrical inspection and the results documented.
(F) The percentage change in resistance between the two patterns of the same substrate would be compared.

5.4 Sample Development

The second generation stretchable conductive ink with improved binder quality and TPU substrates were selected for this research work. This was because of the acceptable performance of these materials observed during the work carried out in

79

Chapter 4. The pattern was printed on a DEK LPiX printer (Fig 26) using the equipment settings in Table 4.

PARAMETER	DETAIL
Mesh type	Stainless steel
Mesh Count	325
Screen Tension	25 Newtons/cm
Screen Emulsion Thickness	25 microns
Squeegee	Polyurethane squeegee with diamond shape
Squeegee hardness	80 durometers
Squeegee Attack angle	45 degrees

Table # 4: Equipment Parameter Details for Screen Printing

The viscosity of the stretchable conductive ink used was 10Kcps and it had ~70% silver content. The resistivity of the ink was .010 ohms per square for 1 mil thick line and the ink curing was performed at 120 C for 10 minutes in a Despatch Loc1 batch oven (Fig 27) using ambient air. The printed samples were collected and subjected to optical, dimensional and electrical reading. The following pattern (Fig. 74) was developed for the stretchability comparison tests using 100 microns and 150 microns straight lines and sine wave patterns.
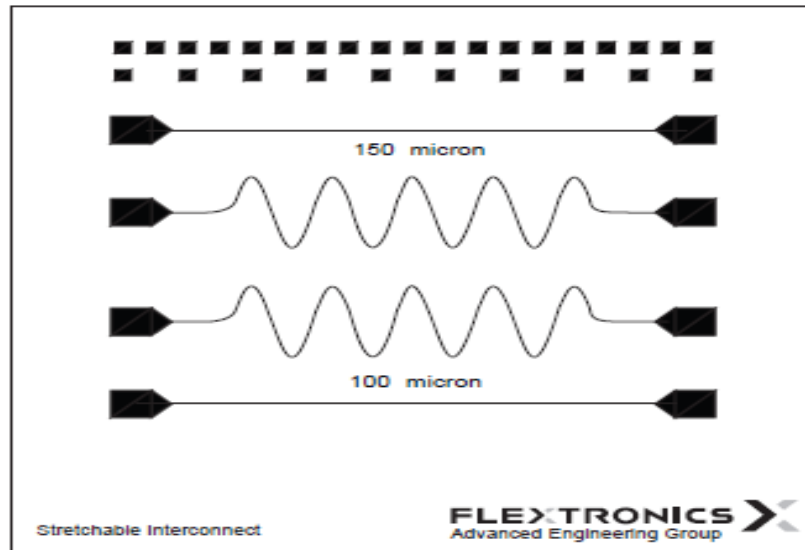
FIG # 74: Screen Pattern Created for Stretchability Comparison

The test samples were stressed by 20% for a total of 100 cycles using a Dage Instron meter (Fig. 31). In situ resistivity reading was recorded for each of the 100 cycles.

5.5 Results

Figure 75 below shows a picture of a TPU substrate printed with Gen 2 ink (N6301X) using the special screen pattern with a straight line pattern printed simultaneously on the same substrate, side by side and cured under similar conditions.
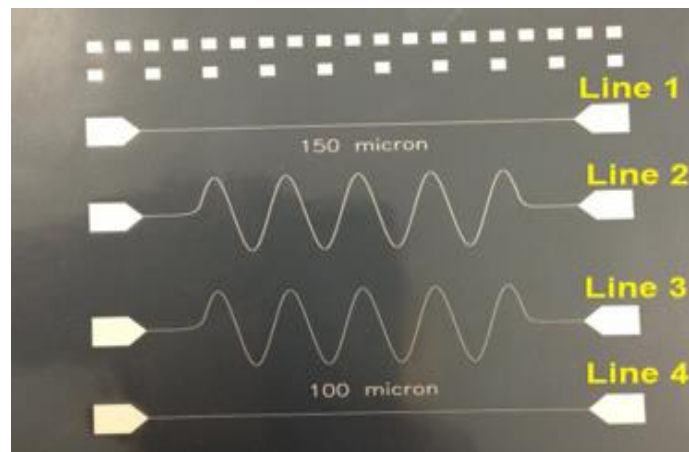
FIG # 75: GEN 2 INK Printed on TPU Substrate for Stretchability Comparison

The experimental results demonstrate that the printed sine wave pattern has better stretchability compared to a straight line pattern. The sine wave pattern behaves like a coil and opens up under stretch whereas the straight line does not have that capability. The results are similar to what is available in the literature [84, 85] for a horse shoe type pattern which was not screen printed, and also similar to what was predicted in our FEA analysis in section 5.2. The FEA estimated the stretchability of the straight line to be 1.5 times worse than the sine wave pattern after a 20% strain exposure. The experimental studies carried out during this research to compare the resistivity changes between a straight line and a sinusoidal line under 20% strain at 100 cycles yielded the graph shown in figure 76.
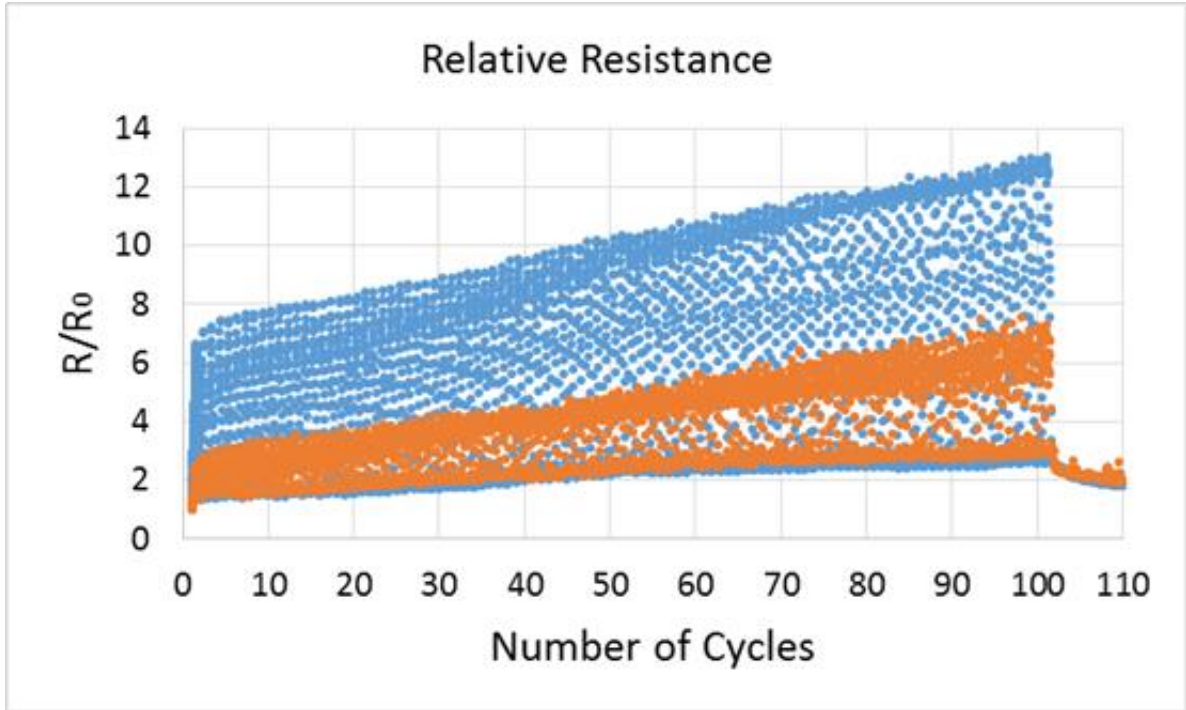
Figure # 76: Experimental Data comparing the Relative Change in Resistance between a Straight Line (Top, Blue) and a Sine Wave Pattern (Bottom, Orange) for 100 Cycles at 20% Strain

The final resistance (R) divided by the initial resistance (Ro) after 100 cycles is approximately 1.7. The FEA estimation, using maximum principal strain give us an approximate ratio of 1.5. The FEA number assumes an ideal situation with no delamination between the ink and the substrate, no stress cycling and no variations during the manufacturing process. Nevertheless, the FEA model does validate our assumption and the experimental results, that a sine wave pattern will tend to behave like a spring coil and will exhibit less strain versus a straight line. Another assumption being made here is that the quantum of the principal strain delta will manifest one to one as the difference in resistivity, which may not be accurate. Hence it is not reasonable to expect the FEA numbers to coincide with the experimental numbers however the FEA number is a good indicator of what to expect.

After demonstrating some experimental data depicting the spring coil behavior of a sine wave pattern, few other meandering patterns were developed that could improve the stretchability (Fig 77) for screen printed, stretchable conductive inks.
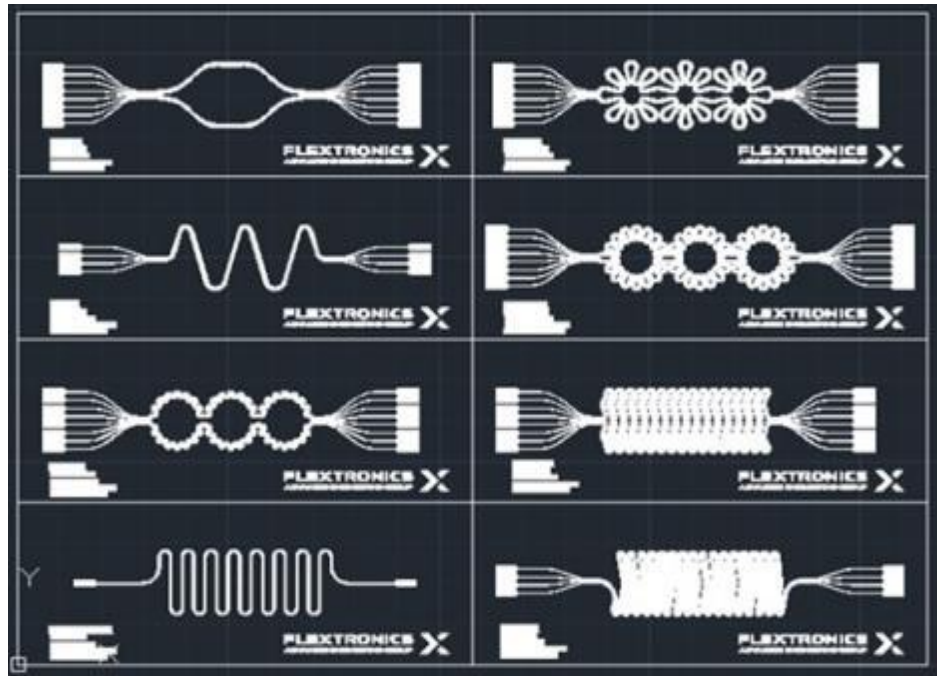
FIG # 77: Wavy Patterns for Enhancing Stretchability of Conductive Ink.

5.6 Determining Optimum Pattern for Stretchability through FEA

Having demonstrated that a sine wave pattern exhibits better stretchability during stretching compared to a straight line and that FEA modeling could assist us in estimating the stretchability, the next step was to explore the possibilities of determining an optimum pattern for enhanced stretchability, using FEA modeling.

Six different types of meandering patterns (Fig. 78) were developed and screen printed using similar approaches from sections 5.4 and 5.5. The parts were then stretched for 50 cycles at 25% strain with in situ resistance reading. FEA modeling was performed on each of the 6 patterns and the total principal strain for each of the 6 patterns were calculated assuming that the lowest total principal strain would offer the best stretchability performance. Pattern 6 exhibited the lowest total principal strain followed by 3,5,2,4 and 1 (Fig.78). The experimental data depicting the change in resistance (Rf/Ro) from being stretched 50 cycles at 20 % strain showed the lowest change in resistance in pattern 6 followed by 3,4,2,5 and 1 (Fig. 78). It should be noted here that patterns 2 and 5 have very similar total principal strain, .82 for pattern 2 and .78 for pattern 5. This experiment suggests that we could come close to the optimal design selection for stretchability using this methodology.

Rf/Ro Changes for Different Patterns

RESISTANCE (RF/RO) CHANGE AFTER 50 CYCLES AT 25% STRAIN PER EXPERIMENT
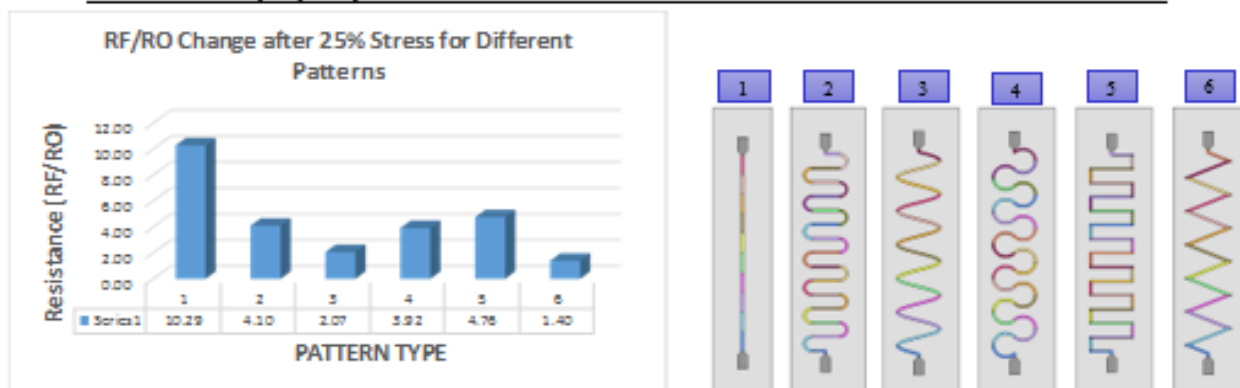
NOTE: LOWEST CHANGE IN RF/RO PEREXPERIMENTAL RESULTS IS SHOWN BY PATTERN 6, FOLLOWED BY 3,4,2,5 AND 1

TOTAL, AVERAGE & MAXIMUM PRINICPAL STRAIN AT 25% STRAIN PER FEA MODELING

	1	2	3	4	5	6	
TOTAL	1.2495	0.8237	0.6404	0.8854	0.7806	0.4970	
AVE	0.2083	0.1373	0.1067	0.1476	0.1301	0.0828	
MAX	0.2171	0.1777	0.1572	0.1509	0.1548	0.1663	

NOTE: LOWEST TOTAL PRINCIPAL STRAIN PER FEA MODELING IS PATTERN 6, FOLLOWED BY 3,5,2,4 AND 1

FIG # 78: Determining Optimal Patterns for Stretchability

5.7 Employing Percolation Theory to explain Resistance Changes

The objective was to determine if Percolation Theory equations could be utilized in explaining and estimating the comparative resistance changes (Rf/Ro) undergone by a straight line pattern and a sine wave pattern during stretching.

Stretchable TPU substrates were printed with a stretchable silver conductive ink and t cured at 180 C. The sine wave pattern and the straight line pattern were printed on the same substrate and under similar processing conditions. The length for the printed patterns was 180 mm each and the width was 2 mm each. The resistance changes (Rf/Ro) on the samples were measured in situ as the samples were stretched from 0% strain to 50% strain at a constant speed of 1mm/sec. This yielded the Strain versus the Rf/Ro graph for the straight line and sine wave pattern in Figure 79.
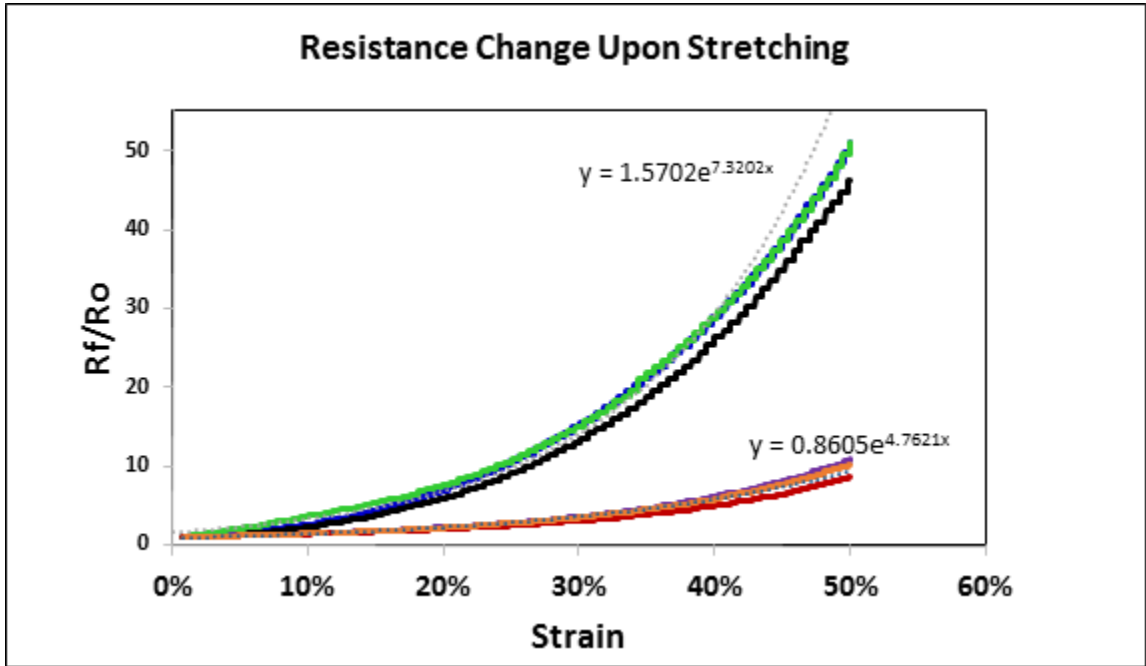
FIG # 79: Rf/Ro versus Strain Curve for Straight Line (top) and Sine Wave (bottom) Patterns

Using SEM analysis and J Image screening techniques, we get the volume fraction of the conductive ink at 0 % stretch (Fig. 80) and 50% stretch (Fig. 81). J Image is a software which can look at the SEM picture and calculate the volume fraction of the silver content in the ink.

Volume Fraction by SEM and J Image: 0 % Stretch

From 3 SEM images, the average volume fraction at 0 % stretch was calculated at 91% using Image J software

Slice	Count	Total Area	Average Size	%Area	Mean
thick 100x.jpg	307	3848387	12535.463	91.202	255
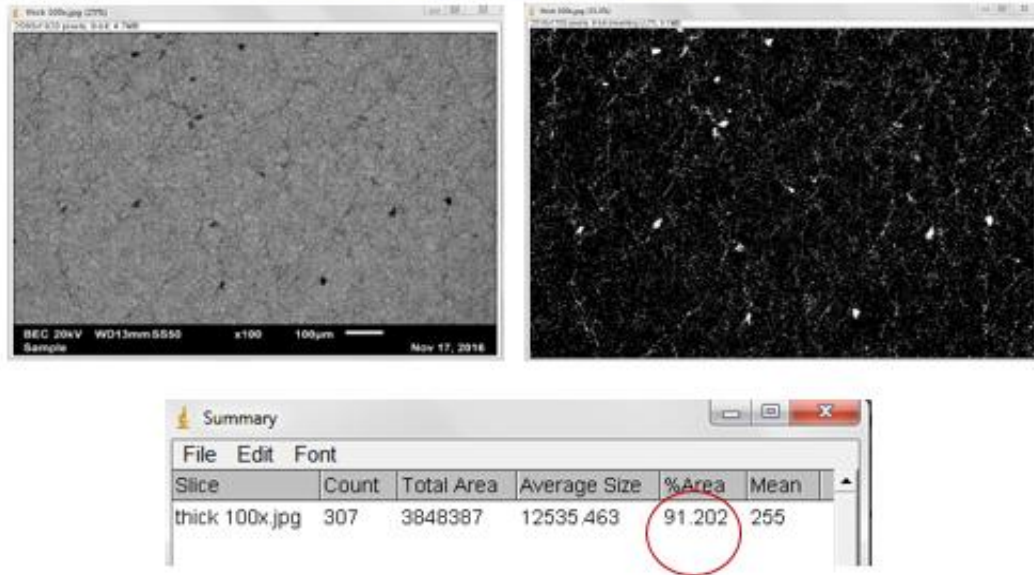
FIG # 80: Volume Fraction Using J IMAGE and SEM at 0% Stretch

Volume Fraction by SEM and J Image: 50 % Stretch

From 3 SEM images, the average volume fraction at 50 % stretch was calculated at 77% using Image J software

Slice	Count	Total Area	Average Size	%Area
thin 100x.jpg	2871	2999054	1044.603	73.38
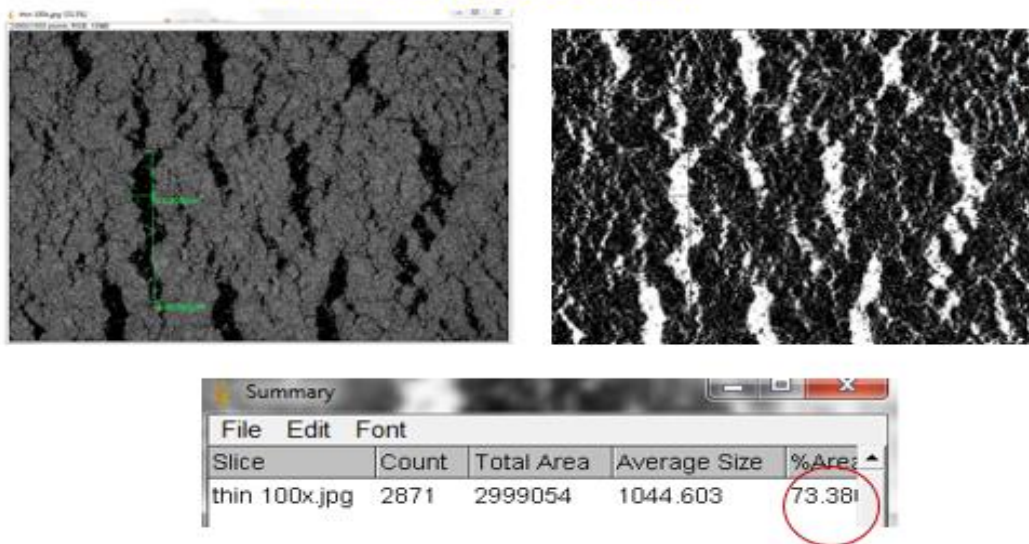
FIG # 81: Volume Fraction Using J IMAGE and SEM at 50% Stretch

Once the volume fraction is calculated a graph can be developed showing the relationship between the volume fraction and percentage strain (Fig. 82) for the straight line and the sine wave patterns. As expected, the volume fraction decreases with additional strain.
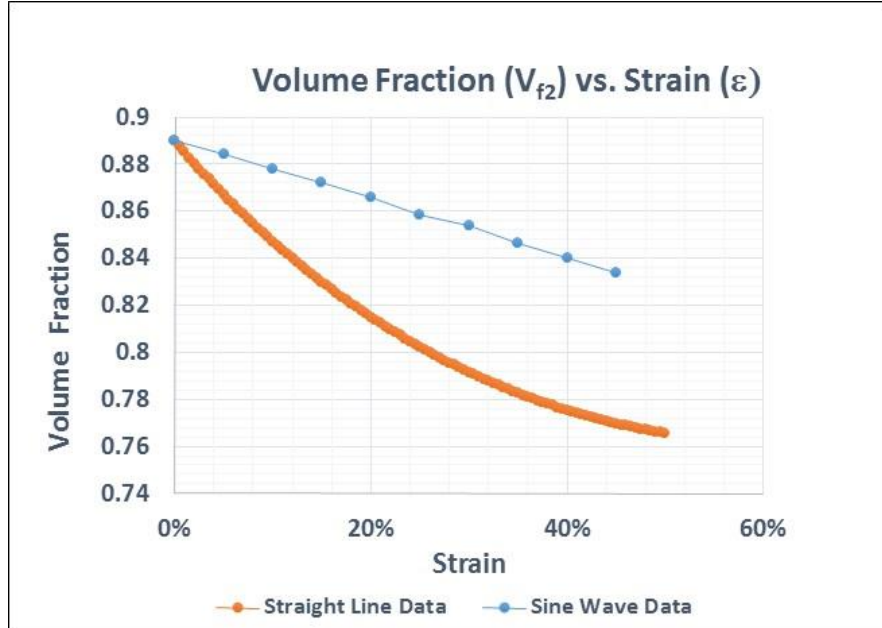
FIG # 82: Calculated Volume Fraction Versus Strain Curve

The relationship between the resistance and the stretch strain can be developed by employing the following equations from Percolation Theory [103]:

$$\sigma = \sigma_{silver}(V_f - V_c)^S \qquad \ldots\ldots\ldots \ldots\ldots\text{EQUATION \# 6}$$

Here, σ is the conductivity of the composite, σ_{silver} is the conductivity of the silver flakes, V_f is the volumetric fraction of the silver flakes, V_c is the critical volumetric fraction at percolation threshold, and S is the fitting exponent. The silver flakes were modeled as being homogenously distributed agglomerates having an average diameter of 10 μm. Ohmic connectivity only happens when V_f is $> V_c$.

The critical volume fraction, V_c can be determined using the carbon nanotubes (CNT) agglomerates model [124] by using equation (7).

$$V_c = \frac{V_{local}\pi}{6} \qquad \ldots\ldots\ldots..\ldots\ldots\text{EQUATION \# 7}$$

Here, V_{local} is the local volume fraction of CNT contained within an agglomerate. In our case, since there we have no CNT inside the agglomerate, $V_{local} = 1$. Hence, we can determine $\frac{\sigma_f}{\sigma_0}$ by combining equations (6) and (7) to obtain equation (8).

$$\frac{\sigma_f}{\sigma_0} = \frac{\sigma_{silver}(V_{f2}-V_c)^S}{\sigma_{silver}(V_{f1}-V_c)^S} = \frac{(V_{f2}-V_c)^S}{(V_{f1}-V_c)^S} \qquad \dots\dots\dots\dots\dots\text{EQUATION \# 8}$$

Here, V_{f1} is the volume fraction of the silver flakes at 0% strain, and V_{f2} is the volume fraction of the silver flakes at a strain of ε. V_{f1} and V_{f2} were derived from SEM images taken on a non-stretched and stretched sample respectively.

The volume fraction of the silver flakes at 0% strain, V_{f1}, and at ε strain, V_{f2}, can be defined as:

$$V_{f1} = \frac{V_{silver}}{V_1}, \; V_{f2} = \frac{V_{silver}}{V_2} \qquad \dots\dots\dots\dots\dots\text{EQUATION \# 9}$$

Here, Vsilver is the total volume of the silver flakes, which remains constant upon stretching, and V1 and V2 are the volumes of the silver ink sample at a strains of 0% and ε% respectively.

$$V_1 = l_1 \cdot w_1 \cdot t_1 \, , V_2 = l_2 \cdot w_2 \, t_2 \qquad \dots\dots\dots \dots\dots\text{EQUATION \# 10}$$

Here, l_1 and l_2 are the ink length at 0% strain and ε% strain, w_1 and w_2 are the ink width at 0% strain and ε% strain, and t_1 and t_2 are the ink thickness at 0% strain and ε% strain. For
the straight line ink pattern, we have:

$l_2 = l_1(1 + \varepsilon)$ ……EQUATION \# 11   and $w_2 = w_1(1 - v\varepsilon)$ ……….EQUATION \# 12

Here, the Poisson's ratio of the ink, v was calculated from the experimental data:

$$v = \frac{w_1 - w_2}{w_1 . \varepsilon} \qquad \dots\dots\dots\dots\dots\text{EQUATION \# 13}$$

Since the ink thickness (~ 10 μm) is significantly smaller than the length (180mm) and width (2mm), we can assume the change of the thickness to be negligible, hence $t_1 = t_2$. In our case, t1 was measured to be 10.9 microns and t2 was at 10 .5 microns (Fig.84).

Change in Thickness from 0% to 50% Stretch

Silver Ink Sample	0% Stretch	50% Stretch
Length	139.09 mm	208.94 mm
Width	2.01 mm	1.61 mm
Thickness	10.9 microns	10.5 microns
Volume Fraction of Silver	91%	77%
Resistance	2.8 ohms	141 Ohms

STRETCHABILITY

$$\varepsilon = \frac{208.94 - 139.09}{139.09} =$$

50.2%

POISSON'S RATIO

$$v = \frac{w_1 - w_2}{w_1 \cdot \varepsilon} = \frac{1.98 - 1.62}{1.98 \times 0.502} =$$

0.36

FIG # 83: Calculating Change in Thickness upon Stretching

Combining equations (11) and (12) we obtain:

$$V_2 = l_1(1 + \varepsilon) \cdot w_1(1 - v\varepsilon) \cdot t_1 = (1 + \varepsilon) \cdot (1 - v\varepsilon) \cdot V_1 \qquad \ldots\ldots\text{EQUATION \# 14}$$

From equation (9) we get: $V_{silver} = V_{f1} \cdot V_1,$

$$V_{f2} = \frac{V_{silver}}{V_2} = \frac{V_{f1} \cdot V_1}{V2} = \frac{89\% V_1}{(1+\varepsilon)\cdot(1-v\varepsilon)\cdot V_1} \qquad \ldots\ldots\text{EQUATION \# 15}$$

$$= \frac{89\%}{(1+\varepsilon)\cdot(1-v\varepsilon)} \qquad \ldots\ldots\text{EQUATION \# 16}$$

Employing Equation (16) we can develop the following graph showing the relation between the change in resistance (Rf/Ro) and stress for a straight line. Similar approach will yield the graph for the sine wave pattern. Figure 85 depicts the data obtained from the Percolation Theory equations overlaying the experimental data from Fig. 80. We see a good fit between the two sets of data, showing the usefulness of the Percolation Theory equations to explain and estimate experimental stretch data.
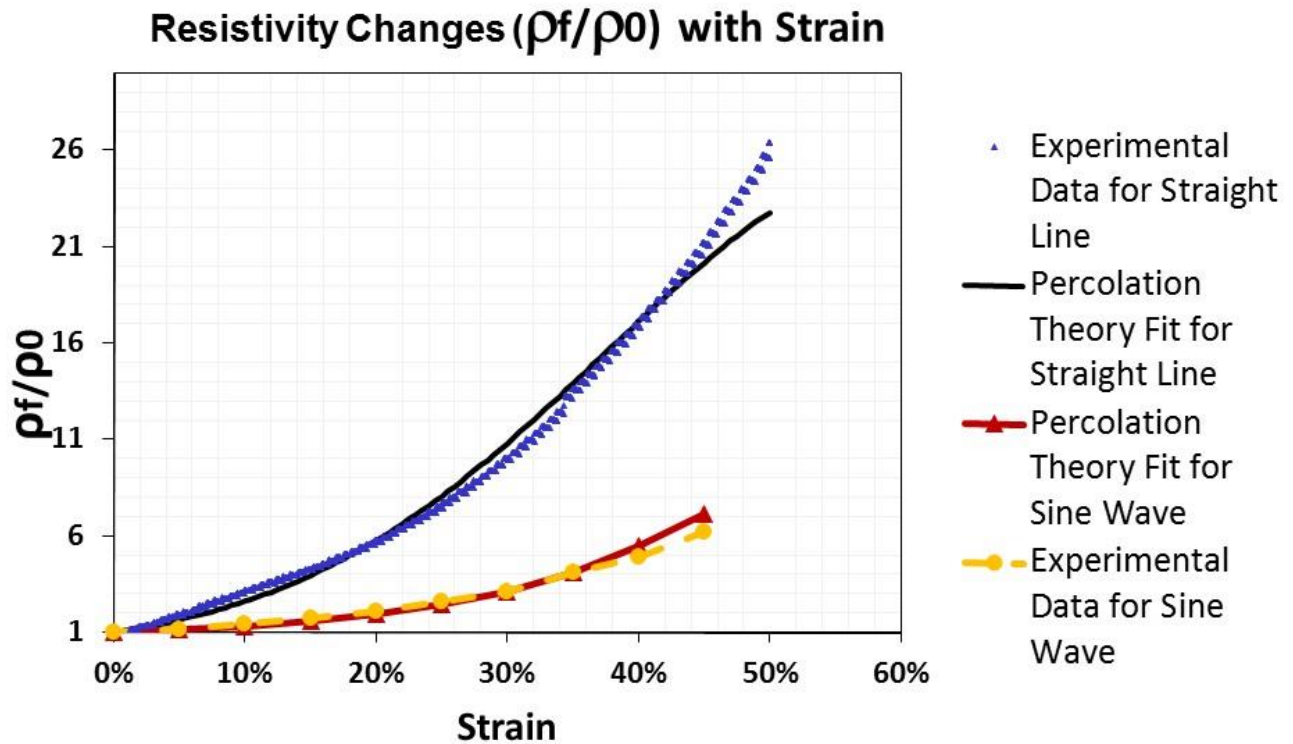
FIG # 84: Percolation Theory Equation Data Overlay on Experimental Data

5.8 Employing FEA Modeling to Estimate Resistance Changes (Rf/Ro)

The objective was to determine if the total principal strain data obtained from FEA modeling could be utilized in estimating the comparative resistance changes undergone by a straight line pattern and a sine wave pattern during stretching. The first step was to obtain the total principal strain data using FEA modeling (Fig.85). The straight line was broken down in to 10 segments and the sine wave was broken down into 25 different segments for determining total principal strain easily.
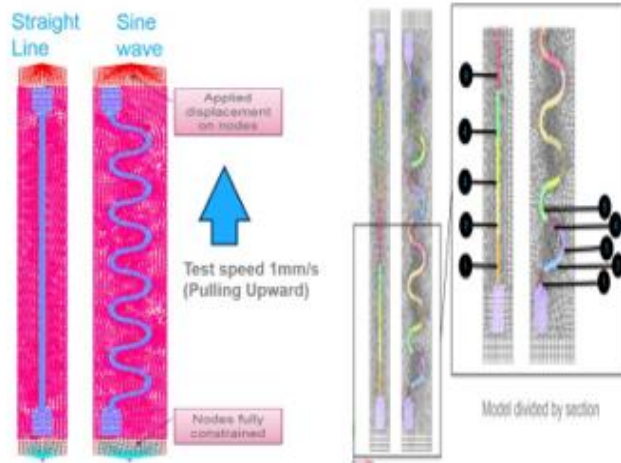
FIG # 85: FEA Modeling of Straight Line and Sine Wave Pattern

The following material and set up information, illustrated in Figure 86 was utilized in setting up the FEA model.

Dimensions and Material Properties

Properties		
Material Property	**Ink (Silver)**	**Substrate (TPU)**
Modulus of Elasticity (MPa)	40	4.3
Poisson's Ratio	0.45	0.42

Dimensions		
Description	**Straight Line**	**Sine Wave**
TPU Substrate Thickness (mm)	0.106	0.106
TPU Substrate Width(mm)	20	30
TPU Substrate Length(mm)	205	205
Ink Thickness(mm)	0.01	0.01
Ink Width(mm)	2	2
Printed Ink Length(mm)	180	180
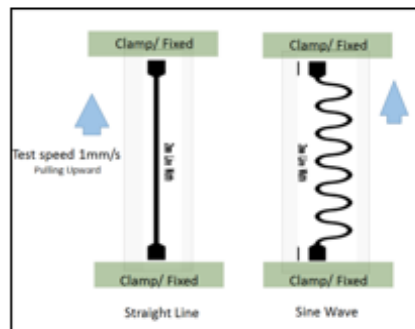
TPU is the thermoplastic urethane substrate with a Poisson's ratio of .42

FIG # 86: FEA Modeling Settings

The following methodology was utilized to arrive at the objective.

- A whole set 3D model approach was used in this analysis.
- Ink and substrate material properties were provided.
- For the substrate, a hyper-elastic material model was used (based on shore 60A).
- Several cases modeled based on different strain rates (from 0 to 50% strain) for both straight line and sine wave patterns.
- Stretching was applied at 1 mm/s.
- Model was divided into smaller sections for better granularity.
- Principal strain was calculated for the two patterns.
- Principal strain was then converted into resistance using the straight line function and a graph was plotted from 0 to 50% strain.
- Compare graph with the curve from the experimental data

The sine wave pattern was broken down into 25 sections and the straight line pattern into 10 equal sections to obtain better granularity for calculating total principal strain.
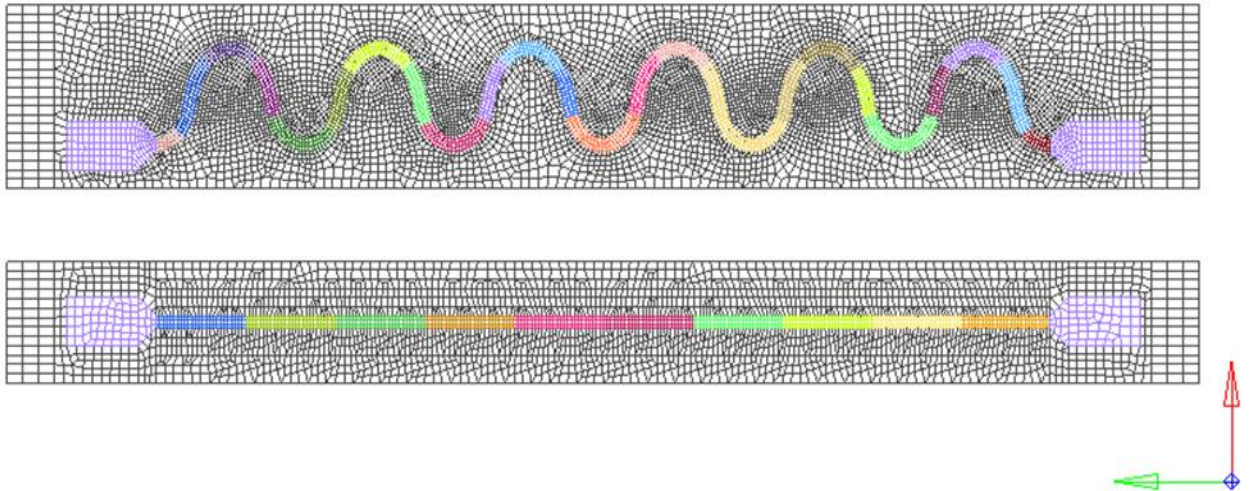
The FEA simulation provide principal strain for each small sections. The principal strain for each small section was converted into resistance, using the quadratic equation from Figure 79. (Equation #17 and 18) for the straight line and sine wave pattern. For simplification, each small section of the sine wave pattern was assumed to behave like a straight line. Resistance from all the sections were added to obtain total resistance. From Figure 79 the following two equations offer us the relationship between strain (ε) and the change in resistance (Rf/Ro) induced by stretching.

$$\frac{R_f}{R_0} = 1.5702e^{7.3202 \cdot \varepsilon} \quad \text{(for straight line)} \qquad \text{…..EQUATION \# 17}$$

$$\frac{R_f}{R_0} = .8605e^{4.7621 \cdot \varepsilon} \quad \text{(for sine wave)} \qquad \text{…..EQUATION \# 18}$$

After calculating the total principal strain from FEA modeling, we can replace the strain (ε) from the equation with principal strain and obtain the FEA fit component for the following graph in Figure 87, where we see the overlay of the FEA Modeling data and the Percolation Theory equation data on the experimental data, showing an acceptably good fit between the three approaches. Hence we can see the that the resistance changes induced by stretching, on different screen printed patterns, can be estimated using FEA modeling data and explained by using Percolation Theory data.
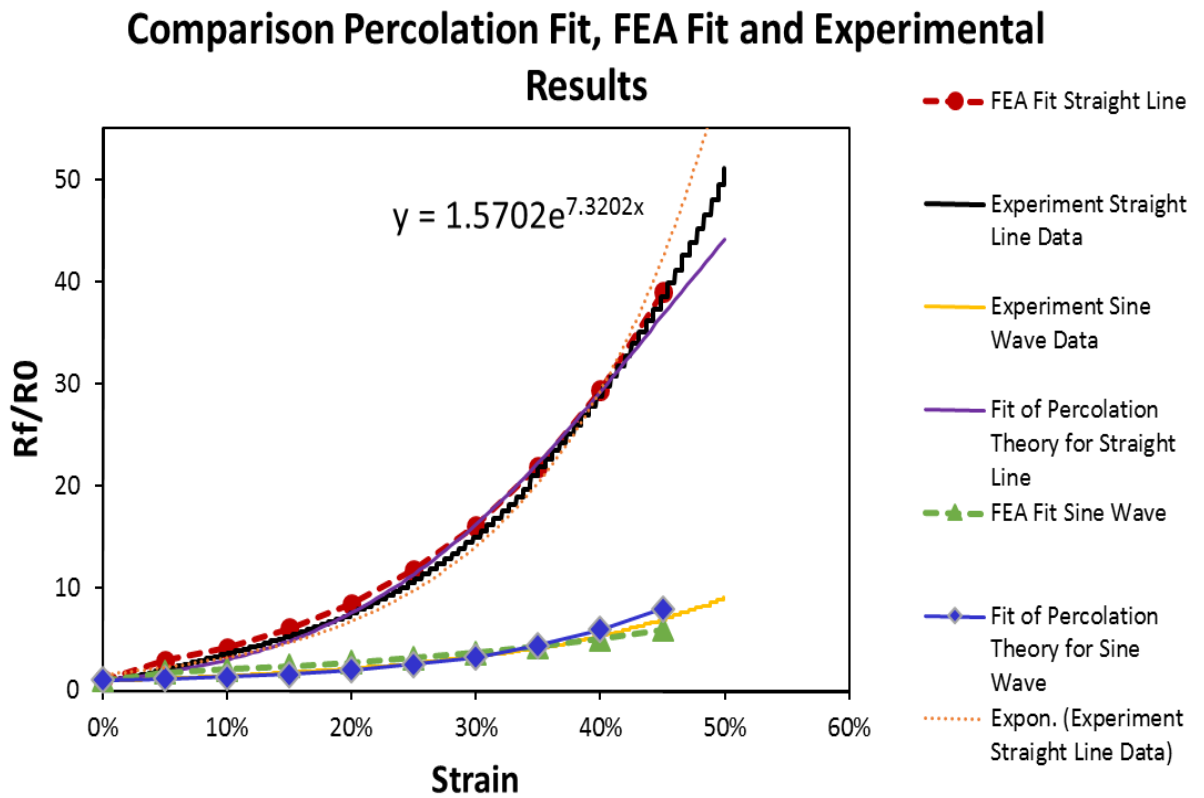
FIG \# 87: Experimental Data with Percolation Data AND FEA Data

5.9 Additional Experiments

The next set of experiments was an effort to determine if the approach of estimating the change in resistance induced by stretching would also work on other meandering patterns like the sine wave pattern. Fig. 88 shows that this approach would also work on other meandering patterns and can enable us to select the most optimal pattern for stretchability during the design phase.

FIG # 88: Rf/Ro Changes for Different Patterns with Gen 2 Ink

Most of the experimental work for this chapter studied the comparative change in DC resistance between a straight line and sine wave pattern. It was decided to run an experiment monitoring the change in AC impedance between the straight line and sine wave pattern. Results show that the sine line pattern still performs better (Figure 89) even for AC applications.

Straight Line versus Sine Wave under AC Load and 10% Stretch

- **Greater power loss in straight line pattern**
- **Both patterns show deterioration of signal integrity**
- **Greater signal noise was seen on straight line pattern**
- **Straight line pattern power loss = 326mV**
- **Sine wave pattern power loss = 292mV**

FIG # 89: Straight Line versus Sine Wave under AC Load and 10% Stretch

5.10 Conclusion

The research carried out was successful in demonstrating that that the comparative change in resistance caused by stretching, between a screen printed straight line pattern and a sine wave pattern can be estimated by calculating the total principal strain using FEA modeling and explained by using Percolation theory. Both the data obtained from FEA modeling and the Percolation data exhibited a good fit with the experimental data.

The data showed that the change in thickness when the ink was stretched from 0% to 50%, was very nominal (from 10.9 microns to 10.5 microns, 4%) and that would not explain the change in resistance from 2.8 ohms to 141 ohms.

When the ink was stretched to failure a typical fatigue curve was seen where, as the stress was increased the number of cycles to failure decreased. Failure was defined as the point the ink exhibited a reading more than 30 times the original (Ro) reading at a constant stress. Hence the change in resistance during stretching could also be explained by fatigue in addition to Percolation theory and it could be estimated using the maximum principal strain obtained through FEA modeling.

The research also helped develop some complex wavy patterns that should further enhance the printed ink stretchability, albeit it will require fine line screen printing capabilities. The research also demonstrated that the optimal screen printed pattern for stretchability can be designed using FEA modeling and that total maximum strain could be used to estimate the increase in the change in resistance.

Chapter 6: Screen printing of 50 micron lines using the stretchable ink

6.1 Introduction

In this section, we cover the last aspect of the thesis work dealing with fine line screen printing of the stretchable conductive inks. Miniaturization is a very powerful enabler for WE and IoT products hence it would be important to develop a stretchable conductive ink which could also be fine printed to lines as narrow as 50 microns. Typical width of screen printed conductive links on current microelectronics product is around 125 to 200 microns [133, 134]. There are available technologies that use photoresist and lithographic technologies to obtain finer lines around 50 microns for special applications, especially on 99% smooth, ceramic substrates. The current thesis will demonstrate the capability of screen printing 50 micron lines using stretchable conductive inks on stretchable polyurethane type substrates. It should be borne in mind that stretchable conductive inks rely on stretchable polymer binders to exhibit stretchability and that makes it harder to print fine lines. In contrast highly conductive, non -stretchable inks have very high metal filler content, making it more amenable for fine line printing.

6.2 Brief Overview of Screen Printing Process

Before discussing fine line screen printing using stretchable conductive ink, a brief overview is presented to establish some basic components of the screen printing process. We will cover briefly the following key areas: Ink rheology and composition, screen and squeegee parameters, screen printer setup parameters, substrate and the print environment.

6.2.1   Ink Rheology and Composition

The rheology and composition of the printed ink are important contributors for achieving acceptable screen printing qualities in microelectronics applications. Good screen printed inks will depict a non -Newtonian rheology [135], meaning that the viscosity of the ink will remain high when the ink is sitting on the screen and will not flow through the screen mesh but when the ink is subjected to a high shear stress, like when the ink is pushed through the openings of a screen by a squeegee, it will exhibit very low viscosity and will flow easily to cover the printed area. When the stress is removed the ink quickly regains its high viscosity and will not flow further. The conductive ink composition generally includes a functional phase which includes metal powders like Ag, Au or Cu and it may include some nano materials technology to improve the sintering and low temperature curing of the ink. The binder phase of the conductive ink is designed to attach the ink to the substrate, during and before the curing process. The role of the vehicle phase is to become the carrier for the metal powders before the curing process and it includes volatile solvents and non-volatile organic

polymers. Lastly we have the solvent phase which essentially determines the viscosity of the ink. [136, 137]

The solids content, meaning the percentage of functional phase materials, the ink rheology, the ink morphology, meaning the dispersion and flake size and distribution of the metal powder and the evaporation rate of the vehicle phase will all play a role in determining the printability of the conductive ink. The paste viscosity is the most important rheological quality of the paste that has significant impact on fine line printing [138, 139, 140].

The following picture (Figure 90) illustrates the basic screen printing principles.
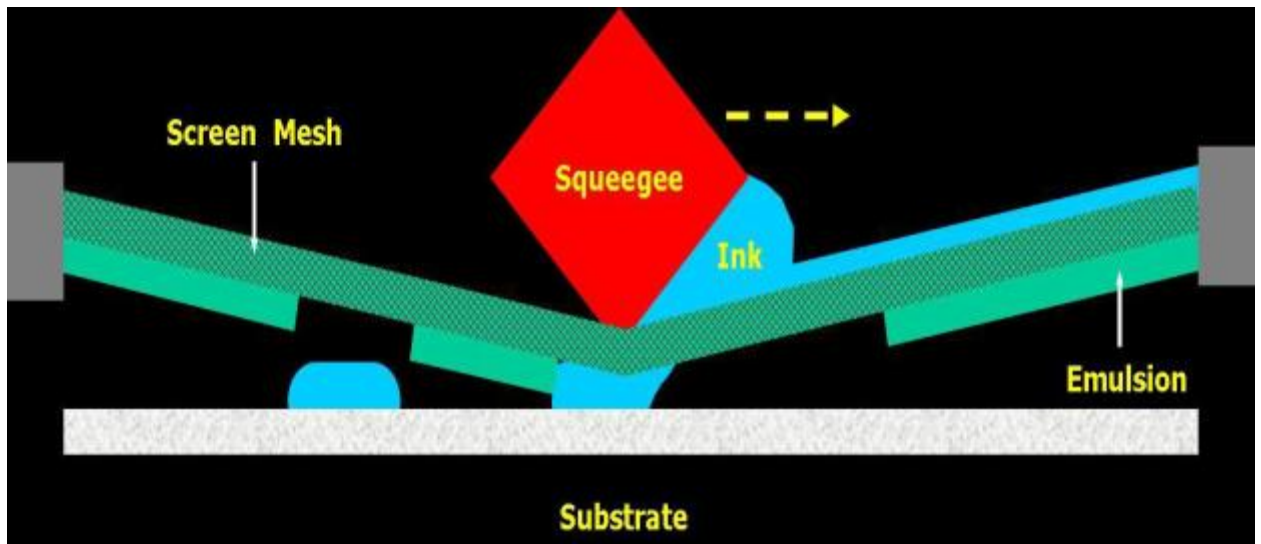
FIG # 90: Basic Screen Printing Process

(1) The rubber squeegee transfers the conductive ink across the screen mesh
(2) The screen emulsion defines the printed pattern
(3) The mesh count of the squeegee, the mesh angle, the screen wire diameter and the emulsion thickness will have an effect on the resulting print.

6.2.2   Screen and Squeegee Parameters

The screen plays a very important role in the screen printing process. This is even more important when printing of fine lines is required. Mesh count is the number of wires or openings that are contained in one linear inch. Hence the higher the mesh count the thinner is the wire diameter and the less the percent open area. Generally, a higher mesh count screen is desirable for fine line printing. Fine line printing will generally require a screen mesh count of 325 mesh (Figure 91) or higher. The emulsion thickness acts like

the gasket for the screen and it also defines the screen pattern. Usually the higher the screen emulsion the thicker will be the height of the printed ink. Finer mesh angle 45 degrees or lower tends to yield finer printed lines and a lose screen tension will result into coarser lines. The screen tension is the tautness of the stretched screen mesh measured in Newtons per centimeter. High tensile strength wires also tend to support finer printed lines. The screen mesh parameters play an important role in achieving fine line printability [141, 142]. Other screen factors that are important to control besides the screen mesh, and the wire angle are the screen tension and the proper alignment of the printed pattern along the angled screen wires. The angle that the squeegee head makes with the screen plane, commonly referred as the squeegee angle is also an important parameter to control. The hardness of the squeegee material is the most important parameter for enabling fine line printing [133] and the geometry of the squeegee material [134] is also important to monitor and control. Generally, a squeegee hardness of 80 durometer or higher, with a diamond pattern will enable fine line printing. Squeegee material, squeegee parallelism to the screen and the squeegee length compared to the print size are all important factors to consider [133].
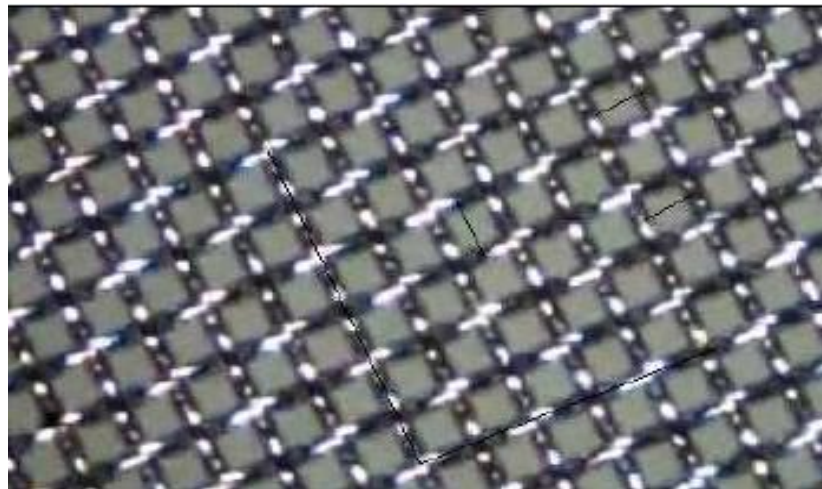
FIG # 91: 325 Mesh Stainless Steel Mesh with 22.5 Degree Angle

6.2.3   Screen Printer and Setup Procedures

The proper setup of the screen printer (Fig # 92) is also vital for achieving fine line printing. Some important parameters to monitor are squeegee pressure, squeegee angle, print direction, printing speed, stroke length and the snap off distance. The stroke

length is the distance the squeegee travels and the snap off distance is the space between the screen and the substrate prior to the printing stroke.

FIGURE # 92: DEK Printer- Model # LPiX used for fine Line Printing

6.2.4 Substrates

The substrate is where the screen printed ink gets deposited. There are many different types of substrates in the industry like Alumina substrates, Aluminum Nitride substrates, Glass substrates, FR4 substrates, flex PCB substrates, HTCC (High Temperature Co-fired Ceramics), LTCC (Low Temperature Co-fired Ceramics) and many others. Generally, the smoother the substrate finish the better are the chances of printing fine lines. It is much easier to print fine lines on 99% polished Alumina substrates than for example on FR4 substrate.

An ideal stretchable substrate should also be planar, insulative and resistant to most chemicals while offering excellent bondability, hydrolytic stability and strong mechanical support with a melting point which is higher than 200°C. Silicones, polyethylene terephthalate (PET), polyurethane (PUT), thermoplastic poly urethanes

(TPU) and poly dimethyl siloxane (PDMS) are some examples of available stretchable substrates. The challenging part is that these substrates do not tend to be very smooth and have very low glass transition temperature (Tg) hence they have to be cured generally under 150 C. After being stretched a number of times most of them do not fully recover to their original relaxed state. Compatibility issues with the stretchable conductive ink is another challenge. This could lead to metal delamination under thermal or mechanical stress. Hence careful consideration is required in selecting the appropriate substrate.

Another important concern with stretchable substrate is that they tend to be quite thin (1 mil to 5 mils thick) so that it is easier to stretch them. Because they are so thin they get deformed during the vacuum hold process when the printing takes place leading to distortions in the print image. Some companies like BEMIS use an adhesive layer to hold the thin substrate during the printing process and releasing it after printing is completed. American Polyfilm, BEMIS and DuPont are some key suppliers of stretchable substrates in the industry.

6.2.5 Printing Environment

A clean environment is necessary for printing fine line patterns otherwise the contaminants in the air can easily cause a clog in the screen leading to open failures in the printed patterns. Fine line printing is generally carried out in a class 10K clean room environment where strict cleanliness rules are applied like wearing booties and head cover. Since the viscosity of the ink is very important it is critical to control the temperature and humidity of the printing room environment. The recommended temperature for fine line printing is 72C +/- 3C and the recommended humidity is 30 to 40%.

6.2.6 Holistic Approach

To obtain fine line printing a holistic approach needs to be considered because there are many parameters that end up affecting the final result. Proper set up of the screen printer equipment, matched appropriately with the proper squeegee, screen, ink, substrate and the environment, are all required for a successful process. This is depicted in Table 5 below.

FACTORS AFFECTING THE QUALITY OF FINE LINE SCREEN PRINTING					
PRINTER SETUP	**SQUEEGEE**	**SCREEN**	**INK**	**SUBSTRATE**	**ENVIRONMENT**
Print Speed	Hardness	Mesh Count	Viscosity	Surface Roughness	Temperature
Print Direction	Parallelism	Wire Material	Rheology	Planarity	Humidity
Snap Off Distance	Size and Shape	Wire Diameter	Percent Solid	Compatibility with Ink	Contaminants
Squeegee Pressure	Material	Mesh Opening	Morphology	Mechanical Strength	
Squeegee Down stop	Attack angle	Mesh Thickness	Particle Size	Chemical Resistance	
Stroke Length		Mesh Weave	Particle Distribution	Glass Transition (Tg)	
Amount of Ink on screen		Mesh Angle	Homogeneity	Cleanliness	
		Emulsion type	Stability		
		Emulsion Thickness	Compatibility with Substrate		
		Screen Tension	Binder System		
		Screen Size	Vehicle System		
		Pattern Positioning	Shelf Life		

TABLE # 5 Screen Printing Factors Affecting Fine Line Printing

6.3 Methodology

The objective of this research section is to demonstrate capabilities for printing straight lines which are 50- micron wide or thinner, using stretchable conductive inks on stretchable substrates to enable miniaturization.

The first phase was to determine the best line width we could print repeatedly, using a stretchable conductive ink on a PET substrate. Even though a PET substrate is not very stretchable it is flexible and has a very smooth surface which is very conducive to fine line printing. This would allow us to understand the behavior of the stretchable ink on a substrate which is commonly used for fine line printing because of its smoothness.

The second phase was to determine if we could print 100 micron lines repeatedly using the stretchable conductive ink on a selected stretchable substrate. This would be closer to our objective of printing stretchable conductive inks on selected stretchable substrates.

The third and final phase was to determine the finest line width we could print using the selected stretchable conductive ink from phase two on the selected stretchable substrate from phase two.

6.4 Sample Development

The stretchable conductive ink used to print fine line straight lines was the second generation stretchable (Gen 2) ink. The ink was chosen because of its superior stretchability and high conductivity. The ink also exhibited excellent adhesion to thermoplastic polyurethane substrates. The ink viscosity used was 10Kcps and it had ~85% silver content. The ink resistivity was 30 milliohms per square for 1 mil thick line and the ink was cured at 120 C for 10 minutes in an ambient air oven. The stretchable substrate used was a TPU from Bemis. The screen printer (Figure 90) used was a DEK Lxpi printer with the following settings depicted in Table 6.

PARAMETER	DETAIL
Mesh type	Stainless steel
Mesh Count	325
Screen Tension	25 Newtons/cm
Screen Emulsion Thickness	25 microns
Squeegee	Polyurethane squeegee with diamond shape
Squeegee hardness	80 durometers
Squeegee Attack angle	45 degrees

TABLE # 6: Recommended Settings for Fine Line Printing on DEK Lxpi Printer

6.5 Results

6.5.1   Phase One Results

For the first phase the Generation 1 stretchable conductive ink was printed on PET substrate using straight lines which were 400 microns wide. This was planned to develop a baseline to ensure that the printing process was under control. PET, which is a known good substrate was used to ensure there were no compatibility issue.

There were some initial issues with regards to using the appropriate screen mesh and squeegee material. Once that was solved, the results were quite promising and there were no other issues encountered. (Figure 93) The screen mesh used for this case was 325 mesh screen, 45-degree mesh angle and a 70 durometer, polyurethane squeegee with a diamond shape.
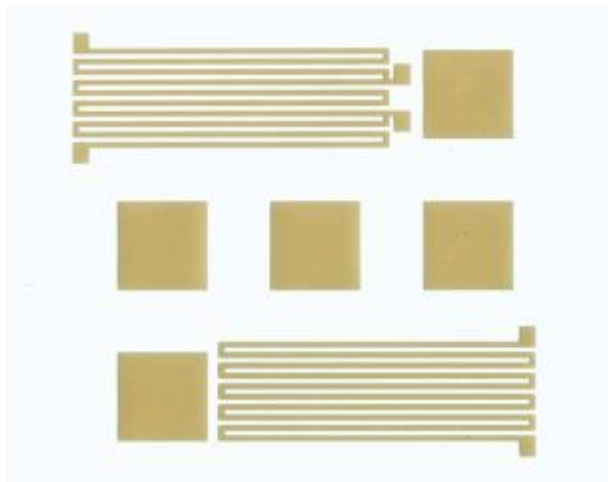
FIG # 93: 400 Micron Lines on PET Substrate with GEN 1 INK

6.5.2   Phase Two Results

The second phase needed some decisions to be made. The PET substrate printed well but it was a flexible substrate and not stretchable. Few stretchable substrates were evaluated from American Polyfilm and Du Pont and initial testing showed that the best stretchable substrate seemed like the American Polyfilm Polyurethane VLM 3301. The first generation stretchable ink exhibited fine printing capabilities and 100 microns and 150 micron fine lines were achieved using both straight line and sine wave pattern. (Figure 94). Phase two leveraged the same ink, the same printer and screen setting used for phase one. Unfortunately, upon stretch testing, it became quickly evident that the first generation ink was delaminating from the stretchable substrate upon 20 % stress. This necessitated the need for a second generation (Gen 2) ink for phase three.
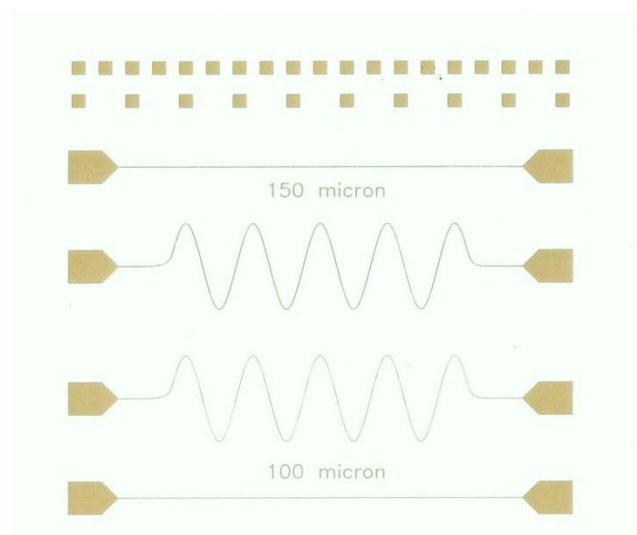
FIG # 94: 100 & 150 Micron Lines on VLM 3301 Substrate with GEN 1 Ink

6.5.3 Phase Three Results

A new screen (Figure 95) was designed for phase three to determine if it was possible to print lines narrower than 100 microns using Generation 2 ink. The stretchable substrate used was a TPU supplied by BEMIS and the parts were fabricated on the DEK machine using screen printing parameters developed in phase two.
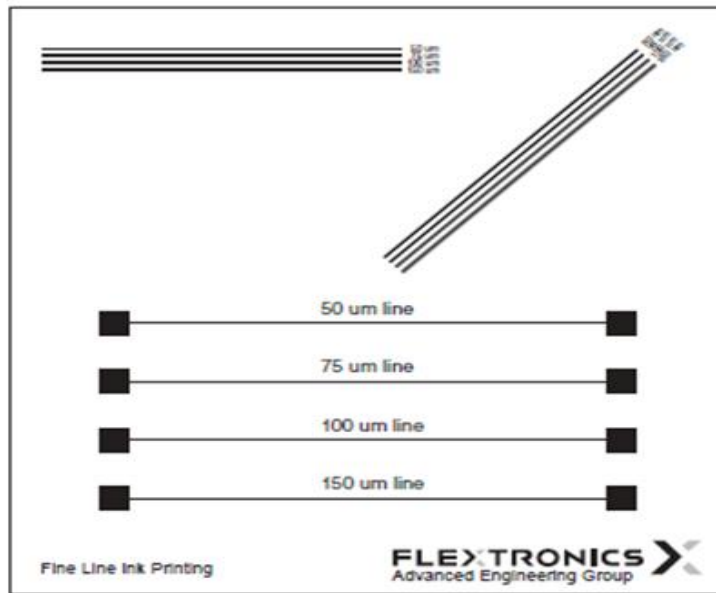
FIG # 95: Screen Pattern Designed for 50 to 150 Micron Thin Lines

Using the new screen pattern and following screen printing parameters gleaned from the phase two efforts it was possible to demonstrate the printing of 75 micron lines (Fig 96- 98) with good (> 85%) yields. 50 micron lines were also printed but the yield was lower (~ 70%).
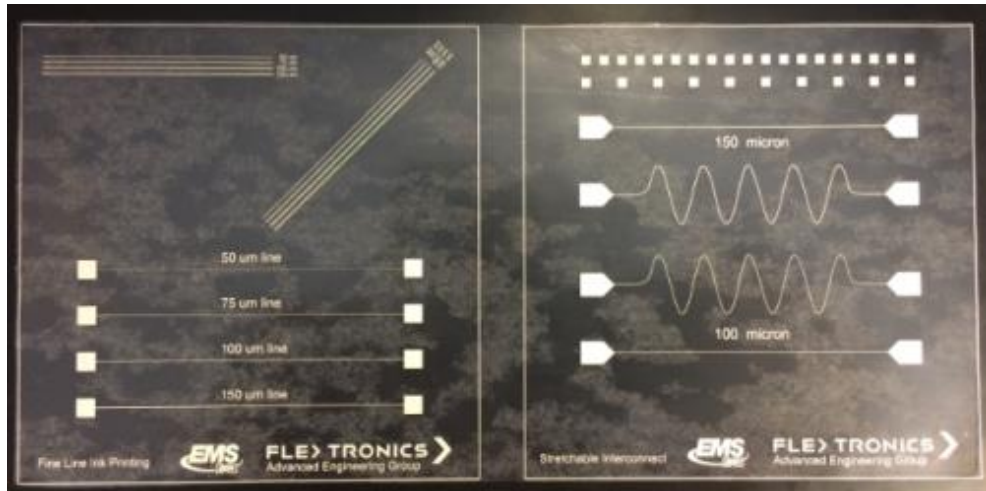
FIG # 96: GEN 2 Ink on TPU Substrate Printed with 50 to 150 Microns Thin Lines

Line Resistance, Width and Thickness
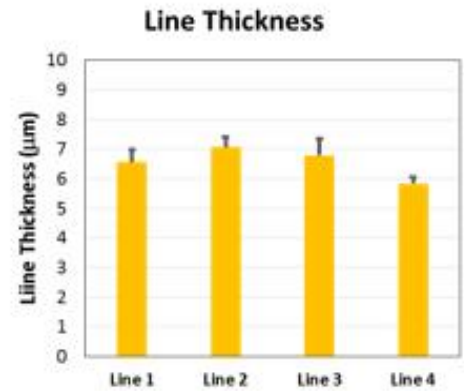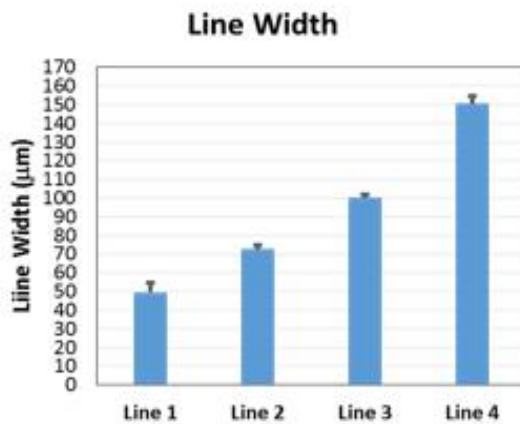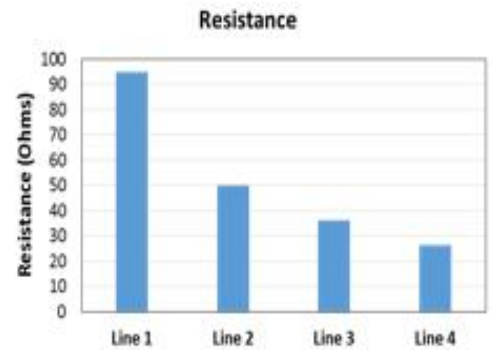
FIG # 97: Resistance, Width and Thickness of 50, 75, 100 and 150 Micron Thin Lines
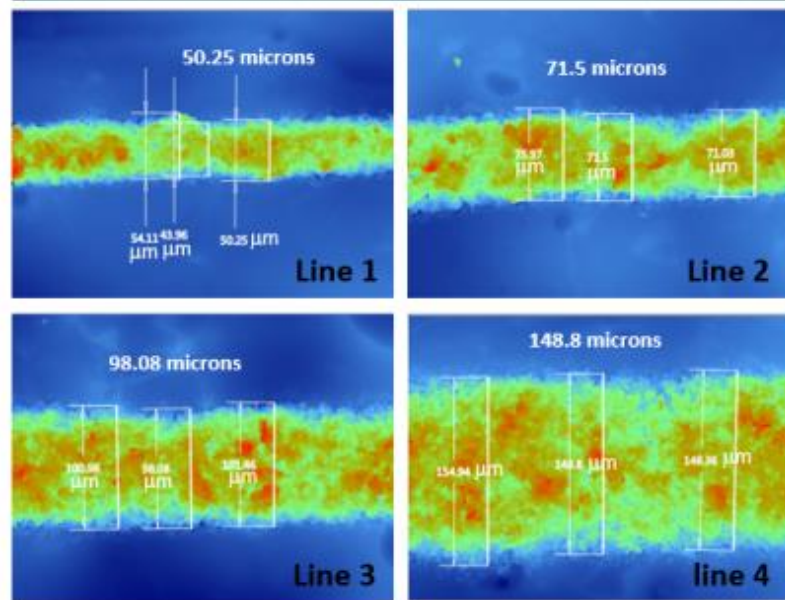
FIG # 98: 3D Camera Validation of 50, 75, 100 and 150 Micron Thin Lines

6.6 Conclusions

The current thesis work was successful in meeting the stated objective of printing straight lines which were 50 microns wide or thinner using stretchable conductive inks on stretchable substrates. The work also went ahead to prove that 50-micron thick sine wave patterns were also printable. The work also demonstrated that 50 micron lines could be achieved on at least two different types of stretchable substrates. Screen printing parameters for fine line printing were enumerated and recommendations offered.

Chapter 7: Summary and Conclusion

7.1 Introduction

In this section the summary of the key research results is presented in section 7.2, the limitations of the current work are pointed out in section 7.3, recommended directions for future work, to keep on expanding this new technology of stretchable interconnects are offered in section 7.4 and section 7.5 ends with some concluding remarks.

7.2 Summary of Results

The current thesis was able to achieve all three of the initially established objectives;

(1) Demonstrate the development of a new screen printable and stretchable conductive ink, that can withstand over 500 cycles of stretching at 20% strain without increasing the resistance by more than 30 X. This is a key contribution enhancing the current state of the art.

(2) Demonstrate that the comparative change in resistance caused by stretching, between a screen printed straight line pattern and a sine wave pattern can be estimated by calculating the total principal strain by FEA modeling and explained by using equations from Percolation theory. This is also a key contribution enhancing the current state of the art.

(3) Demonstrate the printability of stretchable conductive lines which are 50 microns wide or thinner. Even though this is the first study of its kind on printing 50 micron lines using a screen printable conductive ink, this is not claimed as an achievement that enhances the current state of the art because this has been achieved on screen printable, non-stretchable ink.

This ink was developed by running a set of experiments and failure analyses studies of available conductive inks with 'limited stretchability', to understand the causes of stretchability failures. After some critical analyses and experimentation, I developed solutions to overcome these failures. It was my research leading to two key critical insights (bimodal flake distribution and elastomeric chain polymerization) which led me to the development of this new stretchable and screen printable conductive ink. This stretches the current state of the art because prior to my research, the best screen printable and 'stretchable' conductive ink exhibited around 30 cycles of stretchability at 20% strain with an increase in resistance by more than 1000 X.

The stretchable conductive ink was also tested for preliminary reliability testing like thermal cycling and 85/85 relative humidity. Using a similar approach and replacing the metal flakes with glass, a stretchable dielectric was also developed to enable multi-

layer circuitry and stretchable capacitors. A universal flex tester was also designed and developed to assist in testing the stretchability, bendability, flexibility and some other mechanical characteristics of the stretchable conductive ink.

The research was able to demonstrate that by employing FEA modeling and calculating the total principal strain it was possible to estimate the change in resistance. The research also showed that Percolation Theory equations could be used to explain the change in resistance induced by stretching. The research also showed that it was possible to develop optimum designs for enhanced stretchability by leveraging FEA modeling and calculating the total principal strain for the design pattern. Some complex, meandering patterns were also developed which would be able to augment the stretchability.

Finally, the research demonstrated the capability of printing stretchable conductive inks with fine lines which were 50 microns in width. Recommendations for printing techniques and screen parameters were offered for the fine line screen printing of stretchable conductive inks. This capability would be very helpful for enabling the miniaturization of wearable products.

7.3 Limitations of Current Work

The stretchable ink developed during the current research is much better than what was previously available, however it still needs to be developed further. A good target would be to meet at least 2000 cycles of stretch at 20 % strain. The current research was only able to develop few different types of TPU substrates, more work needs to be done to evaluate different types of stretchable substrates to meet the different needs of the market. The stretchable electronic used within a human body, or the stretchable jersey of a soccer player or the insole of an athlete's shoe will all require different types of substrates. The increase in resistance of the printed conductive ink induced by stretching should be predictable and preferably less than 2X the original resistance, hence the current ink needs significant improvement. The current stretchable conductive ink is not solderable or wirebondable and cannot be printed directly to a fabric.

7.4 Recommendations for Future Work

Stretchable electronics is a brand new field, it is a new paradigm which will offer new capabilities and possibilities for electronic products. The current research is just the tip of the iceberg. There is much more work to be covered in this technology space, some recommendations are offered below.

- Develop stretchable and screen printable conductive inks to last more than 2000 stretch cycles at 20% or higher strain without changing its resistance by more than 2X. The current research focused only on uni-axial strain, future work should also consider torsional strain.

- Develop a stretchable and screen printable, multi- layer electrical structure with stretchable substrates, conductives, resistives, dielectric and encapsulants.
- More research needs to be done in developing polymers that could be used as effective binders for stretchable conductive inks. New elastomers need to be developed for substrates with minimal mechanical hysteresis effect.
- Develop stretchable conductive inks with silver combined with new stretchable materials like graphene, silver nano-flowers and carbon nano tubes [134, 143, 144].
- Various techniques to significantly increase the flake surface area and inter-connect points need to be developed.
- Develop industry standards for testing various tests like stretching, bending, flexing using the universal flex tester.
- Understand why the conductivity improves after the stretchable conductive ink gets exposed to 85C/85% RH testing
- Develop protective encapsulants with controlled stretching. This will prevent circuit failures by over stretching.
- Develop stretchable die attach adhesives to handle CTE mismatch between the die and the substrate.
- Develop stretchable conductive inks that are solderable and wirebondable
- Develop stretchable conductive inks that could be printed directly to fabrics [145,146].
- Develop stretchable conductive inks for artificial skin and soft robotics [147].
- Enhance theoretical understanding of the stretchability of conductive inks [148-151].

7.5 Concluding Remarks

Stretchable electronics is very well poised to participate in emerging new technologies like Wearable Electronics (WE), Internet of Things (IoT) and Flexible Displays (FD). This is a new technology in the engineer's tool kit and psyche. It will give rise to new products like the bio inspired camera that mimics the human eye or the stretchable electronic monitoring patch used for a Brain Trauma Injury (BTI) patient. This nascent technology will need a lot of research and development work to keep pace with the rapid demands of the world of the future. The current research is definitely a very tiny step towards this long and exciting journey.

REFERENCES

[1] Mark Weiser, "The computer for the 21st Century", *Scientific American,* 1991: 94-104

[2] Rajiv R. Singh, "Preventing Road Accidents with Wearable Biosensors and Innovative Architectural Design", *2nd ISSS National Conference,* Nov 2007: 1-8

[3] S. Patel, H. Park, P. Bonato, L. Chan and M. Rodgers, "A review of wearable sensors and systems with application in rehabilitation", *Journal of Neuro Engineering and Rehabilitation,* 2012, 9:21,

[4] Teng X.F, Zhang Y.T, Poon CCY and Bonato P, *IEEE Reviews in Biomedical Engineering,* 2008, 1:62-74.

[5] M. Hilder, B. W. Jensen and N.B. Clark, *Journal of Power Sources,* 2009,194, 1135

[6] C.C. Ho, K. Murata, D.A. Steingart, J.W. Evans, and P.K. Wright, *J of Micromechanical Engineering,* 2009, 19, 940

[7] Preradovic, S., Roy, S. and M. Karmakar, N.C., *Antennas & Propagation Magazine,* Volume 53: 5

[6] Haopeng Wang, Debao Zhou and Jianguo Cao, *IEE Transactions on Nanotechnology,* Volume12:4

[7] T. Braun, F. Hausel, J. Bauer, O. Witler, R. Mrossko et al., "Nano particle enhanced encapsulants for improved humidity resistance", *58th ECTC Conference*, May, 2008

[8] P.A. Muennig and S.A. Giled, "What changes in survival rates tell us about US health care", *Health Affair*, 2010, 29: 2105-2113

[9] S.P. Gulley, E.K. Rasch and L. Chan, "If we build it who will come?" *Medical Care* 2011, 49: 149-155

[10] Rogers, J. A., Someya, T. & Huang, Y., "Materials and mechanics for stretchable electronics", *Science* 327, 1603–1607 (2010) CAS

[11] Fan, Z. et al., "Toward the development of printable nanowire electronics and sensors", *Adv. Mater.* 21 (2009) CAS: 3730–3743

[12] Nolfi, S. and Floreano, D., "Evolutionary Robotics: The Biology, Intelligence, and Technology of Self-Organizing Machines", (MIT Press, 2000)

[13] Ko H C et al, "A hemispherical electronic eye camera based on compressible silicon photo electronics", *Nature,* 2008, 454: 748–753

[14] Schuettler M, Pfau D, Ordonez S, Henle C, Woias P and Stieglitz T, "Stretchable tracks for laser-machined neural electrode arrays", Conf. *Proc. IEEE Eng. Med. Biol. Soc.,* 2009: 1612–1615

[15] J. A. Rogers, Z. Bao, K. Baldwin, A. Dodabalapur, B. Crone, V. R. Raju, V. Kuck, H. Katz, K. Amundson, J. Ewing, and P. Drzaic, *Proc. Natl. Acad. Sci. U.S.A.* 98 (2001) 4835

[16] H. O. Jacobs, A. R. Tao, A. Schwartz, D. H. Gracias, and G. M. Whitesides: *Science* 296 (2002) 323

[17] M. Kaltenbrunner, M. S. White, E. D. Głowacki, T. Sekitani, T. Someya, N. S. Sariciftci, and S. Bauer: *Nat. Commun*. 3 (2012) 770.

[18] Yoonseob Kim et al, "Stretchable nanoparticle conductors with self-organized conductive pathways", *Nature*, 500, (01 August 2013): 59–63

[19] John A. Rogers, Takao Someya and Yonggang Huang, "Materials and Mechanics for Stretchable Electronics", *Sciencemag,* January 27, 2011

[20] S.P. Gulley, E.K. Rasch and L. Chan, "Ongoing coverage of ongoing care", *Am J Public Health* 2011, 101:368-375

[21] S.S. Goonawardene, K. Baloch and I. Sargeant, "Road traffic collision case fatality rate", *Am Surgeon* 2010, 76: 977-981

[22] Patel et al, *Journal of NeuroEngineering and Rehabilitation* 2012: 9:21

[23] X.F. Teng, Y.T. Zhang, C.Y. Poon and P. Bonato, "Wearable Medical System for p-Health", *IEEE Reviews in Biomedical Engineering*, 2008, 1: 62-74

[24] P. Bonato, Wearable Sensors and systems. "From enabling technology to clinical applications", *IEEE Eng. Med Biol Mag* 2010, 29: 25-36

[25] Health Care Disparities in Rural areas, National Healthcare Disparities Report for 2004, Agency *for Healthcare Research and Quality*, 2005

[26] L. Chan, L.G. Hart and D.C. Goodman, "Geographic access to health care for rural Medicare beneficiaries", *J Rural Health 2006,* 22: 140-146

[27] T.S. Caudill, R. Lofgren, C.D. Jennings and M. Karpf, "Commentary: Health Care reform and primary care: Training physicians for tomorrow's challenges", *Acad Med 2011*, 86: 158-160

[28] M.J. Mathie, A.C. Coster, N.H. Lovell, B.G. Celler, S.R. Lord and A. Tiedemann, "A pilot study of long term monitoring of human movements in the home using accelerometry", *J Telemed Telecare*, 2004,10: 144-151

[29] D. Giansanti, G. Maccioni and S. Morelli, "An experience of health technology assessment in new models of care for subject with Parkinson's disease by means of a new wearable device", *Telemed J E Health,* 2008, 14: 467-472

[30] O. Aziz, L. Atallah, B. Lo, M. Elhelw, L. Wang, GZ Yang, and A Darzi, "A pervasive body sensor network for measuring postoperative recovery at home", *Surg Innov* 2007 14: 83-90

[31] E.S. Sazonov, G. Fulk, N. Sazonova and S. Shuckers, "Automatic recognition of postures and activities in stroke patients" *Conf Proc IEEE Eng Med Biol Soc* 2009, 2009: 2200-2203

[32] O. Amft and G. Troster, "Recognition of dietary activity events using on-body sensors" *Artif Intell Med* 2008, 42: 121-136

[33] O. Amft, M. Kusserow and G. Troster, "Bite weight prediction from acoustic recognition of chewing" *IEEE Trans Biomed Eng* 2009, 56: 1662-1672

[34] M.G. Benedetti, A.D. Gioia, L. Conti, L. Berti, L.D. Eposti, G. Tarrini and NG Melchionda "Physical activity monitoring in obese people in the real life environment", *J Neuroeng Rehab* 2009 6:47

[35] E.S. Sazonov, S.A. Shuckers, P. Lopez-Meyer, O. Mekeyev, E.L. Melanson, M.R. Neuman and O.J. Hill, "Toward objective monitoring of ingestive behavior in free-living population", *Obesity (Silver Spring)* 2009, 17: 1971-1975

[36] J. Merilahti, J. Parkka, K. Antila, P. Paavilainen, E. Mattila, E.J. Maim, A. Saarinen and I. Korhonen, "Compliance and Technical feasibility of long-term health monitoring with wearable and ambient technologies", *J Techmed Telecare* 2009, 15: 302-309

[37] A. Siacqua, M. Valentine, A. Gualtieri, F. Perticone, A. Faini, G. Zacharioudakis, I. Karatzanis, F. Chianugi, C. Assimakopoulau and P. Merrigi, "Validation of a flexible and innovative platform for the home monitoring of heart failure patients: preliminary results", *Computers in Cardiology* 2009, 36: 97-100

[38] Rajiv R. Singh, "Preventing Road accidents with wearable bio sensors and innovative architectural designs", *2nd ISSS National Conf on MEMS*, ISSS- MEMS-2007

[39] M. Sung, C. Marci and A. Pentland, "Wearable Feedback System for Rehabilitation", *J Neuroeng Rehab*, 2005, 2:17

[40] C.W. Mundt, K.N. Montgomery, U.E. Udah, V.N. Barker, G.C. Thonier, A.M. Tellier et al, "A multi-parameter wearable physiological monitoring system for space and terrestrial applications", *IEEE Tran Inf Technol Biomed*, 2005, 9:382-391

[41] U. Anliker, J.A. Ward, P. Lukowicz, G. Troster, F. Dolveck et al, "AMON: a wearable multi parameter medical monitoring and alert system" IEEE *Trans Inf Technol Biomed,* 2004, 8:415-427

[42] D. Rienzo, M. Rizzo, F. Parati, G. Brambilla et al, "MagIc system: a new textile based wearable device for biological signal monitoring applicability in daily life and clinical setting" *Conf Proc IEEE Eng Med Biol Soc 2005:* 7167-7179

[43] D. Rienzo, M. Rizzo, P. Bordoni, G. Brambilla et al, "Applications of a textile based wearable system for vital signs monitoring" *Conf Proc IEEE Eng Med Biol Soc* 2006: 2223-2226

[44] J. Habetha, "The MyHeart project-fighting cardiovascular diseases by prevention and early diagnosis", *Conf Proc IEEE Eng Med Biol Soc* 2006: 6746-6749

[45] M.I. May, S.J. Mentzer and J.J. Reilly, "Ambulatory monitoring of cumulative free living activity", *IEEE Eng Med Biol Mag*, 2003: 22:89-95

[46] D.M. Sherill, M.I. May, J.J. Reilly and P. Bonato, "Using hierarchy of clustering methods to classify motor activities of COPD patients from wearable sensor data", *J Neuroeng Rehabil,* 2005, 2:16

[47] N. Noury, A. Dittmar, C. Corroy, R. Baghai, J.L. Weber et al, "VTAMN- a smart clothe for ambulatory remote monitoring of physiological parameters and activity", *Conf Proc IEEE, Eng Med Biol Soc*, 2004, 5: 3266-3269

[48] I. Atallah, J. Zhang, B.P.L. Lo, D. Shrikrishna, J.L. Kelly et al, "Validation of an ear worn sensor for activity monitoring in COPD", *Am J of Respir Crit Care Med,* 2010, 181: A1211

[49] B. Belza, B.G. Steele, J. Hunziker, S. Lakshminarayan, I. Holt and D.M. Buchner, "Correlates of physical activity in chronic obstructive pulmonary disease", *Nurs Res*, 2001, 50: 195-202

[50] B.G. Steele, I. Holt, B. Belza, S. Ferris, S. Laksminarayan and D.M. Buchner, "Quantitating physical activity in COPD using a triaxial accelerometer", *Chest, 2000,* 117: 1359-1367

[51] Zheng H, Wang H, Wang H, Jeffers P, Jeffers P, Nikamalfard H, et al., "Monitoring and visualizing of night time activity patterns of people with early dementia", *International Journal of Integrated Care*, 2011;11(6). DOI: http://doi.org/10.5334/ijic.727

[52] T.L. Hayes, F. Abendroth, A. Adami, M. Pavel, T.A. Zitzelberger and J.A. Kaye, "Unobtrusive assessment of activity patterns associated with mild cognitive impairment", *Alzheimers Dement,* 2008, 4:395- 405

[53] D. Giansanti, G. Ricci and G. Maccioni, "Toward the design of a wearable system for the remote monitoring of epileptic crisis", *Telemed J E Health,* 2008, 14: 1130 -1135

[54] U. Kramer, S. Kippervasser, A. Shitner and R. Kuzniecky, "A novel portable seizure detection alarm system: preliminary results", *J Clin Neurophysiol,* 2011

[55] S. Patel, C. Mancinelli, A. Dalton, B. Patritti, T. Pang et al "Detecting epileptic seizures using wearable sensors", *Book. Detecting epileptic seizures using wearable sensors.* 2009 (Editor). City

[56] M.Z. Pah, T. Laddenkemper, N.C. Swenson, S. Goyal, J.R. Madsen and R.W. Pickard, "Continuous monitoring of epidermal activity during epileptic seizures using wearable sensors", *Conf Proc IEEE Eng Med Biol Soc* 2010: 4415-4418

[57] A. Dalton, S. Patel, A.C. Roy, M. Welsh, T. Pang et al "Detecting epileptic seizures using wearable sensors", *Book. Detecting epileptic seizures using wearable sensors*. 2010 (Editor). City

[58] M. Lanz, A. Nahapetian, A. Vahdatpourz, L. Kaiserz, M. Sarrafzadeh et al, SmartFall: an automatic fall detection system based on subsequent matching for the smart cane, *Inter Conf on Body Area Networks,* 2009

[59] A. Bourke, P. Vande, A. Ven, V. Chaya, G. OLaighn and J. Nelson, "Testing of a long term fall detection system incorporated into a custom vest for the elderly", *Conf Proc IEEE Eng Med Biol Soc* 2008, 2008:2844-2847

[60] F. Bianchi, S. Redmond, M. Narayan, S. Cerutti and N. Lovell, "Barometric pressure and triaxial accelerometry-based fall event detection", *IEEE Trans Neural Syst Rehabil Eng* 2010 18:619-627

[61] F. Sposaro and G. Tyson, "IFall: an android application for fall monitoring and response", *Conf Proc IEEE Eng Med Biol Soc 2009*, 2009:6119-6122

[62] J. Dai, X. Bai, Z. Yang, Z. Shen and D. Xuan, "PerFallD: A pervasive fall detection system using mobile phones", *IEEE Inter Conf on Pervasive Computing and Communication Workshops*, Mannheim 2010:292-297

[63] G. Yavuz, M. Kocak, G. Ergun, H. Alemdar, H. Yalcin et al, "A smart phone based fall detector with online location support", *Intl Workshop on Sensing for Ap Phones*, Zurich, 2010:31-35

[64] CSEM, Centre Suisse d'electronique Et de Microtechnique. [http//www.csem.ch/docs/ Show.aspx? id=6026]

[65] K. Fukaya and M. Uchida, "Protection against impact with the ground using wearable airbags", *Ind Health* 2008, 46:59-65

[66] O. Brand, Microsensor integration into systems-on-chip, *Proc of the IEEE,* 2006, 94:1160-1176

[67] R. DeVaul, M. Sung, J. Gips and A. Pentland, MIThril 2003: applications and architecture, *Seventh IEEE Int Symp on Wearable Comput,* 2003:4-11

[68] D. Curone, E. Secco, A. Tognetti, G. Loriga, G. Dudnik, M. Risatti et al, "Smart Garments for Emergency Operators: The ProeTex project, *Infor Tech in Bio Med, IEEE Trans*, 2010, 14:694-701

[69] http://rogers.matse.illinois.edu/files%5C2008%5Cadvmatstrnews.pdf

[70] Sekitani T, Nakajima H, Maeda H, Fukushima T, Aida T, Hata K and Someya T, "Stretchable active-matrix organic light-emitting diode display using printable elastic conductors", *Nature Materials2009*; 8:494–9.

[71] Stephanie J. Benight1, Chao Wang1, Jeffrey B.H. Tok and Zhenan Bao, "Stretchable and self-healing polymers and devices for electronic skin", *Progress in Polymer Science 38*, (2013):1961– 1977

[72] Jeong GS, Baek DH, Jung HC, Song JH, Moon JH, Hong SW, Kim IY and Lee SH, "Solderable and electroplatable flexible electronic circuit on a porous stretchable elastomer", *Nature Communications 2012*, 3:1–8, 977

[73] Araki T, Nogi M, Suganuma K, Kogure M and Kirihara, "Printable and stretchable conductive wirings comprising silver flakes and elastomers", *IEEE Electron Device Letters 2011*, 32:1424–6.

[74] Irimia-Vladu M, Troshin PA, Reisinger M, Schwabegger G, Ullah, M, Schwoediauer R, Mumyatov A, Bodea M, Fergus JW and Razumov VF, "Environmentally sustainable organic field effect transistors", *Organic Electronics 2010*;11:1974–90.

[75] Wenzhe Cao, "Fabrication and modeling of stretchable conductors for traumatic brain injury research", *Princeton PhD Dissertation Research*, 2013

[76] Lee P, Lee J, Lee H, Yeo J, Hong S, Nam KH, Lee D, Lee SS, Ko SH, "Highly stretchable and highly conductive metal electrode by very long metal nanowire percolation network", *Advanced Materials* 2012, 24:3326–332.

[77] Ko H C *et al, "*A hemispherical electronic eye camera based on compressible silicon photoelectronics", *Nature,* 2008, 454:748–753

[78] Schuettler M, Pfau D, Ordonez J S, Henle C, Woias P and Stieglitz T, "Stretchable tracks for laser-machined neural electrode arrays", Conf. *Proc. IEEE Eng. Med. Biol. Soc.* 2009: 1612–1615

[79] J. A. Rogers, Z. Bao, K. Baldwin, A. Dodabalapur, B. Crone, V. R. Raju, V. Kuck, H. Katz, K. Amundson, J. Ewing, and P. Drzaic, *Proc. Natl. Acad. Sci. U.S.A.* 98, 2001, 4835

[80] H. O. Jacobs, A. R. Tao, A. Schwartz, D. H. Gracias, and G. M. Whitesides: *Science 296,* 2002, 323

[81] M. Kaltenbrunner, M. S. White, E. D. Głowacki, T. Sekitani, T. Someya, N. S. Sariciftci, and S. Bauer: *Nat. Commun.* 3, 2012, 770.

[82] Lacour S P, Wagner S, Huang Z and Suo Z, "Stretchable gold conductors on elastomeric substrates", Appl. *Phys. Lett.,* 82: 2003: 2404–2406

[83] Wagner S, Lacour S P, Jones J, Hsu P I, Sturm J C, Li T and Suo Z, "Electronic skin: architecture and components", *Physica E*., 2004, 25: 326– 334

[84] Yung-Yu Hsu, Mario Gonzalez, Frederick Bossuyt, Fabrice Axisa, Jan Vanfleteren and Ingrid DeWolf, "The effect of pitch on deformation behavior and the stretching-induced failure of a polymer-encapsulated stretchable circuit", *J. Micromech. Microeng,* 20**,** 2010: 75036-75046

[85] Amir Jahanshahi, Mario Gonzalez, Jeroen van den Brand, Frederick Bossuyt, Thomas Vervust et al, "Stretchable Circuits with Horseshoe Shaped Conductors embedded in Elastic Polymers", *Japanese Journal of Applied Physics* 52, 2013, 05DA 18-1 to18-7

[86] Astrid-Sofie Borge Vardoy, Andreas Larrson, Knut Olav Gislerud, Hamzah Bhatti, Kristin Imenes et al, "Stretchable Conductors enabled by Metal Coated Polymer Spheres", IEEE *Sensors Journal,* Vol 13, No 10, October 2013

[87] Tino Töpper, Bekim Osmani, Florian M. Weiss, Carla Winterhalter and Fabian Wohlfender, "Strain-dependent characterization of electrode and polymer network of electrically activated polymer actuators ", *Proc. SPIE 9430, Electroactive Polymer Actuators and Devices (EAPAD*) 2015, 94300B (April 1, 2015

[88] https://isen.northwestern.edu/doc/pdf/news/scholarlypapers/Booster_YHuang.March10.pdf

[89] http://feml.skku.edu/publications/2012/JPS-0022-3727_45_10_103001.pdf

[90] Shu Gong, Daniel T, H. Lai, Bin Su, Kae Jye Si, Zheng Ma, Lim Wei Yap, Penzhen Guo and Wenlon Cheng, "Highly Stretchy Black Gold E-Skin Nanopatches as Highly Sensitive Wearable Biomedical Sensors", *Advanced Electronics Materials,* Vol 1, Issue 4, April 2015

[91] Shahshan Yao and Yong Zhou, "Nanomaterial-Enabled Stretchable Conductors: Strategies, Materials and Devices", *Advanced Materials,* Volume 27, Issue 9, March 4, 2015, Pages 1480–1511

[92] H. Jang, Y.J. Park, X. Chen, T. Das, M.S. Kim and J.H. Ahn, "Graphene based flexible and stretchable electronics", *Adv Mater* 28 (22), 4184-4202. 2016 Jan 05.

[93] V. Kumar and G. Khandanval, "Graphene-based Flexible and Stretchable Bioelectronics in Health Care Systems *"Journal of Analytical and Pharmaceutical Research,* Volume 3 Issue 2 – 2016

[94] http://rogers.matse.illinois.edu/files%5C2008%5Cadvmatstrnews.pdf

[95] http://feml.skku.edu/publications/2012/JPS-0022-3727_45_10_103001.pdf

[96] http://rogers.matse.illinois.edu/files/2012/mrsbull.pdf

[97] http://www.seas.harvard.edu/suo/papers/261.pdf

[98] http://dataspace.princeton.edu/jspui/bitstream/88435/dsp012227mp70n/1/Cao princeton.pdf

[99] Araki T, Nogi M, Suganuma K, Kogure M and Kirihara, "Printable and stretchable conductive wirings comprising silver flakes and elastomers", *IEEE Electron Device Letters 2011*, 32:1424–6.

[100] S. Merilampi, T. Laine-Ma, P. Ruuskanen, "The characterization of electrically conductive silver ink patterns on flexible substrates" *Microelectronics Reliability,* 49, 2009:782–790

[101] Merilampi, S.; Björninen, T.; Haukka, V.; Ruuskanen, P.; Ukkonen, L.; Sydänheimo, L. Analysis of electrically conductive silver ink on stretchable substrates under tensile load. *Microelectron. Reliab.* 2010, *50*: 2001–2011.

 [102] Jianbao Pan, Gregory Tonkay, Alejandro Quintero, "Screen Printing Process Design of Experiments for fine line printing of Thick Film Ceramic Substrates", *Journal of Electronics Manufacturing* **09**, 203, 1999

[103] M. Taya, W.J. Kim and K. Ono, "Piezo resistivity of a short fiber/elastomer composite", *Mechanics of Material,* 28 (1998): 53-59

[104] H Lee, K Chou, and Z Shih. Effect of nano-sized silver particles on the resistivity of polymeric conductive adhesives. *International Journal of Adhesion and Adhesives*, pp 5, Feb 2005.

[105] Y Rao and C Wong, "A novel ultra high dielectric constant epoxy silver composite For embedded capacitor application", *Advanced Packaging Materials*, Jan 2002.

[106] C Pecharromn and J Moya, "Experimental evidence of a giant capacitance in insulator/conductor
composites at the percolation threshold". *Adv. Mater*, Jan 2000.

[107] David Roberson, Ryan Wicker, Lawrence Murr, Ken church and Eric MacDonald, "Microstructural and Process Characterization of Conductive Traces Printed from Ag Particulate Inks", *Materials*, 2011, 4, 963-979

[108] Qin, X.Y.; Zhang, W.; Zhang, L.D.; Jiang, L.D.; Liu, X.J. and Jin, D. "Low-temperature resistance and its temperature dependence in nanostructured silver", *Phys. Rev. B* 1997, *56*: 10596-10604.

[109] Huang, C.; Becker, M.F.; Keto, J.W. and Kovar, D. "Annealing of nanostructured silver films produced by supersonic deposition of nanoparticles", *J. Appl. Phys.* 2007, *102*, 054308:1-054308:8.

[110] Greer, J.R.; Street, R.A. Thermal cure effects on electrical performance of nanoparticle silver inks. *Acta Mater.* 2007, *55*: 6345-6349.

[111] R F Saraf, J M Roldan., R Jagannathan, C Sambucetti. J Marino and C Jahnes, "Polymer/ metal composite for interconnection technology", *Electronic Manufacturing Technology Symposium, 1995, 18th IEEE/CPMT International,* 1995, 18: 1051-1053

[112] D. A. Porter and K. E. Easterling "Phase Transformations in Metals and Alloys". 2nd edition, Chapman & Hall, 1992.

[113] Sungmee Park, Kyunghee Chung and Sundaresan Jayaraman, Chapter 1.1 - Wearables: Fundamentals, Advancements, and a Roadmap for the Future. Wearable Sensors, 1-23 (2014)

[114] Marie Chan, Daniel Estève, Jean-Yves Fourniols, Christophe Escriba, Eric Campo, "Smart wearable systems: Current status and future challenges", *Artificial Intelligence in Medicine*, 56: 137-156 (2012)

[115] Tsuyoshi Sekitani, Yoshiaki Noguchi, Kenji Hata, Takanori Fukushima, Takuzo Aida, and Takao Someya, "A Rubberlike Stretchable Active Matrix Using Elastic Conductors", *Science* 321 (5895): 1468-1472 (2008)

[116] John A. Rogers and Yonggang Huang, "A curvy, stretchy future for electronics", *Proc. Natl. Acad. Sci. USA*, 10875-10876 (2009)

[117] Dae-Hyeong Kim, Jong-Hyun Ahn, Won Mook Choi, Hoon-Sik Kim, Tae-Ho Kim, Jizhou Song, Yonggang Y. Huang, Zhuangjian Liu, Chun Lu, and John A. Rogers, "Stretchable and Foldable Silicon Integrated Circuits", *Science,* 320 (5875): 507-511 (2008)

[118] Zhenqiang Ma, "An Electronic Second Skin", *Science* 333 pp. 830-831 (2011)

[119] John A. Rogers, Takao Someya, Yonggang Huang, "Materials and Mechanics for Stretchable Electronics", *Science*, 327: 1603-1607 (2010)

[120] Z. Suo, E. Y. Ma, H. Gleskova, and S. Wagner, "Mechanics of rollable and foldable film-on-foil electronics", *Applied Physics Letters*, 74, 1177 (1999)

[121] Nanshu Lu, "Mechanics, Materials, and Functionalities of Bio Integrated Electronics", *The Bridge on Frontiers of Engineering*, 43 (4), 31-38 (2013).

[122] Sonia Grego, Jay Lewis, Erik Vick, Dorota Temple, "Development and evaluation of bend-testing techniques for flexible-display applications", *Journal of the SID*, 13/7, 575-581 (2005)

[123] F. Bossuyt, J. Guenther, T. Löher, M. Seckel, T. Sterken, J. de Vries, *"Cyclic endurance reliability of stretchable electronic substrates", Microelectronics Reliability,* 51, 628–635 (2011)

[124] Zhong Chen, Brian Cotterell, Wei Wang, Ewald Guenther, Soo-Jin Chua, "A mechanical assessment of flexible optoelectronic devices", *Thin Solid Films,* 394: 201-205 (2001)

[125] Helena Gleskova, I-Chun Cheng, Sigurd Wagner, James C. Sturm, Zhigang Suo, "Mechanics of thin-film transistors and solar cells on flexible substrates", *Solar Energy*, 80: 687-693 (2006)

[126] Sekitani, T., Kato, Y., Iba, S. ; Shinaoka, Hiroshi, Someya, T., Sakurai, T., Takagi, S., "Bending experiment on pentacene field-effect transistors on plastic films", *Applied Physics Letters,* 86: 073511 - 073513 (2009)

[127] Y.C. Lee and T.S. Liu, "Deformation of Multilayer Flexible Electronics Subjected to Torque", *Experimental Techniques*, 38: 13-20 (2014)

[128] Chen, Q., Xu, L., Salo, A., Neto, G., and Freitas, G., "Reliability Study of Flexible Display Module by Experiments", *International Conference on Electronic Packaging Technology & High Density Packaging*: 1–6 (2008).

[129] M. Taya, W.J. Kim, K. Ono, "Piezo resistivity of a short fiber elastomer matrix composite", *Mechanics of Materials*, 28, 53-59 (1998)

[130] Krishna Rajan, Ignazio Roppolo, Annalisa Chiappone, Sergio Bocchini, Denis Perrone, and Alessandro Chiolerio, "Silver nanoparticle ink technology: state of the art", *Nanotechnol Sci Appl*. 2016; 9:1–13. Jan 2016

[131] Abhinav VK, Rao VR, Karthik PS, Singh SP, "Copper conductive inks: synthesis and utilization in flexible electronics", *RSC Adv*. 2015;46(39):63985–64030.

[132] Jing Li and Jang-Kyo Kim, "Percolation threshold of conducting polymer composites containing 3D randomly distributed graphite nano platelets", *Comp. Sci. Tech.,* 67: 2114-2120 (2007)

[133] Jianbao Pan, Gregory Tonkay, Alejandro Quintero, "Screen Printing Process Design of Experiments for fine line printing of Thick Film Ceramic Substrates", *1998 Proceedings of the International Symposium on Microelectronics,* 1998, San Diego, CA: 264-269

[134] Shapee, S.M., Alias, R., Yusoff, M.Z.M., Ibrahim, A., Ambak, Z., & Saad, M.R., "Screen Printing Resolution of Different Paste Rheology for Printed Multilayer LTCC Tape", *Proceedings of International Conference on Electronic Packaging 2010 (ICEP2010)*, Hokkaido, Japan, May 2010: 255-258.

[135] Chhabra, R.P. & Richardson, R.F. "Non-Newtonian Flow in the Process Industries: Fundamental and Engineering Applications", Butterworth-Heinemann*,* Oxford. 1999

[136] Rane, S.B., Seth, T., Phatak, G.J., Amalnerkar, D.P. & Ghatpande, M., "Effect of Inorganic Binders on the Properties of Silver Thick Films", *Journal of Materials Science: Materials in Electronics*, Vol. 15, 2004: 103-106.

[137] Sergent, J.E. "Screen Printing" in *Ceramic Interconnect Technology Handbook* edited by Fred D. Barlow and Aicha Elshabini, CRC Press, 2007: 199-233.

[138] K.C. Chiu, "Application of Neural Network on LTCC Fine Line Screen Printing Process*". Proc. Of the International Joint Conference on Neural Network.* Vol. 2, 2003: 1043-1047.

[139] Gilleo, K., "Rheology and Surface Chemistry for Screen Printing". *Screen Printing*, 1989:128-132

[140] Hoornstra, J., Weeber, A.W., Moor, H.H.C. & Simke, W.C., "The Importance of Paste Rheology in Improving Fine Line, Thick Film Screen Printing of Front Side Metallization", *Proceedings of 14th EPSEC*, Barcelona, 1997:823-826.

[141] Yin, W., Lee, D.H., Choi, J., Park, C. and Cho, S.M., "Screen Printing of Silver Nanoparticle Suspension for Metal Interconnects", *Korean Journal of Chemistry,* Vol. 25, No. 6, (April 2008): 1358-1361.

[142] Stalnecker, Jr., S. G., "Stencils Screens for Fine-Line Printing", *Electrocomponent Science and Technology*, Vol. 7, 1980:47-53.

[143] Ma R, Kang B, Cho S, Choi M, Baik S, "Extraordinarily High Conductivity of Stretchable Fibers of Polyurethane and Silver Nano-flowers". *ACS Nano.* 2015 Nov 24;9(11):10876-86.

[144] Lee H, Kim M, Kim I, "Flexible and Stretchable Optoelectronic Devices using Silver Nanowires and Graphene", *Adv Mater.* 2016 Jun;28(22):4541-8

 [145] W. G. Whittow, A. Chauraya, J. C. Vardaxoglou, L. Yi, R. Torah, K. Yang, S. Beeby, and J. Tudor, "Inkjet Printed Microstrip Patch Antennas Realized on Textile for Wearable Applications," *IEEE Antennas and Wireless. Propag. Lett*, 2014, Vol. 13, 2014:71–74

[146] Aris Tsolis, William G. Whittow, Antonis A. Alexandridis, J. (Yiannis) C and Vardaxoglou**,** "Embroidery and Related Manufacturing Techniques for Wearable Antennas: Challenges and Opportunities", *Electronics*, Vol *3*: 314-338

[147] Inoue M, Yamasaki Y, Suganuma K.," Development of super-flexible wires using conductive adhesives for artificial skin applications of robots and related equipment", *Proceedings of the 5th international conference polymer adhesives in microelectronics and photonics*, Wroclaw, Poland, October 23–26; 2005: 90- 95.

[148] T Li, Z Suo, SP Lacour and S Wagner, "Compliant thin film patterns of stiff materials as platforms for stretchable electronics", *Journal of Materials Research,* 20, 3274-3277 (2005).

[149] Widlund, Thomas, Shixuan Yang, Yung-Yu Hsu, and Nanshu Lu. "Stretchability and compliance of freestanding serpentine-shaped ribbons." *International Journal of Solids and Structures* 51, no. 23 (2014): 4026-4037.-4037.

[150] Y.E and P Mamunya, "Electrical and thermal conductivity of polymers filled with metal powders" *European Polymer J*ournal, **38**, 2002

[151] Nanshu Lu, Shixuan Yang · Becky Su and Ghassan Bitar, "Stretchability of indium tin oxide (ITO) serpentine thin films supported by Kapton substrates" *International Journal of Fracture,* 190(1-2), Nov 2014: 99-110. DOI: 10.1007/s10704-014-9977-x